The Messenger

No. 169 – September 2017

ESO Australia partnership
100 ESO Observing Periods
SPHERE view of protoplanetary disks
ALMA looks at high-redshift quasars

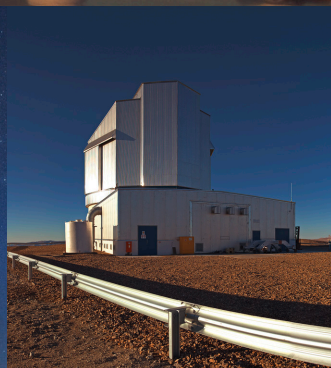

DOI: 10.18727/0722-6691/5030

The Strategic Partnership between ESO and Australia

Laura Comendador Frutos[1]
Tim de Zeeuw[1]
Patrick Geeraert[1]

[1] ESO

On 11 July 2017, ESO and the Australian government signed a ten-year Strategic Partnership arrangement giving Australian astronomers access to the La Silla Paranal facilities. The path towards this arrangement is briefly outlined and the details of the Partnership and its implications for both the Australian and ESO astronomical communities are summarised.

Informal discussions between the Australian astronomical community, Australian government representatives, and ESO concerning Australian membership of ESO have taken place several times since the 1990s. In March 2014 the ESO Director General was invited to present colloquia in Sydney, Melbourne, Canberra and Perth, and had the opportunity to meet senior government officials. Following this visit, an informal Working Group was created consisting of members of the Australian astronomical community and representatives of the Australian government and ESO Management.

Following further meetings with senior Australian astronomers, it was agreed to formally approach the Australian government, given that the timing coincided with a government review of the funding and organisation of astronomy. Australia had informally expressed its desire to participate in the currently existing optical and infrared telescopes at the La Silla Paranal Observatory (LPO) in Chile through a Strategic Partnership, with the intention of becoming an ESO Member State in the future.

The Director General wrote to Sue Weston, Deputy Secretary of the Australian Department for Industry, Innovation and Science (DIIS), to formally open negotiations. Follow-up discussions revealed that the informally discussed Strategic Partnership was of significant interest to the new Australian government and was seen as an excellent candidate for inclusion in the roadmap for new investments in research infrastructures. In addition, the Australian representatives confirmed that full membership of ESO was the goal and that for financial and other reasons the proposed ten-year partnership would be the ideal first step.

On 9 May 2017 the Australian Minister for Industry, Innovation and Science, Arthur Sinodinos, announced, as part of the presentation of the Australian national budget for 2018, that the Australian government was opening formal negotiations on a ten-year Strategic Partnership arrangement with ESO for access to LPO.

Following formal discussions between the Australian government and ESO-Management, the arrangement was signed on 11 July 2017 to begin the ten-year Strategic Partnership between ESO and Australia. The signature ceremony was held at the Australian National University (ANU) in Canberra, during the annual meeting of the Astronomical Society of Australia. Introductions were made by Nobel Laureate and ANU Vice-Chancellor Brian Schmidt and were followed by speeches from Tim de Zeeuw and Arthur Sinodinos, who then together signed the arrangement. Figure 1 shows the participants at the signing ceremony.

The timing of the signature of the arrangement has enabled astronomers in Australia to apply for observing time under the next Call for Proposals, issued in late August, for observations in Period 101 starting on 1 April 2018.

Scope of the Strategic Partnership

The arrangement stipulates that Australia will benefit from participation in activities relating to LPO facilities in the same way and to the same extent as the ESO Member States. In particular:

1. Astronomers based in Australia have access to LPO facilities, specifically the Very Large Telescope (VLT), the Very Large Telescope Interferometer (VLTI), the Visible and Infrared Survey Telescope for Astronomy (VISTA), the VLT Survey Telescope (VST), the ESO 3.6-metre telescope, and the New Technology Telescope (NTT) under the same scientific conditions as those applying to the ESO Member States and through the same procedure, i.e., the Observing Programmes Committee process.

2. Australian companies are placed on the same footing as companies in ESO Member States with regard to participation in ESO procurements relating to LPO facilities. Similarly, Australian institutions are placed on the same footing as institutions in the ESO Member States in respect of involvement in instrumentation for LPO. Under the arrangement, Australian industry and Australian institutions do not have access to contracts and involvement in instrumentation for the ELT. This latter condition would change if Australia became an ESO Member State.

3. In order to facilitate its transition to full membership, Australia is entitled to be represented as an observer at meetings of the ESO Council, Finance Committee (FC), Scientific and Technical Committee (STC) and the Users Committee (UC) in matters dealing with LPO facilities. Australia has no voting rights in the ESO Council because the ESO Convention, which is the founding treaty of the Organisation, only foresees voting options in the ESO Council for Member States. At meetings of the FC, Australia has voting options exclusively for the award of contracts relating to LPO facilities. At meetings of the STC and the UC, Australia has voting options exclusively for matters relating to LPO facilities.

4. Australia is now included along with the Member States in the list of preferred nationalities for all job vacancies at ESO. This applies even if the vacancy is not related to LPO.

In return, Australia:

1. Contributes to the annual total (direct and indirect) costs of the operation of the LPO facilities and the LPO instrumentation programme with payment in cash of an amount corresponding to the Australian Net National Income (NNI) share of the total cost.

2. Annually contributes to the amortised costs of the net assets of the LPO

Figure 1. The participants from the Australian government and ESO at the signing of the Strategic Partnership in Canberra in July 2017[1]. From left to right: Virginia Kilborn, President of the Astronomical Society of Australia; Warrick Couch, Director of the Australian Astronomical Observatory; Sue Weston, Deputy Secretary, Department of Industry, Innovation and Science; Arthur Sinodinos, Minister for Industry, Innovation and Science; Tim de Zeeuw, ESO Director General; Brian Schmidt, Vice Chancellor of the Australian National University; Laura Comendador Frutos, Head of the ESO Cabinet; and Patrick Geeraert, ESO Director of Administration.

facilities with payment in cash of an amount corresponding to the Australian NNI share.

In practical terms, this means that Australia will pay annually about 7.8 million euros (2018 economic conditions) over the ten-year period, which, through the financial contribution will help to bring the ELT Phase II forward. In particular, it will allow to ensure that the entire ELT primary mirror, including the five inner rings of segments and the seventh sector, which are important for adaptive optics operation of the ELT, will be in place at first light. The annual amount of Australia's contribution to the LPO operational costs in each calendar year can vary slightly, and will be set relative to Australia's national share of the projected LPO operational budget, including instrumentation and overheads. This national share is calculated by a standard formula using Organisation of Economic and Community Development (OECD) economic data.

Should Australia accede to ESO during the ten years of the Strategic Partnership or shortly thereafter, the payments related to the La Silla Paranal net assets will be deducted from the special contribution (the "entrance fee"). If Australia does not apply for membership after the expiry of the Strategic Partnership, it will have no claim on this amount.

Implications of the Partnership for the Australian and ESO astronomical communities

From the point of view of Australia, its astronomy community has gained immediate access to many of the best telescopes in the southern hemisphere for a long period, fulfilling a key recommendation of the Australian Decadal Plan for Astronomy. The partnership offers the possibility of a return on investment for Australian industry through participation in instrumentation consortia. Investment in ESO infrastructure is an important element of the support provided by the Australian government. Most significantly, Australia views the partnership as a clear strategy towards achieving full ESO membership in the future.

From the point of view of ESO, the Strategic Partnership represents a vital strategic expansion of the Organisation that will secure ESO's status as the world leader in optical and infrared astronomy. Australia has a long and rich history of internationally acclaimed astronomical research. Its already very active and successful astronomical community will undoubtedly thrive given long-term access to ESO's cutting-edge facilities. Australia's scientific community is very mature, not only in terms of research but also in the development of front-line ground-based instrumentation, and both will be extremely beneficial to ESO. The partnership will further strengthen ESO's programme, both scientifically and technically. The results of such collaborations are eagerly anticipated by the ESO community. This ESO–Australia collaboration will undoubtedly lead to fundamental new advances in science and technology that neither could hope to achieve alone.

With regard to the Strategic Partnership's being a first step towards Australia becoming an ESO Member State, given the relatively large size of the Australian economy and the increasing growth of ESO's assets, the Strategic Partnership will serve to reduce future barriers to Australia's accession to ESO by offering a substantial down-payment on the special contribution. Thus, the decade-long partnership will strengthen the technical, scientific and political cooperation between Australia and ESO, offering fertile ground for future membership discussions, as the Portuguese and Spanish precedents successfully demonstrated.

Links

[1] ESO Release: http://www.eso.org/public/news/eso1721/

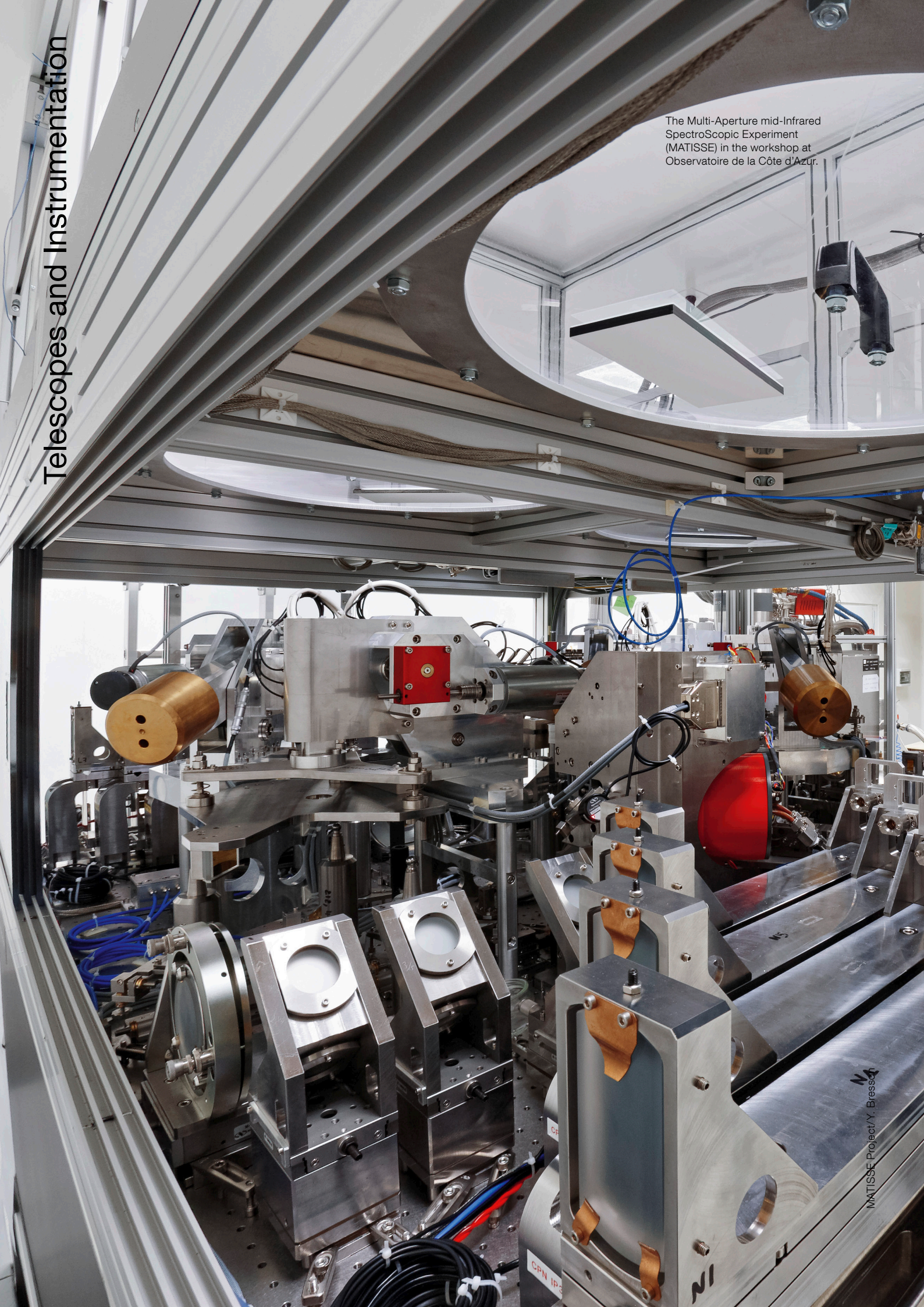

The Multi-Aperture mid-Infrared SpectroScopic Experiment (MATISSE) in the workshop at Observatoire de la Côte d'Azur.

MATISSE Project/Y. Bresson

DOI: 10.18727/0722-6691/5031

Period 100: The Past, Present and Future of ESO Observing Programmes

Ferdinando Patat[1]
Gaitee Hussain[1]
Dimitri Gadotti[1]
Francesca Primas[1]

[1] ESO

1 October 2017 marks the start of ESO Period 100. To celebrate this centenary we look back at the evolution of observing time proposals at ESO. This article examines the way that science is facilitated by ESO and how this has evolved as new technologies mature in order to take advantage of new ideas from astronomers and engineers from across the ESO Member States and beyond. We look at how the first ESO observing periods were defined and how different the calls for proposals and proposal reviews were at that time. We then detail how these processes changed as the VLT started, showing how Service Mode has fundamentally changed how astronomy is being done on the VLT. Finally we look to the future, describing forthcoming instruments and experiments on ESO telescopes and at other facilities hosted onsite. We conclude by describing some of the challenges faced by ESO and the user community and how procedures will need to evolve further to accommodate these.

Table 1

Specification of the periods for which observing time was allocated to Visiting Astronomers

Reference number	Period from noon	Period to noon	Notes
1	Nov. 1, 1968	May 1, 1969	only 1 m telescope
2	May 1, 1969	Sept. 1, 1969	only 1 m telescope
3	Sept. 1, 1969	March 2, 1970	1.52 m tel. and GPO added
4	March 2, 1970	Sept. 1, 1970	
5	Sept. 1, 1970	March 2, 1971	
6	March 2, 1971	July 1, 1971	
7	July 1, 1971	Oct. 1, 1971	
8	Oct. 1, 1971	Apr. 1, 1972	50 cm tel. added
9	Apr. 1, 1972	Oct. 1, 1972	
10	Oct. 1, 1972	Apr. 1, 1973	
11	Apr. 1, 1973	Oct. 1, 1973	

Figure 1. This table from the ESO Annual Report 1972 shows how the duration of the observing periods at ESO varied over the first 2–3 years until operations settled down in 1971. The numbering system of these observing periods was agreed with the OPC at the time.

In the beginning

ESO astronomers have regularly been invited to apply for observing time on ESO facilities since November 1968, which marks the start of Period 1. In the beginning the only telescope offered was the recently commissioned ESO 1-metre photometric telescope. The 1.52-metre spectrographic telescope and the Grand Prisme Objectif soon followed and they came into regular use from September 1969. Over the next two years ESO experimented with how often telescopes should be offered, trialling observing period lengths of between four and six months (see Figure 1), and finally settling on six-month periods running October–March and April–September; a definition that continues to this day. The numbering system for the first observing periods was retroactively assigned and published in the 1972 ESO Annual Report[1]. This includes a description of the importance of the October–March period which "includes the meteorologically most favourable months and also coincides with the Magellanic Clouds season". Standard application forms, in which astronomers could describe their observing plans in detail, were only introduced from Period 4, which began in March 1970.

The announcement inviting ESO observing proposals for Period 2 (March to September 1969) can be found in ESO Bulletin No. 4[2] and reveals some fascinating insights into what observing trips looked like for visiting astronomers at that time. From the beginning, ESO would cover costs for travel, lodging and food for qualifying visiting astronomers; this is much the same today. However, there are also some key differences: additional funds could be sourced to contribute towards the travel costs incurred by "accompanying wives ... only in case the observer will have to stay in Chile for periods of at least 6 months". It is clear from this announcement that the community was predominantly male and that observing stays of weeks to months were not unusual. The announcement was published in both English and French until Period 53 and proposals were accepted in both languages during this time.

Until 1971 the Scientific Programmes Committee (first chaired by Bengt Strömgren) oversaw both scientific policy at ESO and the review of the observing proposals submitted every period[3] (Madsen, 2012). In that year the responsibility for time allocation moved to the new Observing Programmes Committee (first chaired by Paul Ledoux). The initial panel constituted six senior scientists and was extended to eight in 1981. Over the next few years, the success of the Observatory meant the numbers of proposals submitted continued to increase and put the review process under correspondingly increasing pressure. In 1988, 350 proposals per period were received, necessitating the recruitment of extra "Members-at-Large" to balance the workload for all the reviewers.

By 1994, with over 500 proposals being submitted every semester, even this was not sufficient and it became necessary to significantly revise the procedure[3]. This led to the two-step process that continues to this day, whereby proposals are first reviewed by astronomers organised into panels with specific areas of scientific expertise, and then the Observing Programmes Committee (OPC) reviews the panel rankings across all scientific areas and issues final recommendations to the Director General. This model has largely been successful and has not substantially changed over more than 20 years, even though the numbers involved are very different. The first such review involved 34 panellists, of which 12 were OPC members (eight national representatives and four Members-at-Large). This was progressively increased to 48 (2000), 60 (2004) and 72 (2007). Since 2010 the

process has involved 79 astronomers per period, of which 17 are in the OPC-proper (including the OPC Chair).

Part of the challenge with organising peer reviews is to ensure that the pressure on reviewers is even across all scientific categories. The categories into which proposals were organised were initially defined as follows:
– Galaxies, Clusters of Galaxies and Cosmology
– Active Galactic Nuclei and Quasars
– Intergalactic and Interstellar Mediums
– High-mass and/or Hot Stars
– Low-mass and/or Cool Stars
– Solar System.

Four years later, some of these were updated and the list was as follows:
– Nearby Normal Galaxies and Stellar Systems
– Physics of AGNs, QSOs and Starburst Galaxies
– Interstellar Medium and Star formation
– High-mass and/or Hot Stars
– Low-mass and/or Cool Stars
– Solar System.

By June 2000, as the community started to avail itself of the new opportunities presented by access to the VLT, the OPC scientific categories were reassessed and four broad categories were defined, which remain substantially unchanged to the present day:
– Cosmology
– Galaxies and Galactic Nuclei
– ISM, Star Formation and Planetary Systems
– Stellar Evolution.

For reviews of the detailed procedures governing the review, selection and scheduling of observing time proposals at ESO the reader is referred to Breysacher & Waelkens (2001) and Patat & Hussain (2012).

From the La Silla boom to the VLT explosion

The proposal submission history at ESO during the last 40 years (1977–2017) is presented in Figure 2. This also shows the entry periods of the various Member countries and other significant events related to ESO telescopes and instrumentation. The pre-VLT era is characterised by steady growth, peaking in Period 54 (1995), when 556 proposals were submitted for the ten telescopes offered at La Silla. Immediately after, the New Technology Telescope (NTT), which had first been offered in 1990, was taken out of operation for the so-called "big-bang". During this phase, in which the NTT was used as a test bench for the hardware and software to be deployed at the Very Large Telescope, the number of proposals per semester stabilised at around 475. That was only a temporary pause, preceding the significant jump that was seen in Period 63 when Unit Telescope 1 (UT1, *Antu*), equipped with FORS1 (the FOcal Reducer/low dispersion Spectrograph 1) and ISAAC (the Infrared Spectrometer And Array Camera), was offered to the community for the first time. After that the number of submissions kept growing, peaking in Period 84 when, following the deployment of the first second-generation VLT instrument, X-shooter (a wideband ultraviolet-infrared spectrograph), ESO received almost 1100 proposals. Following this (still unchallenged) high point, the number of proposals has decreased to about 890, with another bump corresponding to the start of operations of other second-generation instruments (KMOS, SPHERE and MUSE).

Although it may be too early to draw firm conclusions, there are indications that the number of proposals is levelling out, at an average value slightly below 900 proposals per semester.

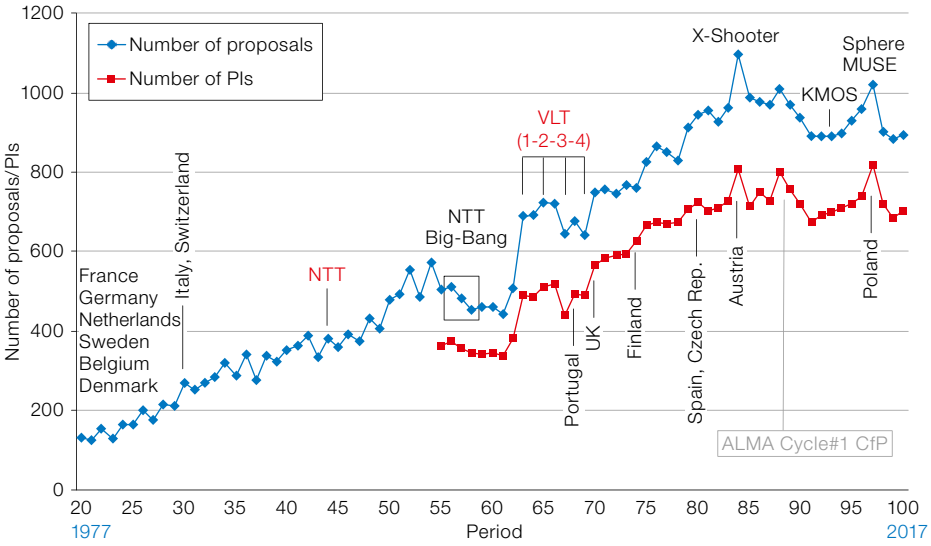

Figure 2. The "Breysacher" plot showing the evolution of the number of proposals submitted over time, for the last 40 years of ESO operations (1977–2017); this is named after Jacques Breysacher, who oversaw the proposal selection process at ESO between 1978 and 2003. The figure also shows the number of distinct Principal Investigators (PIs) from Period 55 (the period from which proposers data were digitally stored). The semesters during which new Member State countries joined are also indicated, as are significant events related to telescopes and instrumentation.

The ALMA Cycle #1 Call for Proposals opened on 31 May 2012 during ESO Period 89. This also corresponds to the time the first Public Spectroscopic Surveys started; both the ESO-Gaia survey and the Public ESO Spectroscopic Survey for Transient Objects (PESSTO) involve very large collaborative efforts. These factors probably contributed to the observed "plateau", although signs of flattening may already be visible as early as Period 85 (see Figure 2). This may indicate that the proposal submission capacity of the community has been reached.

It is interesting to note that a pause in the proposal growth is visible also in the phase immediately following the start of VLT operations (Periods 63 to 69) during which the average submission rate stabilised at around 700. The accession of the United Kingdom (Period 70) marked a new phase, characterised by other Member States joining and bringing new active users into the picture.

The shift from La Silla to Paranal

The trends in the number of proposals submitted over time to each site are shown in Figure 3, which illustrates the gradual shift from La Silla to Paranal from the start of VLT operations in Period 63. In this Period, only UT1 was offered on the VLT, and ESO received 400 proposals for La Silla and 237 for Paranal. This number quickly ramped up, with Paranal taking over from Period 70 and La Silla steadily decreasing with time. While La Silla receives fewer than 100 proposals per semester from Period 91 onwards, the overall demand for Paranal telescopes has remained roughly constant as at Period 82, with the two remarkable exceptions mentioned above. While there was some interest in joint La Silla-Paranal projects (about 40 proposals in Period 63), this has dropped with time to the relatively low level observed today (about 10 proposals per semester). The overall decrease that started in Period 85 can be explained as the combined decline in the number of submissions for La Silla and APEX (the Atacama Pathfinder EXperiment). For the La Silla telescopes, we note that there is a clear trend towards Large Programmes submitted by large teams. On the contrary, the request at the VLT is largely dominated by normal programmes (about 85 %), with a median time request of below 15 hours.

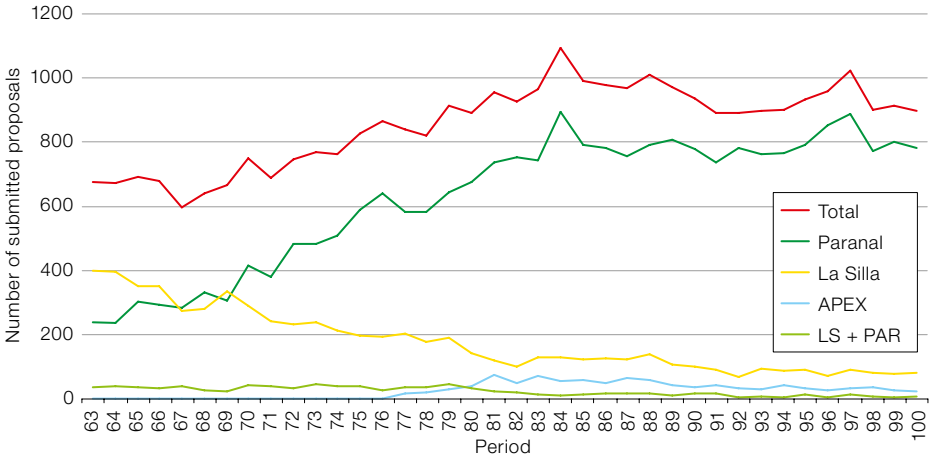

Figure 3. (Upper) Evolution in the number of proposals per site in the VLT era (starting from Period 63).

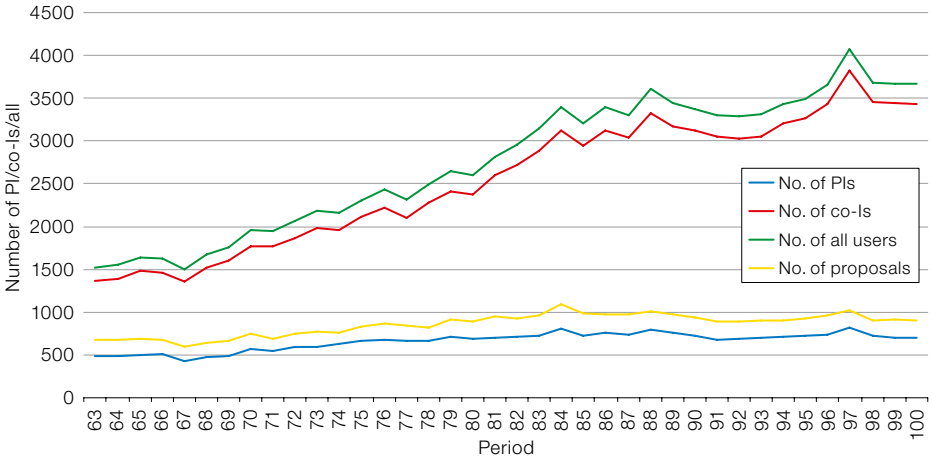

Figure 4. (Lower) Trends in the number of investigators over time in the VLT era. The figure shows the evolution of the number of distinct Principal Investigators, co-Investigators (co-Is), total users and proposals per semester.

The evolution of the user community and the shift in scientific interests

The evolution of the ESO user community is presented in Figure 4, where we have plotted various indicators for the VLT era. After the initial, comparatively flat part (from Periods 63 to 67), in which the total number of users (distinct scientists, both PIs and co-Is) was slightly above 1500, a steady rise commences. The number of scientists involved in ESO proposals has kept growing, exceeding 3500 proposers in Period 88, and reaching its maximum value (4078) in Period 97, to stabilise at about 3700 researchers in the last few semesters. The size of the active ESO community has more than doubled since the start of the VLT era.

Despite the significant growth in the number of proposals, the submission rate per PI (in terms of average number of proposals per semester) has remained practically constant at about 1.3 proposals per semester per PI. This is shown in Figure 5 and it is due to the combined evolution of the number of proposals and distinct PIs, which practically balance out; the observed increase is totally driven by the rise in the number of active PIs (and not by an enhanced submission rate per PI). A similar stability is observed for the average number of proposals per co-investigator; on average, each co-investigator is connected with about two proposals every semester.

On the other hand, the size of proposing teams has continued to get larger, with no signs of saturation across the whole VLT era (see Figure 5). While at the start of VLT operations the average team included two co-investigators, by P100 this number has almost doubled (to 3.8).

To illustrate the changes in the scientific interests in the community, we present in Figure 6 the fractions of the number of proposals for each of the four categories introduced in Period 66 (A: cosmology; B: galaxies and galactic nuclei; C: interstellar medium, star formation and planetary systems; D: stellar evolution). The most significant development is the pronounced growth of the C category, from about 21 % in Period 66 to the 36 % peak attained in Period 83. This trend is certainly related to the expansion of the exoplanet field sparked by the announcement of the first detection by Mayor & Queloz (1995), a discovery that led to the development of efficient planet-hunting instrumentation at ESO.

Another interesting aspect concerns the A and B categories. While these fields lost some interest since the start of VLT operations in favour of the more popular categories C and D, each regained at least part of it in the last five years. In addition, around Periods 80 to 83 there was an inversion in the trend; cosmology took over from galaxies and galactic nuclei studies. This, coupled with the increase in the overall number of proposals, motivated ESO to introduce an extra panel in the A category in Period 85 which, like B, traditionally had only two panels (in contrast to the C and D categories, which have four panels each). In P100, C and D categories include 61 % of the proposals, while A and B account for the remaining 39 %.

The move to Service Mode

One of the most important changes introduced by ESO in its operating model is the deployment of Service Mode. As stated in the VLT/VLTI Science Operations Policy[4], at least 50 % of the time at the VLT is reserved for this mode, while at least 40 % of the available time is reserved for Visitor Mode observations. The policy ensured some flexibility, stating that "these figures may be subject to periodic adjustments, depending on the experience gained at ESO and the evolution of the community demands".

The way the repartition of time evolved in practice is presented in Figure 7, which plots the fractions of requested time at the VLT only. As it turns out, the community quickly moved away from the 50/50 request seen in the first few semesters, gradually and steadily increasing the Service Mode fraction. After levelling out at around 70/30 between Periods 78 and 88, the Service Mode demand started growing again, to reach a peak in P100 (about 87 %). The reasons for the observed behaviour are probably manifold. The efficiency of the operational schema, its satisfactory science return and the increase in the number of short time requests (for which observing trips to Chilean sites are inefficient) have certainly contributed to the current status. ESO has not taken any action to counter this trend, which may lead to a loss of contact with the Observatory and the telescopes, with potentially negative effects on the next generation of astronomers.

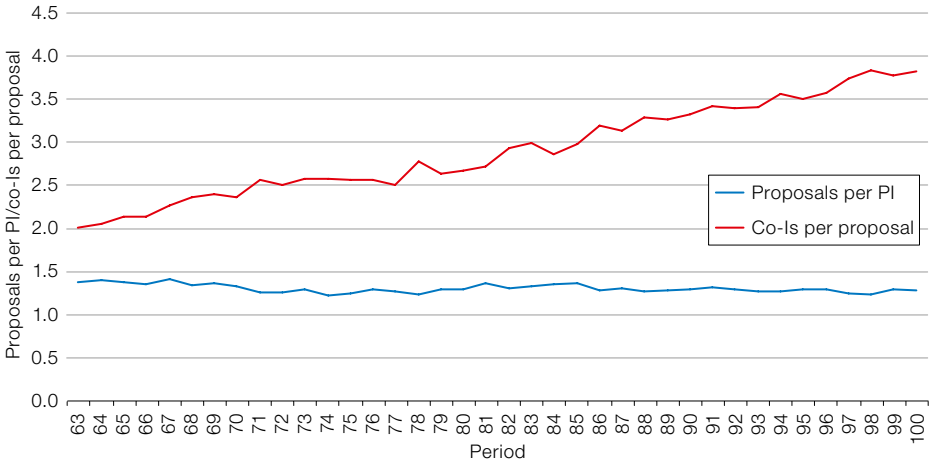

Figure 5. (Upper) Evolution of the average number of proposals per Principal Investigator and the average number of co-Investigators per proposal during the VLT era.

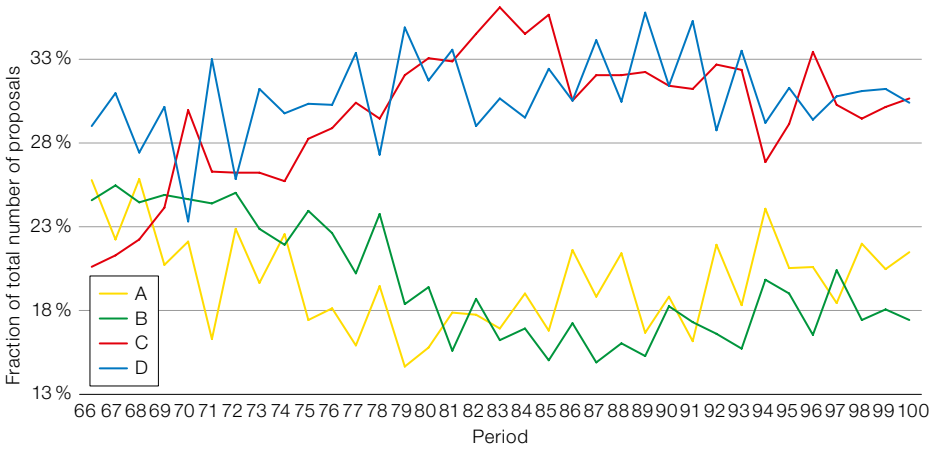

Figure 6. (Lower) Evolution of the number of proposals per scientific category since Period 66 (A: Cosmology, B: Galaxies, C: Star formation and planetary systems, D: Stellar evolution).

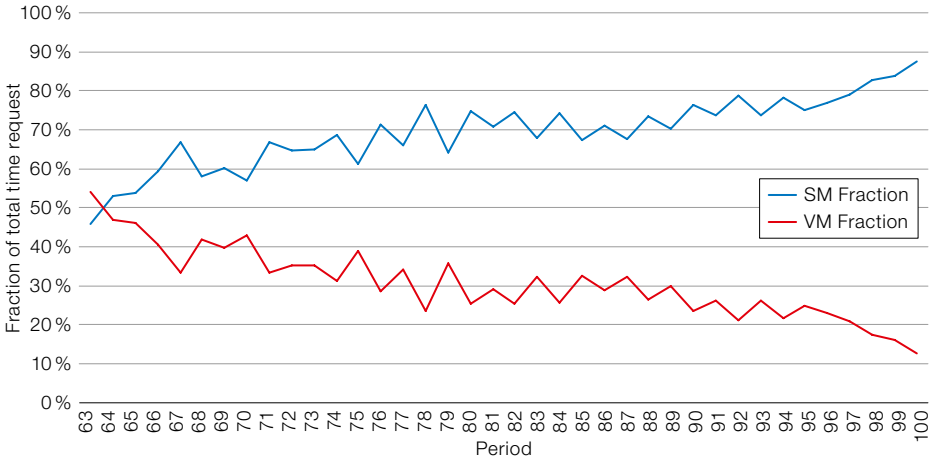

However, it is worth noting that the effectively allocated Service/Visitor Mode fraction is different, because the GTO as well as the Public Spectroscopic Surveys on

Figure 7. Service Mode (SM) *vs.* Visitor Mode (VM) time requests. This includes proposals for the VLT only. Large Programmes, Public Spectroscopic Surveys and Guaranteed Time Observations proposals are excluded.

the VLT are all scheduled in Visitor Mode, hence partially balancing the repartition, especially in the last five years. However, Figure 7 reveals a clear trend that requires consideration by both ESO and its user community.

Looking ahead

The history of ESO is marked by the constant development of new instrumentation and facilities, and an operating model that is capable of adapting to these changes. Likewise, the processes involved in the selection of the most promising observing programmes and the allocation of telescope time have to develop accordingly. Often this is accompanied by an evolution of the tools used at ESO. Figure 8 compares draft telescope schedules from Periods 22 (1978) and 100 (2017). Whilst in Period 22 this was done manually on paper, schedulers have used the TaToo time allocation tool since Period 73 (Alves, 2005).

Since there are virtually no pauses in the operation of ESO telescopes, new frameworks have to be tried at the same time as regular support to the ESO user community is provided, resulting in a number of additional challenges. This also means that the consequences of changes are seen immediately, and new ideas are constantly scrutinised and adapted in a feedback process between ESO and its user community. As the pace of technological progress and the ESO community both increase, so does the pressure on the different ESO systems, which grow in complexity to facilitate quick scientific exploitation.

In the very near future, the current framework will be challenged by ESPRESSO (the Echelle SPectrograph for Rocky Exoplanet and Stable Spectroscopic Observations) and 4MOST (the 4-metre Multi-Object Spectroscopic Telescope). As of 2018, ESPRESSO will be the first instrument to use the incoherent focus at the VLTI laboratory, employing either one or multiple UTs. When using multiple UTs it will be similar to the VLTI with the UTs as regards time allocation. However, in what is considered its basic operating mode, i.e. using a single UT, ESPRESSO allows the possibility of using any UT for the execution of a given Observing Block for the first time, hence adding extra complexity to the scheduling. Furthermore, when ESPRESSO is occupying a single UT, the VLTI coherent focus can still be used at the same time with either the Auxiliary Telescopes (ATs) or the other UTs.

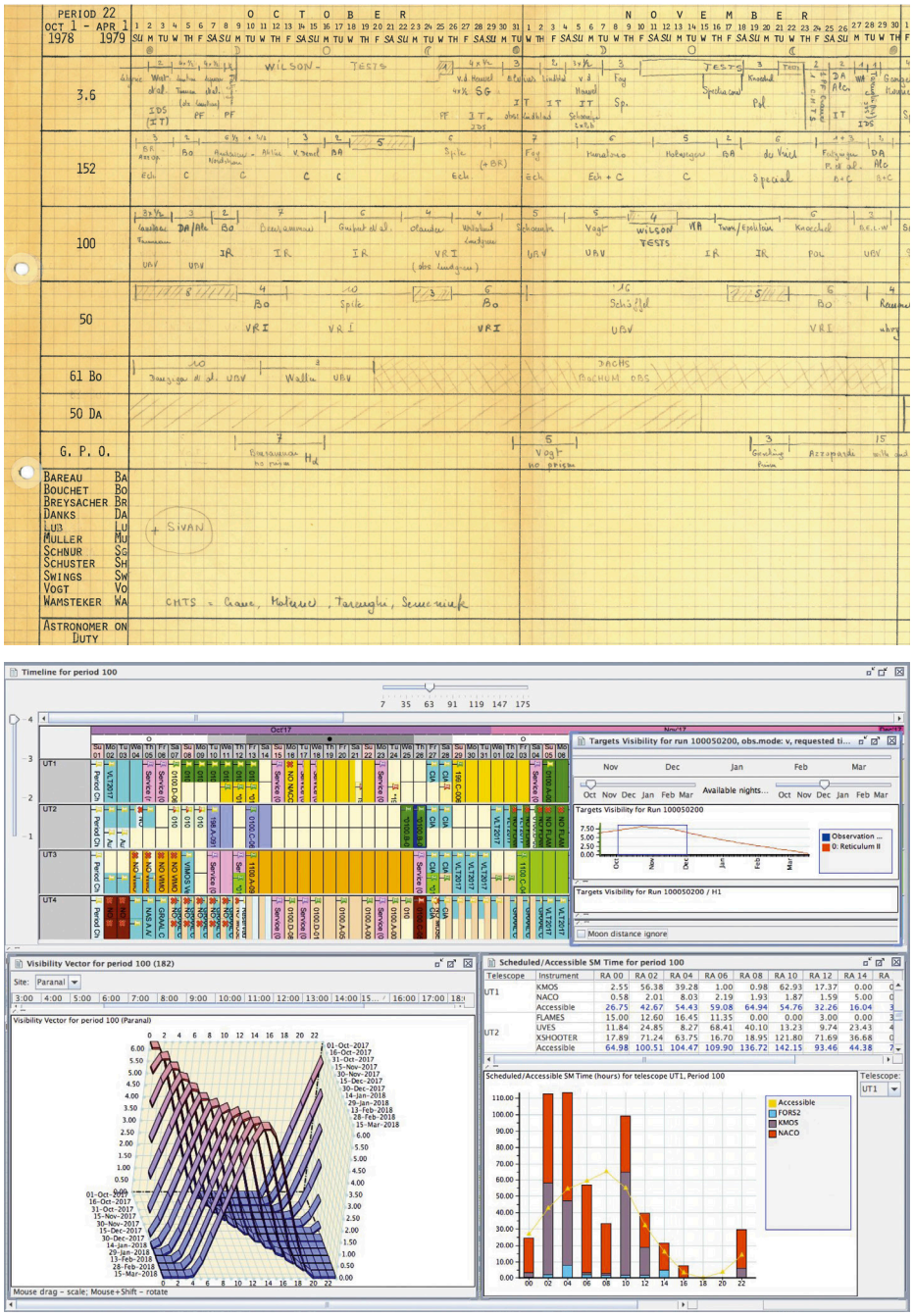

Figure 8. Draft telescope schedules in Periods 22 (top) and 100 (bottom). Until Period 73, scheduling the telescopes was done manually on paper.

4MOST (to be installed on the VISTA telescope in 2021, replacing the VISTA InfraRed CAMera, VIRCAM) will bring about an entirely new concept as regards surveys at ESO. Whilst the selection of the most compelling observing proposals will still be the responsibility of a committee of experts from the community, the

preparation and queuing of Observing Blocks will be a joint effort between ESO and the consortium building the instrument. Most of the time, the observations of targets from multiple surveys will be done in parallel within the same Observing Block. A tool developed by the consortium — the 4MOST Facility Simulator — will be used to assess the execution and completion of observations corresponding to both community and consortium surveys (Boller & Dwelly, 2012). The tool will also have a built-in exposure time calculator to estimate the execution time of observations of large sets of targets.

Furthermore, 4MOST will provide ample opportunity for spectroscopic follow-up of transient objects discovered with the Large Synoptic Survey Telescope (LSST), which will also be located in Chile, its first light expected in 2020. Given that the LSST will discover thousands of new transient sources (for example, supernovae and QSOs) every night, studies of such phenomena will push strongly for more dynamical scheduling.

After the installation of the HARPS (High Accuracy Radial velocity Planetary Searcher) instrument on the ESO 3.6-metre telescope in La Silla, this site has become a key player in research on extrasolar planetary systems. The unique capabilities of HARPS in studying the radial motion of extrasolar planets will be complemented in the near-infrared with the commissioning of the NIRPS (Near-InfraRed Planet Searcher) instrument, expected in 2019 (Bouchy et al., p. 21). The ESO 3.6-metre telescope becomes therefore an “extrasolar planet telescope”, i.e., a telescope dedicated to tackling a particular set of science questions, with a significant impact on a specific yet substantial fraction of the community — a potentially interesting prospect for other ESO telescopes.
A number of small telescopes hosted at La Silla are addressing similar questions using a wide variety of approaches: for example, TRAPPIST (TRAnsiting Planets and PlanetesImals Small Telescope; first light in 2010); and two projects that have first light in 2017, the MASCARA (Multisite All Sky CAmeRA) station, and the ExTrA project (Exoplanets in Transits and their Atmospheres). Similarly, Paranal has been hosting the NGTS (Next-Generation Transit Survey) since 2015, which is also dedicated to extrasolar planets.

Planning for the Extremely Large Telescope

After first light in 2024, the Extremely Large Telescope (ELT) will become part of the suite of facilities offered to the ESO community. The ELT will enable discoveries of a transformational nature. It will be one unique telescope serving a large community with a diverse range of science cases. Depending on the operational model adopted for the VLT during the ELT era, this may have an impact and cause the review and scheduling process to develop further. This is a good time to re-examine the framework within which observing programmes are selected and allocated time, in consultation with the community. The exercise should not only consider the ELT but also the VLT, which will take on additional roles to support ELT discoveries. ESO is working to ensure that members of the user community can realise their ambitions to carry out the planned experiments and make the exciting discoveries that are foreseen with the ELT, while leaving enough space to facilitate unpredictable discoveries and address long-standing questions. This amounts to a significant challenge. The goal is a *modus operandi* that benefits the community as a whole. In this context, it is worth noting that the expected ELT discoveries in respect of fundamental physics will expand the expertise required to evaluate proposals, which is already very broad.

Despite the significant growth of the user community, which makes ESO one of the largest astronomical facilities in the world, the way that telescope time applications are reviewed has remained substantially the same since 1993. Barring the necessary increase in the number of reviewers, the procedure has changed in the details, but not in its substance. The current review load (about 70 proposals per panel member, and up to 100 for OPC-proper members) has reached critical levels once again, requiring a re-evaluation of the procedures and an examination of the effectiveness of peer review. This has been the subject of study by the ESO OPC Working Group (Brinks, Leibundgut & Mathys, 2012) and the Time Allocation Working Group (Patat et al., in preparation), which was convened as a spin-off of the ESO2020 exercise (Primas et al., 2015). A clear outcome from these studies is that it is generally agreed that peer review still remains the most satisfactory way of selecting time applications. How this is organised and carried out remains a matter of ongoing discussion that continues to take place between ESO and the community. This will necessarily touch upon a number of aspects, including the way time will be allocated at the ELT.

Acknowledgements

We wish to thank Silvia Cristiani and Elisabeth Hoppe for useful discussions that helped with the preparation of this paper, and without whom it is not possible to manage the scale of the process described here.

References

Alves, J. 2005, The Messenger, 119, 20
Boller, T. & Dwelly, T. 2012, SPIE, 8448, 0XB
Breysacher, J. & Waelkens, C. 2001, in *Organizations and Strategies in Astronomy, Vol. 2*, ed. Heck, A., (Dordrecht: Kluwer Acad. Publ.), 149
Brinks, E., Leibundgut, B. & Mathys, G. 2012, The Messenger, 150, 21
Madsen, C. 2012, *The Jewel on the Mountaintop: The European Southern Observatory through Fifty Years,* (Weinheim: Wiley-VCH)
Mayor, M. & Queloz, D. 1995, Nature, 378, 355
Primas, F. et al. 2015, The Messenger, 161, 6
Patat, F. & Hussain, G. 2013, in *Organizations, People and Strategies in Astronomy, Vol. 2*, ed. Heck, A., (Duttlenheim: Venngeist), 231

Links

[1] ESO Annual Report 1972: https://www.eso.org/public/archives/annualreports/pdf/ar_1972.pdf
[2] ESO Bulletin No. 4: www.eso.org/public/archives/bulletins/pdf/bulletin_0004.pdf
[3] ESO Annual Report 1993: https://www.eso.org/public/archives/annualreports/pdf/ar_1993.pdf
[4] VLT/VLTI ESO Science Operations Policy: https://www.eso.org/sci/observing/policies/cou996-rev.pdf

DOI: 10.18727/0722-6691/5032

Scientific Return from VLT instruments

Bruno Leibundgut[1]
Dominic Bordelon[1]
Uta Grothkopf[1]
Ferdinando Patat[1]

[1] ESO

A statistical analysis of metrics probing the use of VLT instruments yields a perspective on the demand, productivity and impact of individual instruments. The trends in the usage of these instruments provide information that may be useful in determining the timing of potential future instrument upgrades and replacements. We look at the evolution of observing time requests on VLT instruments; this is measured using the number of proposals submitted each semester as well as the requested time. We also look at the publication statistics on all VLT instruments and find that the older workhorse instruments have produced over 1000 publications to date. The most successful VLT instruments produce over 80 publications per year. After an initial increase as they enter operation, most instruments reach a constant rate of publications after between four and eight years and the number of publications and citations only starts to decline after decommissioning. We find that all instruments currently operating show increasing citation counts every year. ESO has regularly upgraded instruments to strengthen their scientific impact.

Introduction

Assessing the scientific impact of scientific institutes, observatories, telescopes and their instrumentation has a long history. Several different methods have been employed in the past (Abt, 1994; Trimble, 1995; Bergeron & Grothkopf, 1999; Benn & Sanchez, 2001; Meylan, Madrid & Macchetto, 2003; Madrid & Macchetto, 2007). The advent of electronic bibliographies has greatly increased the power of statistical analyses. The ESO telescope bibliography telbib[1] (see Grothkopf & Meakins, 2012, 2015 for recent descriptions) has been used in several analyses (for example, Leibundgut, Grothkopf & Treumann, 2003; Grothkopf et al., 2005, 2007) and can be compared to other observatories (Crabtree, 2014, 2016). Sterzik et al. (2015) recently presented a detailed analysis of the science return from VLT observing programmes, identifying connections to operational modes.

Recently, Kulkarni (2016) proposed a new metric to investigate the scientific return of individual instruments. In addition to the publication statistics, he proposes investigating the citations every (calendar) year collected by publications based on a specific instrument. He refers to this as the “citation flux”. A further criterion for the success of an instrument is its capability to provide landmark results universally accepted by a large fraction of the community as yielding new insights; such publications are typically cited very often. The demand by the community is another factor that can be used to describe the popularity and science potential of instruments. The number of proposals and the requested time are good indicators of whether an instrument caters for the scientific needs of the community.

In this analysis we focus on Very Large Telescope (VLT) instruments only. The VLT has been operating since April 1999. There are currently 12 instruments in operation (see Table 1), two have been decommissioned (FORS1 and ISAAC) and one is currently being upgraded (CRIRES).

Our analysis encompasses statistics of the instrument demand (popularity), publications (science return), citations (science impact) and most-cited publications (landmark contributions). We focus on results up to the end of 2016. The proposal statistics therefore include Period 99 (deadline October 2016; observations from 1 April until 30 September 2017) and the citation statistics are also until the end of 2016 (from statistics gathered in July 2017). The proposal database at ESO and telbib[1] were used. Citations are drawn from the SAO/NASA Astrophysics Data System (ADS). The ESO telescope bibliography collects refereed publications based on ESO instruments. We note that several instruments canbe associated with a single proposal or publication.

Overview of the demand for VLT instruments

Figure 1a presents the evolution of the demand per instrument over the past 12 years (i.e., 24 observing periods since April 2005) as indicated by the number of proposals submitted. In 2005, all four Unit Telescopes (UTs) were fully operational and nine instruments were offered. The graph shows that some instruments are extremely popular and remain so for many years. The most frequently demanded instruments are FORS2, X-shooter and MUSE. These are multi-purpose instruments suitable for many astrophysical applications. X-shooter and MUSE are unique among the instruments available at 8- to 10-metre telescopes.

New instruments display a strong start in demand and exhibit a strong increase in the number of proposals and requested time within a couple of periods to at least 50 proposals per semester (for example, VISIR, CRIRES, HAWK-I, KMOS) and in some cases significantly more (X-shooter, MUSE, SPHERE). The strong increase in the demand for FORS2 after Period 82 is due to the decommissioning of FORS1. We note that some instruments were not offered during specific semesters (ISAAC in Period 91, which was followed with a last call for proposals in Period 92; VISIR between Period 92 and Period 94 during the upgrade; HAWK-I in Period 93).

With a few exceptions, a general trend towards fewer submitted proposals over the years can be observed. This shows the early science interest in new capabilities — sometimes in competition with instruments at other facilities — and the move to newer instruments as they become available. In some cases, the decrease is probably connected to the ageing of instruments (for example, NACO).

The evolution of the demand for observing time is displayed in Figure 1b. Strong fluctuations in demand for time can be due to Large Programme and Public Survey proposals. A sawtooth distribution between even and odd periods is also observed. More time is requested in even periods as they offer access to the Northern Galactic Cap. The separation between very highly demanded instruments and the bulk of regularly requested instruments

Table 1. VLT Instruments

Instrument Name	Instrument Acronym	First offered Period	First offered Date	Comments
FOcal Reducer/low dispersion Spectrograph 1	FORS1	63	April 1999	Decommissioned April 2009
Infrared Spectrometer And Array Camera	ISAAC	63	April 1999	Decommissioned December 2013
FOcal Reducer/low dispersion Spectrograph 2	FORS2	65	April 2000	–
UV-Visual Echelle Spectrograph	UVES	65	April 2000	–
Nasmyth Adaptive Optics System (NAOS-CONICA)	NACO	70	October 2002	–
Fibre Large Array Multi Element Spectrograph	FLAMES	71	April 2003	–
VIsible Multi-Object Spectrograph	VIMOS	71	April 2003	Decommissioning planned for 2018
Spectrograph for INtegral Field Observations in the Near-Infrared	SINFONI	74	October 2004	Upgraded in 2016; upgrade as part of ERIS project
VLT Imager and Spectrometer for mid-InfraRed	VISIR	75	April 2005	Upgraded in 2015
CRyogenic InfraRed Echelle Spectrometer	CRIRES	79	April 2007	Dismounted in Period 93; to return to the VLT in Q1 2018
High Acuity Wide field *K*-band Imager	HAWK-I	81	April 2008	Commissioning instrument for the Adaptive Optics Facility (AOF)
X-shooter	–	84	October 2009	Atmospheric Dispersion Corrector refurbished in 2017
K-band Multi-Object Spectrograph	KMOS	92	October 2013	–
Multi Unit Spectroscopic Explorer	MUSE	94	October 2014	–
Spectro-Polarimetric High-contrast Exoplanet REsearch	SPHERE	95	April 2015	–

remains. Like the number of proposals, the time requested tends to decrease over time for ageing instruments.

A further indication of the popularity of instruments is the number of approved Large Programmes (LPs). This is a strong function of the duration of operation of an instrument. By far the largest number of LPs have been approved on FORS2: 28 programmes in total, covering a wide range of scientific topics from Solar System objects to cosmology. Most other early instruments (FORS1, ISAAC, UVES) and the survey instruments (FLAMES and VIMOS) had allocations of between 14 and 16 LPs. FLAMES and VIMOS are also used in Public Spectroscopic Surveys (Gaia-ESO, LEGA-C and VANDELS). The more recent instruments (HAWK-I, X-shooter, KMOS, MUSE and SPHERE) had smaller LP allocations simply because they have not been offered for the same length of time.

Science return of VLT instruments

Data on the number of publications and citation counts per year have been analysed statistically for all instruments, partially following the methodology presented by Kulkarni (2016). We also looked at the ten most cited publications for each instrument to assess their impact.

The total numbers of publications and citations give a global view of the impact of an instrument. A direct comparison between the instruments is difficult for several reasons. The time between data collection and publication is typically from months

Figure 1a. (Below left) Demand per VLT instrument (number of proposals) over the past 12 years (24 observing periods). The colour assigned to each instrument is the same in the subsequent figures.

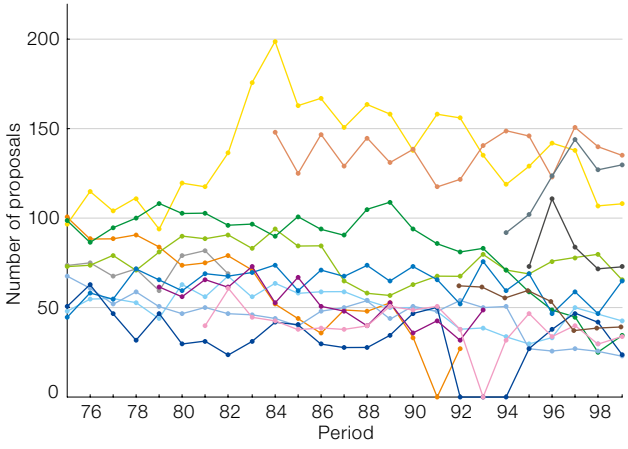

Figure 1b. (Below right) Requested time per VLT instrument over the past 12 years.

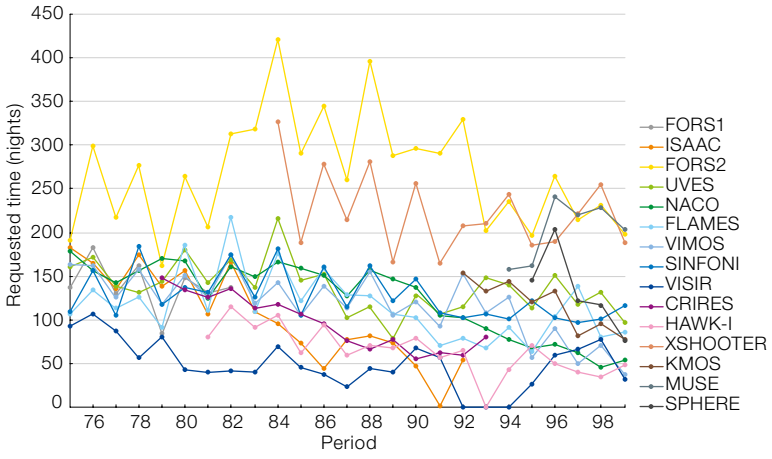

Table 2. Total publications and citations

Instrument	Publications	Citations
FORS1	1000	57265
ISAAC	978	51839
FORS2	1365	62499
UVES	1781	69754
NACO	598	23121
FLAMES	567	22001
VIMOS	715	32807
SINFONI	365	16075
VISIR	167	4225
CRIRES	168	4251
HAWK-I	199	6794
X-shooter	383	8072
KMOS	23	363
MUSE	66	391
SPHERE	45	344

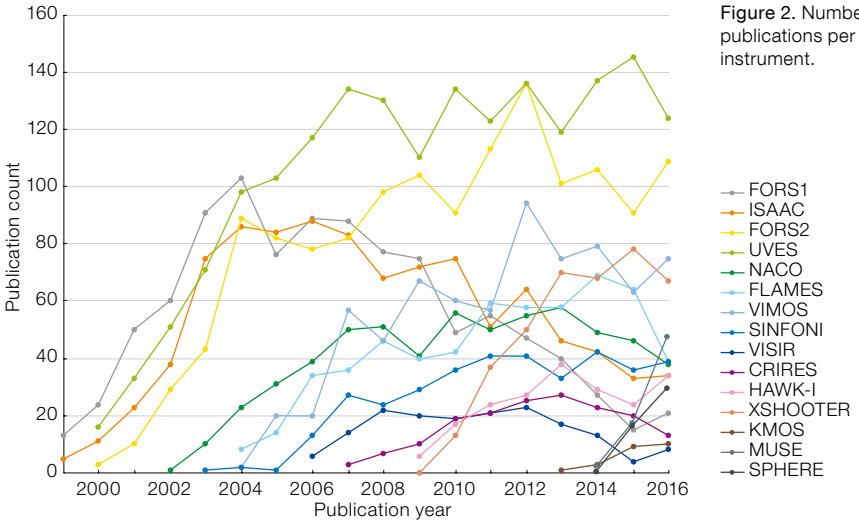

Figure 2. Number of publications per VLT instrument.

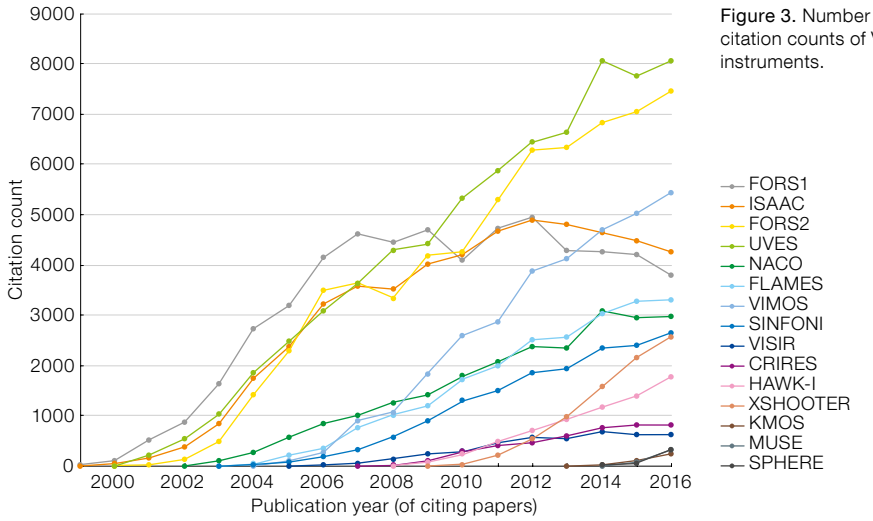

Figure 3. Number of citation counts of VLT instruments.

to years, which means that a lag time from when an instrument is first offered would have to be applied. Similarly, citations build up after publication, and a corresponding lag time would need to be considered. The data in Table 2 should therefore be interpreted with caution.

As might be expected, the earliest instruments have also resulted in the most papers and citations (Figures 2 and 3). UVES has resulted in the most publications and the highest number of citations, while FORS1 and FORS2 have contributed more than 1000 papers each. ISAAC is the fourth VLT instrument with over 50 000 citations to nearly 1000 papers. VIMOS stands out with a large number of papers considering its late arrival and has a high number of citations. On the other hand, SINFONI has produced about half as many publications as VIMOS but joins FORS1, ISAAC, FORS2, and VIMOS as one of the instruments with more than 40 citations per publication on average.

The first VLT instruments (FORS1, ISAAC, FORS2, UVES) showed an early steep rise in publications and citations. It should be noted that not all foci of the available UTs were initially occupied, so the first instruments had a larger fraction of observing time available. While the numbers of papers for FORS1 and ISAAC started to decline after they were decommissioned, FORS2 and UVES have reached a stable level of about 120 (UVES) and 100 (FORS2) papers per year for the past ten years.

The increase in the number of papers for the instruments that came into operation later is more modest (NACO, FLAMES, VIMOS, SINFONI, VISIR and CRIRES). However, these instruments did have smaller shares of telescope time as the UT foci filled up. Specific situations for some instruments apply. As FLAMES and VIMOS are survey instruments, publications often require large samples collected over several semesters. In particular, the early rise in publications for VIMOS is not as steep as those for the FORSs, ISAAC and UVES, but VIMOS publications now match the same level (about 80 publications per year) as the plateau of ISAAC and FORS1 (both decommissioned). NACO and FLAMES had a slower evolution to reach a plateau of about 60 publications every year. SINFONI has contributed to about 40 papers per year for the past 6 years. HAWK-I, VISIR and CRIRES peak below 30 papers per year, but all three instruments were not offered for some time because of upgrades. The second-generation instruments have begun operating too recently to have reached a peak in their paper evolution. X-shooter displays an increase comparable to the most successful instruments, but has levelled at about 70 papers per year for the past three years, while KMOS, MUSE and SPHERE will need several more years to reach equilibrium.

Science impact of VLT instruments

All VLT instruments show rising citation counts, which means that their impact continues to grow. The citation counts seem to separate the VLT instruments into three groups (Figure 3). Obviously, the citation counts strongly correlate with the length of time an instrument has been offered to the community. FORS2 and UVES, the two instruments in operation for the longest time show the highest citation counts. FORS1 and ISAAC levelled off after decommissioning. VIMOS shows a very steep rise in the past years and is now the third most cited VLT instrument. While still showing a steady increase, NACO, FLAMES and SINFONI are on a less accelerated path than the first instruments. This can clearly be seen when comparing the citation counts relative to the start of operations for all instruments (Figure 4).

Here the top group for the first decade of operation includes FORS1, FORS2, ISAAC, UVES, VIMOS and X-shooter. They each reached about 4500 citations per year after a decade. X-shooter has of course not reached the 10-year mark yet, but it is fully on track to match the evolution of the other instruments. A second group of instruments reaches about 2000 to 2500 citations after ten years and includes NACO, FLAMES, SINFONI and HAWK-I. Finally, VISIR and CRIRES had fewer than 1000 citations per year after their first decade; but CRIRES was only in operation for seven years.

Lower demand for an instrument naturally results in fewer observations, leading to fewer publications and citations. This causality can be roughly followed from Figures 1 to 4. A direct comparison of the total number of citations per instrument is not meaningful given the different operating times of the individual instruments. One should also be careful as overall statistics only tell part of the story and some instruments may have an important scientific impact in specific fields while not excelling in the global averages. For example, we note NACO's key role in the measurement of the mass of the supermassive black hole at the centre of the Milky Way.

Most cited papers of VLT instruments

Citation counts can also depend on the specific research topics and communities. When comparing absolute numbers, the time for which an instrument has been in operation is also a deciding factor. The most cited VLT publications (more than 750 citations as at the end of 2016) come from FORS1, FORS2 ISAAC, VIMOS, NACO and SINFONI. The topics include supernova cosmology, deep galaxy surveys (GOODS, COSMOS), supernova–gamma-ray burst connection, dark matter searches, galaxy evolution at high redshifts, a massive pulsar in a compact binary and the Galactic Centre. Most of these publications use data from several major observatories and have large co-author lists (typically more than 20); for example, only five of the 25 most cited VLT papers have fewer than ten co-authors. Table 3 lists the most cited publications per instrument until 2016 based on ESO Publication Statistics[2].

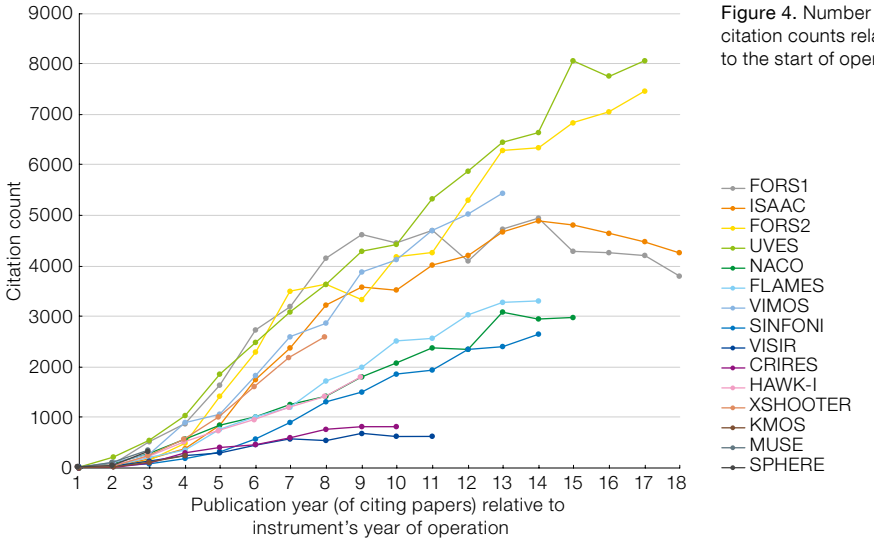

Figure 4. Number of citation counts relative to the start of operation.

Conclusions and outlook

All VLT instruments are in constant demand, display a good scientific return and show significant scientific impact as measured by the proposal statistics, number of publications and citation counts, respectively. According to the criteria set out by Kulkarni (2016), the operational VLT instruments are all delivering. Instruments in operation for a few years show a nearly constant publication rate. Publications from new instruments increase substantially during their first years of operation. Instruments that were not offered for a period, or have been decommissioned, show a decrease in the number of publications after some years. The citation counts continue to increase for all operational instruments, which means that their scientific impact is maintained. A reduction in citation counts would indicate a loss of scientific edge and point toward necessary instrument upgrades or replacements (Kulkarni, 2016). This does not apply to any of the operational VLT instruments at the moment.

The oldest currently operated VLT instruments (FORS2 and UVES) have not received any major upgrades. They are among the VLT instruments with the highest scientific impact and their future operation must be ensured. As workhorse instruments they are the most versatile tools for astrophysics at the VLT and they will remain relevant for the foreseeable future.

ESO has upgraded instruments with low overall impact to improve their science capabilities in recent years (VISIR, CRIRES, HAWK-I). It remains to be seen how these upgrades increase their scientific impact. VISIR will be used for an experiment with the Breakthrough Initiatives (Kasper et al., p. 16). The new CRIRES capabilities will be extremely important in the characterisation of exoplanet atmospheres and HAWK-I will operate with a ground-layer adaptive optics system that will deliver supreme image quality for most of the time.

Table 3. Most cited paper for each instrument (as at end 2016)

Instrument	Bibcode	Publication Title	Authors	Citations
FORS1	2006A&A...447...31A	The Supernova Legacy Survey: Measurement of Ω_M, Ω_Λ and w from the First Year Dataset	Astier et al.	1873
ISAAC	2003ApJ...594....1T	Cosmological Results from High-z Supernovae	Tonry et al.	1450
FORS2	2004ApJ...607..665R	Type Ia Supernova Discoveries at $z > 1$ from the Hubble Space Telescope: Evidence for Past Deceleration and Constraints on Dark Energy Evolution	Riess et al.	3009
UVES	2004A&A...416.1117C	First stars V — Abundance Patterns from C to Zn and Supernova Yields in the Early Galaxy	Cayrel et al.	710
NACO	2009ApJ...692.1075G	Monitoring Stellar Orbits Around the Massive Black Hole in the Galactic Centre	Gillessen et al.	781
FLAMES	2009ARA&A..47..371T	Star-Formation Histories, Abundances, and Kinematics of Dwarf Galaxies in the Local Group	Tolstoy, Hill & Tosi	496
VIMOS	2007ApJS..172....1S	The Cosmic Evolution Survey (COSMOS): Overview	Scoville et al.	823
SINFONI	2009ApJ...692.1075G	Monitoring Stellar Orbits Around the Massive Black Hole in the Galactic Centre	Gillessen et al.	781
VISIR	2010ApJ...716...30A	The Spectral Energy Distribution of Fermi Bright Blazars	Abdo et al.	331
CRIRES	2009A&A...506..287L	Transiting Exoplanets from the CoRoT Space Mission. VIII. CoRoT-7b: the First Super-Earth with Measured Radius	Léger et al.	361
HAWK-I	2009Natur.461.1254T	A γ-ray Burst at a Redshift of $z \sim 8.2$	Tanvir et al.	410
X-shooter	2011A&A...536A.105V	X-shooter, the New Wide Band Intermediate Resolution Spectrograph at the ESO Very Large Telescope	Vernet et al.	285
KMOS	2015ApJ...799..209W	The KMOS 3D Survey: Design, First Results, and the Evolution of Galaxy Kinematics from $0.7 \leq z \leq 2.7$	Wisnioski et al.	74
MUSE	2015MNRAS.449.3393M	The Behaviour of Dark Matter Associated with Four Bright Cluster Galaxies in the 10 kpc Core of Abell 3827	Massey et al.	58
SPHERE	2015A&A...578L...6B	Asymmetric Features in the Protoplanetary Disk MWC 758	Benisty et al.	51

Two VLT instruments have been decommissioned (FORS1 and ISAAC) and VIMOS will follow next year. Instruments under development are either complementary to the current instrument capabilities or will enhance them (such as the Echelle SPectrograph for Rocky Exoplanet and Stable Spectroscopic Observations [ESPRESSO], the Multi Object Optical and Near-infrared Spectrograph [MOONS] and the Enhanced Resolution Imager and Spectrograph [ERIS]). Several instruments have seen extensive interventions to maintain their operability (VIMOS, NACO, X-shooter, KMOS). Others have either recently been upgraded or will be upgraded (for example, VISIR, CRIRES, and SINFONI as part of ERIS).

The second-generation instruments (KMOS, MUSE and SPHERE) began operating within the past three years and will need to fulfil their scientific promise in the coming years. New instruments will replace and improve the capabilities of existing instrumentation: ERIS will replace NACO and SINFONI with improved adaptive optics, ESPRESSO complements UVES as a high-resolution spectrograph while MOONS and 4MOST will massively expand the multiplex capabilities of FLAMES and VIMOS (after 2021). Of course, the Extremely Large Telescope (ELT) will supersede many of the current VLT capabilities (particularly in contrast and depth in the infrared). At the VLT Adaptive Optics (AO) Community Days in 2016, upgrade paths for extreme AO (XAO; upgrade of SPHERE) and Multi-Object AO (MOAO; potentially KMOS) were discussed (Leibundgut, Kasper & Kuntschner, 2016) and a pre-Phase A study for an optical AO imager is currently underway.

Finally, an observatory like the VLT also needs to cover parameter space that will not necessarily yield the highest impact in terms of publications and citations. For example, it has been seen as necessary to offer mid-infrared capabilities to the community to enable research that otherwise would not be possible. In this context, the lower impact of some instruments is expected and acceptable.

Acknowledgements

This research has made use of NASA's Astrophysics Data System. We acknowledge the ESO Telescope Bibliography (telbib), maintained by the ESO Library.

References

Abt, H. 1994, PASP, 106, 107
Benn, C. R. & Sanchez, S. F. 2001, PASP, 113, 385
Bergeron, J. & Grothkopf, U. 1999, The Messenger, 96, 28
Crabtree, D. 2014, SPIE, 9149, 91490A
Crabtree, D. 2016, SPIE, 9910, 991005
Grothkopf, U. & Meakins, S. 2015, ASP Conference Series, 492, 63
Grothkopf, U. & Meakins, S. 2012, The Messenger, 147, 41
Grothkopf, U. et al. 2005, The Messenger, 119, 45
Grothkopf, U. et al. 2007, The Messenger, 128, 62
Kulkarni, R. R. 2016, arXiv:1606:06674
Leibundgut, B., Grothkopf, U. & Treumann, A. 2003, The Messenger, 114, 46
Leibundgut, B., Kasper, M. & Kuntschner, H. 2016, The Messenger, 166, 62
Madrid, J. P. & Macchetto, F. D. 2007, ASPC, 377, 79
Meylan, G., Madrid, J. & Macchetto, F. 2003, STScI Newsletter, 20, no. 2, 1
Sterzik, M. et al. 2015, The Messenger, 162, 2
Trimble, V. 1995, PASP, 107, 977

Links

[1] ESO telescope bibliography telbib: http://telbib.eso.org/
[2] ESO Publication Statistics: http://www.eso.org/sci/libraries/edocs/ESO/ESOstats.pdf

DOI: 10.18727/0722-6691/5033

NEAR: Low-mass Planets in α Cen with VISIR

Markus Kasper[1]
Robin Arsenault[1]
Hans-Ulrich Käufl[1]
Gerd Jakob[1]
Eloy Fuenteseca[1]
Miguel Riquelme[1]
Ralf Siebenmorgen[1]
Michael Sterzik[1]
Gerard Zins[1]
Nancy Ageorges[2]
Sven Gutruf[2]
Arnd Reutlinger[2]
Dirk Kampf[2]
Olivier Absil[3]
Brunella Carlomagno[3]
Olivier Guyon[4,5]
Pete Klupar[6]
Dimitri Mawet[7]
Garreth Ruane[7]
Mikael Karlsson[8]
Eric Pantin[9]
Kjetil Dohlen[10]

[1] ESO
[2] Kampf Telescope Optics, Munich, Germany
[3] Astrophysics Research Institute, Université de Liège, Belgium
[4] Steward Observatory, University of Arizona, Tucson, USA
[5] Subaru Telescope, National Astronomical Observatory of Japan, Hilo, USA
[6] Breakthrough Initiatives, USA
[7] Department of Astronomy, California Institute of Technology, Pasadena, USA
[8] Ångström Laboratory, University Uppsala, Sweden
[9] CEA Saclay, France
[10] Laboratoire d'Astrophysique de Marseille, France

ESO, in collaboration with the Breakthrough Initiatives[1], is working to modify the Very Large Telescope mid-IR imager (VISIR) to greatly enhance its ability to search for potentially habitable planets around both components of the binary Alpha Centauri, part of the closest stellar system to the Earth. Much of the funding for the NEAR (New Earths in the Alpha Cen Region) project is provided by the Breakthrough Initiatives, and ESO mostly provides staff and observing time. The concept combines adaptive optics using the deformable secondary mirror at Unit Telescope 4, a new annular groove phase mask (AGPM) coronagraph optimised for the most sensitive spectral bandpass in the *N*-band, and a novel internal chopper system for noise filtering based on a concept for longer wavelengths invented by the microwave pioneer Robert Dicke. The NEAR experiment is relevant to the mid-infrared METIS instrument on the Extremely Large Telescope, as the knowledge gained and proof of concept will be transferable.

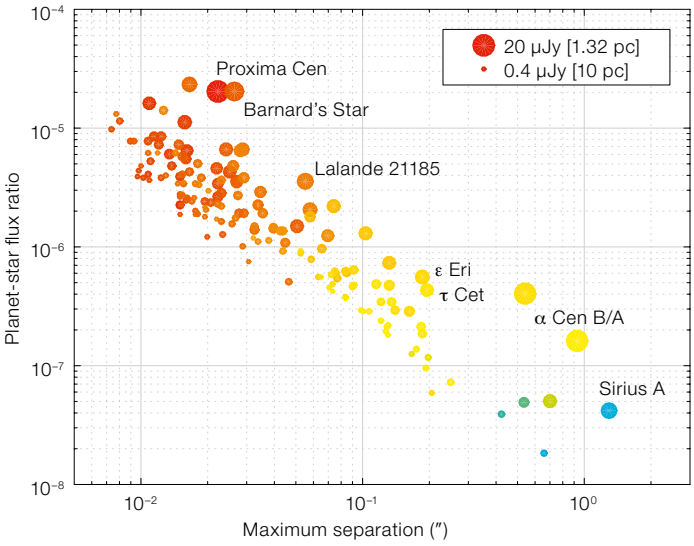

Figure 1. *N*-band flux ratio between Earth-analogue planets and parent stars within 10 pc (from the Hipparcos catalogue). The size of the symbol indicates the planet's apparent brightness, and the colours approximately match those of the stars.

Detecting potentially habitable planets orbiting other stars is a cornerstone of the Extremely Large Telescope (ELT) science case. There are two favourable wavelength regimes for such observations: i) the optical/near-infrared (NIR), where stars emit most of their light and the spectra reflected from planetary atmospheres contain important biosignatures, such as O_2 (transitions in the red and NIR range) and ozone, O_3 (transitions in the ultraviolet); and ii) the *N*-band in the thermal infrared, where the black body emission of potentially habitable planets, i.e., planets with a temperature and an atmospheric pressure suitable to sustain liquid water on the surface, peaks. *N*-band spectral diagnostics are dominated by a very strong O_3 band around 9.6 µm, which is as good a biosignature as O_2.

Earth analogues, that is planets of size and temperature comparable to Earth's, appear at small angular separations from their host star and with very demanding imaging contrasts. Such planets orbit their star in the habitable zone (HZ), which is at about 0.1 au for a red dwarf and around 1 au for a solar-type star, and therefore appear at angular separations between 10 milliarcseconds and 1 arcsecond around stars within 10 pc. The corresponding planet-to-parent-star flux ratio is between 10^{-7} and 10^{-10} in the optical/NIR and between 10^{-5} and 10^{-7} in the *N*-band (Figure 1). The shallower contrasts correspond to the red dwarfs and the more demanding ones to solar-type parent stars.

Such optical/NIR spatial resolution and contrast are not achievable with current 8-metre-class telescopes and will only be achieved with the Giant Segmented Mirror Telescopes (GSMT), such as ESO's ELT. There is, however, a pre-eminent star system in which to search for Earth analogues — α Centauri, which contains the solar-type binary α Cen A and B and the late M star Proxima Cen, around which a likely terrestrial planet has recently been discovered (Anglada-Escudé et al., 2016). At a distance of just 1.35 pc, the α Centauri stars are our nearest neighbours, and Earth-analogue planets there would be significantly brighter than around the next nearest stars (see Figure 1).

As the proximity of α Cen A and B pushes the HZ out to an angular separation from the stars of about one arcsecond, current 8-metre-class telescopes

may already have a chance to reach the required *N*-band spatial resolution, contrast and sensitivity to detect an Earth analogue. The next systems with HZs at sufficient angular separation, Sirius and Procyon, are 15 and 45 times harder to observe, respectively, because the required integration times scale with the inverse of the planet's brightness squared. In addition, both these stars have white dwarf companions in a relatively small (~ 20 au) orbit, which would have negatively impacted on planet habitability during their evolution. Earth analogues in ε Eri, τ Ceti and ε Indi cannot currently be separated from the stars optically and will be observed in the *N*-band with the Mid-infrared ELT Imager and Spectrograph (METIS; Quanz et al., 2015).

Concept

The standard approach for reaching high contrast and sensitivity from the ground uses adaptive optics (AO) and coronagraphy to minimise residual flux from the star and maximise the signal from the planet. The VLT Imager and Spectrometer for mid-InfraRed (VISIR; Lagage et al., 2004), which is currently seeing-limited, will therefore be moved from VLT Unit Telescope 3 (UT3) to UT4, which has recently been upgraded with a Deformable Secondary Mirror (DSM), see Arsenault et al. (2017). Using the DSM at the Cassegrain focus is the most efficient way to equip VISIR with AO because it does not involve additional ambient-temperature mirrors, which are the dominant noise source over large parts of the *N*-band.

At UT3, electrical cables and helium lines between VISIR and its electronics cabinets and compressors located on the azimuth platform are routed through the altitude axis cable wrap. At UT4, the altitude wrap is already rather full and installation of additional cables is arduous. Therefore, NEAR will use a dragging solution, with electrical cables and helium lines being routed through a chain from the primary mirror (M1) cell to the cabinets and compressors on the azimuth platform, as shown in Figure 2. The distances are short enough for the VISIR test cables and helium lines to be used, such that the installation at UT3 can remain untouched.

Most modifications necessary for NEAR are implemented in the non-cryogenic instrument flange of VISIR. This VISIR Flange Module (VFM, see Figure 3) will feature a modified relay for the calibration source, an ESO wavefront sensor (WFS) camera including feed optics, and a vacuum optics unit with the internal chopper. The chopper in this location, behind the dichroic, would not disturb the WFS. The VFM is designed, manufactured and tested by Kampf Telescope Optics, Munich.

The AO WFS is part of the VFM. A dichroic transmits the *N*-band into VISIR and reflects optical light to the WFS unit (WFSU) as shown in Figure 3. The WFSU will provide ±5-arcsecond field selection capability to transmit a 2-arcsecond round field of view (FoV) to the Shack-Hartmann WFS. A spectral long-pass filter allows only wavelengths longer than 800 nm to pass, such that an atmospheric dispersion compensator is not required. The NEAR WFS camera is an ESO standard camera with a 40 × 40 lenslet array. This camera will be connected via a fibre switchboard to the GRound-layer Adaptive optics Assisted by Lasers (GRAAL) real-time computer. Switching between GRAAL and NEAR operation will be done through software configuration only.

A new small electronics rack for the WFS power supply and Peltier controller will be attached to VISIR. Controllers for the other new functions provided by the VFM will be installed in the existing VISIR racks. Fortunately, VISIR currently employs several expendable components, which will be removed in turn such that the NEAR modifications will maintain the weight of the overall instrument.

One of the benefits provided by AO is a corrected point spread function (PSF) with an *N*-band Strehl ratio close to one, which maximises the planet signal. The AO further allows us to control and remove the quasi-static aberrations. These aberrations produce speckle noise in the region around the PSF, where a potential planet would be located, and are the ultimate obstacle to reaching very high imaging contrasts. The minimisation of quasi-static aberrations is helped by the superb optical quality of the dichroic, which is the only optical component in front of the focal plane not seen by the WFS. Optical aberrations in the WFS arm itself will be calibrated with a dedicated light source during integration. Another important task of the AO is to maintain a precise positioning of the PSF on the coronagraphic mask.

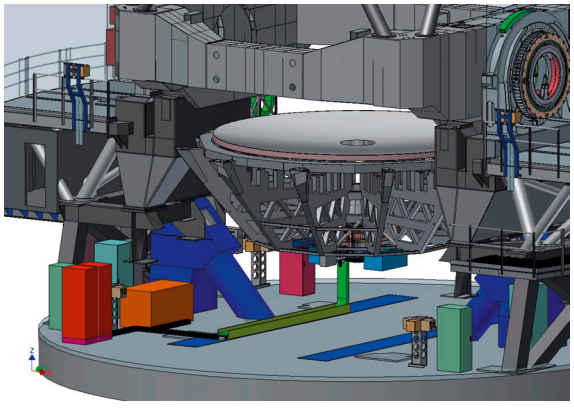

Figure 2. (Left) Cables and He lines routed from the M1 cell though a chain (green) to electronics cabinets (red) and helium compressors (orange). This configuration is very similar to the baseline design accepted at the VISIR Final Design Review in 1999.

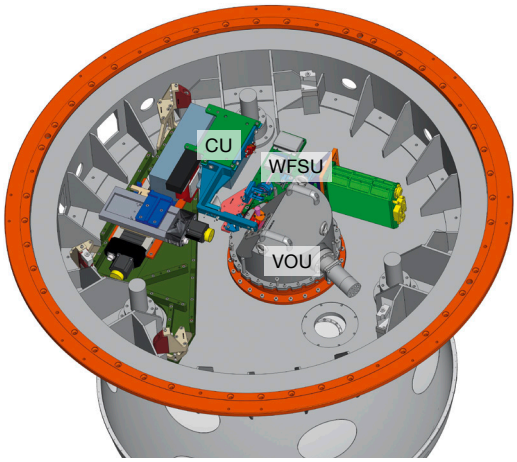

Figure 3. (Right) VISIR Flange Module (VFM) hosting the Wavefront Sensor Unit (WFSU), Vacuum Optics Unit (VOU), and the Calibration Unit (CU). The Dicke switch (see Figure 6) is part of the VOU.

Innovations

A new spectral filter will maximise NEAR's signal-to-noise ratio (SNR) for the detection of an Earth analogue. Figure 4 shows the average Paranal sky background and the expected emission of the telescope with a freshly coated M1. On the one hand, a wide spectral range captures more photons from the object, but on the other hand, even state-of-the art coronagraphs have a limited bandpass, and there are spectral regions which are not favourable for high-SNR observations. At a wavelength shorter than 10 µm, absorption by atmospheric ozone reduces signal transmission and increases sky background. The same happens longward of 12.5 µm because of atmospheric CO_2. The maximum SNR is therefore obtained when observing between 10 and 12.5 µm, where the background is dominated by telescope emission, and sensitivity to atmospheric conditions is reduced.

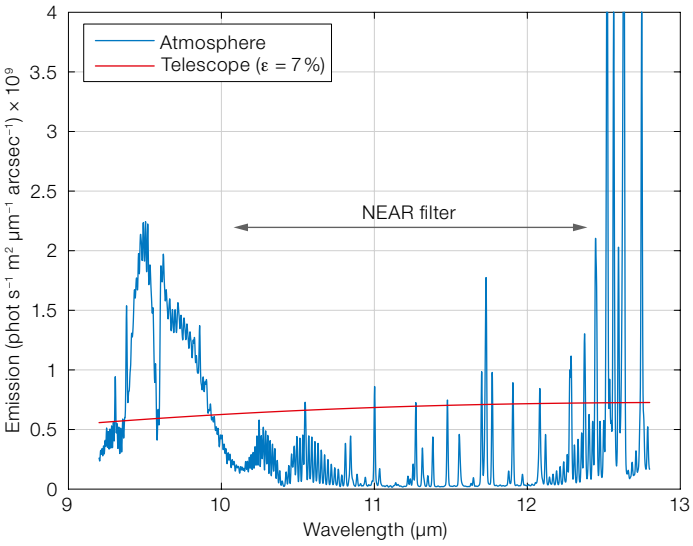

Figure 4. Paranal seasonal average sky background and contribution of the telescope (mirrors at 280 K with a combined emissivity of 7 %) as calculated by the ESO SKYCALC Sky Model Calculator. The spectral band 10–12.5 µm foreseen for the NEAR filter is indicated.

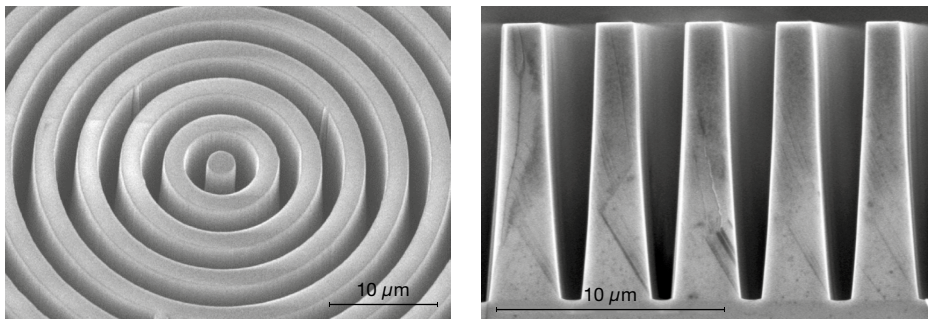

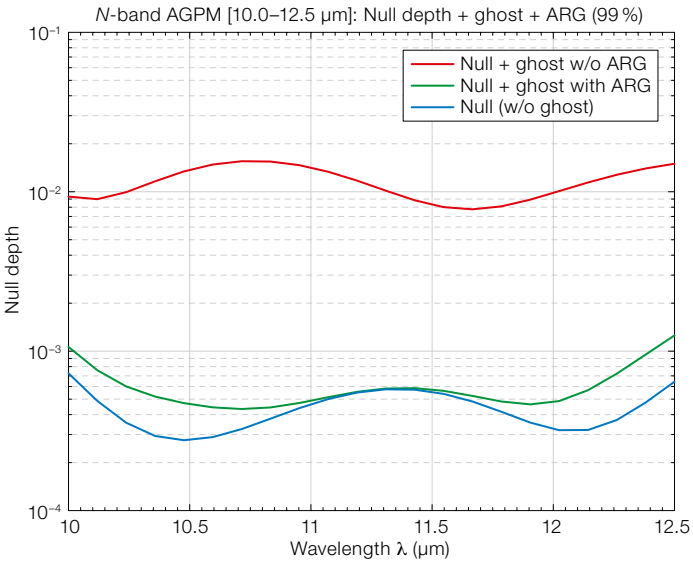

Figure 5. Images and performance of the annular groove phase mask. Microscope pictures of the subwavelength grating are shown above, and the null depth over the NEAR spectral band is shown on the left. See text for more details.

In addition, NEAR will feature a new AGPM (Mawet et al., 2005) coronagraph designed for the NEAR spectral filter. The AGPM is a variation of a vortex coronagraph with very small inner working angle and high throughput. It consists of a rotationally symmetric subwavelength grating (Figure 5) and allows for coronagraphic imaging of close companions and disks around bright stars. The modelled null depth, i.e., the suppression of the PSF's central core, over the NEAR spectral range is shown in Figure 5. The figure also displays the effect of the anti-reflection grating (ARG) on the AGPM's back side, which reduces the intensity of the optical ghost image. Together with a properly designed Lyot stop, the AGPM will provide a raw PSF contrast of the order 10^{-5} at angular separations between 0.7 and 1.5 arcseconds. The NEAR coronagraph will be designed and produced by a team of researchers at the University of Liège, the University of Uppsala and Caltech.

High-SNR observations with VISIR must also consider the excess low frequency noise (ELFN) of the AQARIUS detector. ELFN is temporally correlated noise caused by fluctuations in the space charge, induced by ionisation/recombination in a blocking layer between the pixels. This correlation can be broken by modulating the incidence of light between source and background, i.e., by chopping at sufficiently high speed. ELFN increases rapidly with incident flux levels, and the chopping frequency required to remove it also increases (Ives et al., 2014).

For the expected NEAR flux levels, 10-Hz chopping is needed to effectively sup-

press ELFN. To avoid synchronisation issues and transients with the AO operation, NEAR will employ an internal chopper following the concept of the Dicke switch invented by the microwave pioneer Robert Dicke. A rotating mirror with open areas (in the case of NEAR, a D-shaped mirror with one open section spanning 180 degrees) allows VISIR to alternate between observations of the object and of an internal black body, dynamically adjusted to match sky and background flux (Figure 6).

An efficient alternative to observations with the Dicke switch could be on-sky chopping with the DSM. By chopping between α Cen A and B, one could double the duty cycle of the observations as both stars of the binary are scientifically interesting. The separation between α Cen A and B will be about 5 arcseconds in 2019, which is still in the range for the DSM to efficiently chop with high speed and a transition time of the order of 10 ms. The DSM chopping option will be tested with GRAAL before NEAR goes on-sky.

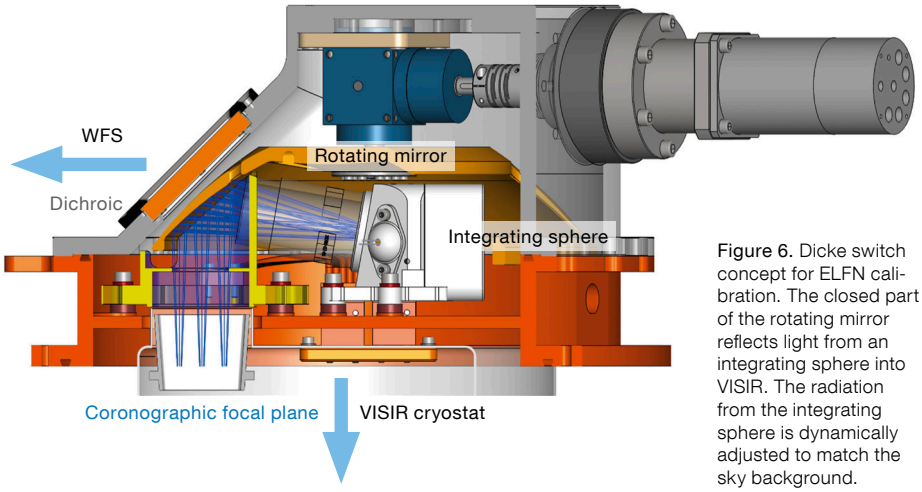

Figure 6. Dicke switch concept for ELFN calibration. The closed part of the rotating mirror reflects light from an integrating sphere into VISIR. The radiation from the integrating sphere is dynamically adjusted to match the sky background.

Performance

Data from an ongoing VISIR programme (098.C-0050, Principal Investigator M. Sterzik) was used to measure the actual point source sensitivity and estimate the expected background-limited imaging performance (BLIP) of NEAR. The data consist of nine one-hour observations of Sirius recorded between December 2016 and March 2017 in the B10.7 filter with 4-Hz chopping. Figure 7 shows the only image of α Cen recorded under the same programme.

We measured the total flux of Sirius and used it to scale the VLT's Airy pattern. This is a reasonable assumption given the nearly perfect AO-corrected PSF in the *N*-band. The background noise per pixel was also measured. The resulting SNR was derived for different photometric aperture diameters. An aperture of 1.25 λ/D diameter containing 60 % of the total flux spread over 50 pixels (the VISIR pixel scale is 45 milliarcseconds per pixel) is optimum and provides an average BLIP sensitivity of 1.1 mJy (5 σ in 1 hr). Scaling the SNR of the classical VISIR data to the new NEAR configuration considering the various changes in the setup (spectral filter, AGPM, Lyot stop, AO correction, dichroic, etc) yields the expected NEAR BLIP sensitivity of 0.7 mJy (5 σ in 1 hr).

We also investigated whether multiple observations would beat down the noise as the inverse of integration time. Pixel intensities over an empty part of the detector were analysed and combined for all the data sets. The analysis shows that the noise is indeed spatially and temporally uncorrelated (the noise covariance matrix between the nine data sets is diagonal), and noise statistics scale with integration time as expected. Therefore, we expect a final sensitivity of the 100-hr NEAR campaign of 70 μJy, which is sufficient to detect a 1.9-Earth-radii planet with an Earth-like emission spectrum or a 1.3-Earth-radii desert planet emitting like a 325 K black body.

Figure 7. Classical VISIR image of α Cen A/B recorded in March 2017 (data obtained through programme 098.C-0050).

Schedule

The NEAR experiment was launched in mid-2016 by ESO and the Breakthrough Initiatives, and it is hosted within ESO's Technology Development Programme. Several reviews (Phase A of the concept, interface and manufacturing readiness of the VFM, and for the overall system) have been carried out since then to mitigate risks involved with the fast track on which NEAR is proceeding.

The next major step will be the delivery of the VFM to ESO early in 2018, where it will be tested with the infrared test facility. In parallel, the components for the cryostat (AGPM, NEAR filter, Lyot stop) will be procured. We also plan for a technical run with GRAAL at UT4 to implement DSM chopping and verify whether it is a viable alternative for the NEAR experiment.

The VFM and all other NEAR components will be shipped to Paranal Observatory in late 2018. VISIR will then be transferred from UT3 to the new integration hall for the modifications, and the infrastructure at UT4 will be prepared. After the integration work, a commissioning run at UT4 will establish the proper functioning of NEAR. During commission-

ing, SINFONI (the Spectrograph for Integral Field Observations in the Near-Infrared) will temporarily be taken off the telescope. The NEAR observing campaign will start around June 2019 once SINFONI has completed observations of the Galactic Centre and is shipped to Europe for integration with the new ERIS instrument.

After the campaign, VISIR will eventually move back to UT3. The WFS camera will be removed, but the modifications of the VFM will remain. Also, the 45-degree dichroic will be exchanged with a 90-degree entrance window providing full access to the *N*- and *Q*-bands. The Dicke switch may prove highly advantageous when observing extended objects, which presently are difficult to observe because of the limited chopper throw.

Observing campaign

The NEAR observing campaign comprises 100 hours of telescope time. The observations of α Cen will be carried out by the NEAR team who will operate the instrument and will use consecutive nights as far as possible. Ideally, the campaign would be concluded within about 20 days, similar to the timespan during which a planet in α Cen at one au from a star would move on its orbit by one diffraction element (~ 0.3 arcseconds at the VLT in *N*-band) on the sky.

The NEAR campaign foresees observations with 10-Hz chopping (ideally chopping between α Cen A and B or alternatively using the internal chopper) and around 4 ms detector integration time (DIT) for a reduced 450 × 450 pixel FoV. The short DITs provide a high observing efficiency for the 10-Hz chopping frequencies needed to reach BLIP performance in the presence of ELFN. The instrument entrance pupil will be stabilised by switching off the Cassegrain rotator and letting the field rotate. This will provide a better performance of the coronagraph, and angular differential imaging techniques can be used to calibrate quasi-static residual speckle noise.

The NEAR observations are otherwise standard with no special needs for day-time calibration or data reduction. One frame per chopping half-cycle will be stored, so 450 × 450 pixel frames will arrive every 50 ms and result in a data rate of 8.1 Mb s^{-1} or 30 Gb hr^{-1}. Assuming an average of six observing hours per night, where α Cen is sufficiently high in the sky, NEAR will produce about 180 Gb of data each night. The Breakthrough Initiatives plan to make these NEAR data publicly available immediately in order to benefit from the expertise of interested astronomers world-wide and to foster excitement for the search for potentially habitable planets around the nearest stars.

References

Anglada-Escudé, G. et al. 2016, Nature, 536, 437
Arsenault, R. et al. 2017, The Messenger, 168, 8
Ives, D. et al. 2014, Proc. SPIE, 9154, 91541J
Lagage, P. O. et al. 2004, The Messenger, 117, 12
Mawet, D. et al. 2005, ApJ, 633, 1191
Quanz, S. et al. 2015, IJAsB, 14, 279

Links

[1] Breakthrough Initiatives: http://breakthroughinitiatives.org

The VLT spectrometer and imager for the mid-infrared (VISIR) mounted at the Cassegrain focus of UT3.

DOI: 10.18727/0722-6691/5034

Near-InfraRed Planet Searcher to Join HARPS on the ESO 3.6-metre Telescope

François Bouchy[1]
René Doyon[2,3]
Étienne Artigau[2,3]
Claudio Melo[4]
Olivier Hernandez[2,3]
François Wildi[1]
Xavier Delfosse[5]
Christophe Lovis[1]
Pedro Figueira[6]
Bruno L. Canto Martins[7]
Jonay I. González Hernández[8]
Simon Thibault[9]
Vladimir Reshetov[10]
Francesco Pepe[1]
Nuno C. Santos[6,11]
José Renan de Medeiros[7]
Rafael Rebolo[8]
Manuel Abreu[12,13]
Vardan Z. Adibekyan[6]
Timothy Bandy[14]
Willy Benz[14]
Nicolas Blind[1]
David Bohlender[10]
Isabelle Boisse[15]
Sébastien Bovay[1]
Christopher Broeg[14]
Denis Brousseau[9]
Alexandre Cabral[12,13]
Bruno Chazelas[1]
Ryan Cloutier[2,16,17]
João Coelho[12,13]
Uriel Conod[1]
Andrew Cumming[2,18]
Bernard Delabre[4]
Ludovic Genolet[1]
Janis Hagelberg[5]
Ray Jayawardhana[19]
Hans-Ulrich Käufl[4]
David Lafrenière[2,3]
Izan de Castro Leão[7]
Lison Malo[2,3]
Allan de Medeiros Martins[7]
Jaymie M. Matthews[20]
Stanimir Metchev[21]
Mahmoudreza Oshagh[6]
Mathieu Ouellet[2,3]
Vanderlei C. Parro[22]
José Luis Rasilla Piñeiro[8]
Pedro Santos[12,13]
Mirsad Sarajlic[14]
Alex Segovia[1]
Michael Sordet[1]
Stéphane Udry[1]
Diana Valencia[16,17]
Philippe Vallée[2,3]
Kim Venn[23]
Gregg A. Wade[24]
Les Saddlemyer[10]

[1] Observatoire Astronomique de l'Université de Genève, Switzerland
[2] Institut de Recherche sur les Exoplanètes (IREx), Université de, Montréal, Canada
[3] Observatoire du Mont-Mégantic, Département de Physique, Université de Montréal, Canada
[4] ESO
[5] Institut de Planétologie et d'Astrophysique de Grenoble (IPAG), Univ. Grenoble Alpes, CNRS, IPAG, France
[6] Instituto de Astrofísica e Ciências do Espaço (IA), Universidade do Porto, CAUP, Portugal
[7] Departamento de Física, Universidade Federal do Rio Grande do Norte (UFRN), Brazil
[8] Instituto de Astrofísica de Canarias (IAC), Spain
[9] Département de physique, de génie physique et d'optique, Université Laval, Canada
[10] National Research Council Canada, Herzberg Institute of Astrophysics, Canada
[11] Departamento de Física e Astronomia, Faculdade de Ciências, Universidade do Porto, Portugal
[12] Laboratório de Óptica, Laser e Sistemas da Faculdade de Ciências da Universidade de Lisboa, Portugal
[13] Instituto de Astrofísica e Ciências do Espaço (IA), Universidade de Lisboa, Portugal
[14] Centre for Space and Habitability, University of Bern, Switzerland
[15] Aix Marseille Université, CNRS, Laboratoire d'Astrophysique de Marseille (LAM) UMR 7326, France
[16] Centre for Planetary Sciences, Department of Physical and Environmental Sciences, University of Toronto Scarborough, Canada
[17] Department of Astronomy & Astrophysics, University of Toronto, Canada
[18] Department of Physics & McGill Space Institute, McGill University, Canada
[19] Department of Physics & Astronomy, York University, Canada
[20] Department of Physics and Astronomy, University of British Columbia, Vancouver, Canada
[21] The University of Western Ontario, Department of Physics and Astronomy, London, Canada
[22] Instituto Mauá de Tecnologia, Praça Mauá, Brazil
[23] Department of Physics and Astronomy, University of Victoria, Canada
[24] Department of Physics, Royal Military College of Canada, Kingston, Canada

The Near-InfraRed Planet Searcher (NIRPS) is a new ultra-stable infrared (*YJH*) spectrograph that will be installed on ESO's 3.6-metre Telescope in La Silla, Chile. Aiming to achieve a precision of 1 m s^{-1}, NIRPS is designed to find rocky planets orbiting M dwarfs, and will operate together with the High Accuracy Radial velocity Planet Searcher (HARPS), also on the 3.6-metre Telescope. In this article we describe the NIRPS science cases and present its main technical characteristics.

In the past two decades, the study of exoplanets has matured from a largely speculative endeavour to the forefront of astronomy. It has moved from the discovery of a handful of massive, close-in giants, called hot Jupiters, to uncovering various populations of planets unlike anything known in our own Solar System (Mayor et al., 2014). Great strides have been made in our understanding of exoplanets, but one notable goal remains to be achieved: the characterisation of terrestrial planets in the temperate zone around a star. While the study of such planets around Sun-like stars is exceedingly challenging with existing facilities, the diminutive red dwarfs offer a significant observational shortcut; their smaller radii, lower temperatures, lower masses and the relatively short orbital periods of planets in their temperate zones make them much easier targets for this type of study.

In response to an ESO call for new instruments for the New Technology Telescope (NTT), the NIRPS consortium proposed a dedicated near-infrared spectrograph to undertake an ambitious survey of planetary systems around M dwarfs. This would nicely complement the surveys that have been running for a decade on HARPS by enlarging the sample of M dwarfs that can be observed, while providing better stellar activity filtering. After the selection of the SOXS[1] (Son Of X-Shooter) spectrograph for the NTT, it was clear that the exoplanet community in the Member States needed another

facility to maintain the leadership built over the last decade thanks, to a large extent, to HARPS. Therefore in May 2015, ESO invited the NIRPS team to adapt the original NIRPS design to the Cassegrain focus of the ESO 3.6-metre Telescope in La Silla for simultaneous observation with the HARPS spectrograph.

In order to be in phase with future space missions such as the Transiting Exoplanet Survey Satellite (TESS), the CHaracterising ExOPlanets Satellite (CHEOPS), the James Webb Space Telescope (JWST) and the PLAnetary Transits and Oscillations of stars (PLATO), NIRPS is being developed on a fast track, its first light is scheduled for the last quarter of 2019. As of mid-2017 the design of the instrument has been finalised and construction has started.

La Silla Paranal Observatory: a hub for extrasolar planet research

Our knowledge of the frequency of planets, the architecture of planetary systems and their nature (mass, size, bulk composition, atmosphere) has been revolutionised in the last two decades thanks to various detection techniques providing complementary measurements. Observational efforts were undertaken with ground- and space-based facilities, notably radial velocity (RV) surveys using high-precision spectrographs and transit surveys from space satellites (Convection, Rotation et Transits planétaires, CoRoT, and Kepler) and from ground-based projects (for example, the Wide Angle Search for Planets, WASP, and the Hungarian Automated Telescope system, HAT). The forthcoming space armada, initiated by the launch of JWST, TESS and CHEOPS in 2018, and PLATO in 2026, will only spark a new revolution in the field of extrasolar planets if it is complemented by efficient ground-based facilities. The La Silla Paranal Observatory has a key role to play as it already hosts prime ground-based planet-finding facilities. These instruments predominantly approach exoplanet study through radial velocity measurements (using, for example, the High Accuracy Radial velocity Planet Searcher, HARPS, CORALIE and the forthcoming Echelle SPectrograph for Rocky Exoplanet and Stable Spectroscopic Observations, ESPRESSO), through detecting and monitoring transits (for example, the Next-Generation Transit Survey, NGTS), and through high-contrast imaging (using the Spectro-Polarimetric High-contrast Exoplanet REsearch instrument, SPHERE, and the planned Planetary Camera and Spectrograph on ESO's Extemely Large Telescope, ELT). NIRPS will enable complementary precise RV measurements in the near-infrared with a precision of 1 m s^{-1}, specifically targeting the detection of low-mass planets around the coolest stars. The NIRPS survey will provide an in-depth monitoring of all southern nearby M dwarfs, complementing large-scale surveys that probe > 1000 M dwarfs for giant planets and brown dwarf companions, such as the Apache Point Observatory Galaxy Evolution Experiment (APOGEE; Deshpande et al., 2013).

M dwarfs: a shortcut to habitability and life

The detection of life beyond Earth is arguably still a few decades away, and will require substantial further technical developments. Regardless of how distant the detection of signs of life might be, the roadmap leading to it has already been traced and consists of well-defined sequential steps:

- Finding transiting or directly imageable planets in the habitable zone of cool stars using ground- and space-based surveys and characterising their orbits, masses, density and bulk composition;
- Characterising planetary atmospheres from space (or from the ground in the most favourable cases);
- Seeking chemical imbalances as tracers of potential biosignatures.

While the detection of an Earth analogue around a Sun-like star requires a precision of better than 10 cm s^{-1}, M dwarfs offer a more accessible and attractive means of achieving the above goals. The amplitude of the RV signal scales with $m^{-2/3}$, where m is the stellar mass. In addition, thanks to their much lower luminosity, the habitable zone of M dwarfs is typically 10 times closer than in the case of Sun-like stars. These combined effects imply that for a star of spectral type mid-M with an Earth-mass planet receiving an Earth-like insolation (i.e., the amount of energy per area per time at this orbital separation, amounting to about 1360 W m^{-2} for the Earth), this RV signal is on the order of 1 m s^{-1} and therefore detectable with state-of-the-art RV spectrographs. As M dwarfs are cool and emit most of their flux in the near-infrared, one ideally needs to obtain RV measurements in this domain to reach the highest possible precision. Furthermore, for a fixed planetary radius, the depth of a planetary transit scales with r^{-2} (where r is the stellar radius), making transit follow-ups of Earth-sized planets around low-mass stars significantly easier.

Although HARPS was optimised to obtain high precision radial velocity measurements for Sun-like G and K dwarfs, a large fraction of HARPS nights over the last decade were allocated to monitor M dwarfs. Following the discovery of a Neptune-like planet around the M3V star Gl581 (Bonfils et al., 2005) more than a decade ago, a large number of planets were uncovered around M dwarfs despite the fact that these stars are particularly faint at optical wavelengths (Astudillo-Defru et al., 2017). Significant discoveries include the first planets orbiting in an M dwarf habitable zone (Gl667Cc; Delfosset al., 2013) and an Earth-mass planet around our nearest celestial neighbour, Proxima Centauri (Anglada-Escudé et al., 2016). In combination with photometric surveys, HARPS played a key role in discovering and characterising transiting planets around M dwarfs, paving the way towards their atmospheric characterisation (Charbonneau et al, 2009; Almenara et al., 2015; Berta-Thompson et al., 2015; Ditmann et al., 2017).

Several studies produced initial estimates of the fraction of M dwarfs hosting Earth-like planets inside the habitable zone. Results based on transits (Dressing & Charbonneau, 2015) and radial velocity measurements from HARPS (Bonfils et al., 2013) all suggest that Earth-sized planets are abundant around M dwarfs, at least 40 % of these stars having such a planet in their habitable zone. Such a high rate is encouraging and provides a strong argument for shifting the attention of exoplanet searches to M dwarfs, which in turn requires a shift towards the near-infrared.

NIRPS main science cases

NIRPS has been designed to explore the exciting prospects offered by the M dwarfs, focusing on three main science cases.

Mass and density measurements of transiting Earths around M dwarfs

Thousands of planets transiting nearby M dwarfs are expected to be found in the coming years, with TESS (Ricket et al., 2014) and PLATO (Rauer et al., 2014), likely to be the main sources of transit candidates. Ground-based surveys such as ExTrA (Exoplanets in Transits and their Atmospheres), TRAPPIST (the TRAnsiting Planets and PlanetesImals Small Telescope), as well as NGTS and SPECULOOS (Search for habitable Planets EClipsing ULtra-cOOl Stars) at the La Silla Paranal Observatory, and MEarth in the USA (Berta et al., 2013) will provide a continuous supply of additional targets.

Given the high fraction of M dwarfs hosting Earth-like planets inside the habitable zone, it is expected that the yield of transiting habitable planets among the M dwarfs will be correspondingly high. Those planets will be the subject of intensive follow-up with RV and photometric observations, and will be the primary targets for atmospheric studies with the JWST. A robust interpretation of the JWST data will ultimately require a constraint on the bulk density of the planet. The planetary radius — from the transit depth — and a mass estimate are required, and these can only be obtained from near-infrared RV data or, in very specific cases, transit-timing variations (TTV). NIRPS is an ideal tool to target M dwarfs, being able to provide masses for a large number of transiting planets and therefore to disentangle transiting planets from diluted background eclipsing binaries. Figure 1 illustrates the parameter space allowed by NIRPS in comparison to state-of-the-art optical spectrographs; considering that most host stars will be M dwarfs, NIRPS will enable the measurement of a large number of masses of super-Earths in their habitable zones.

Preparing for the 2030's: an RV search for planets to image with the ELT

M dwarfs are the preferred targets for direct imaging studies to be carried out with future extreme adaptive optics imagers on the ELT-class telescopes (Snellen et al., 2015). NIRPS will monitor a sample of the closest ~ 100 southern M dwarfs with the goal of finding the closest habitable worlds to the Sun (Figures 2 and 3). As these planets are most likely members of multi-planetary systems, this survey requires a relatively large number of visits per star (100 to 200), as demonstrated by the HARPS experience. Although such a programme can be performed by NIRPS alone, simultaneous HARPS observations will increase the overall efficiency of the telescope, as that will improve the photon noise budget by 15–40 %, depending on the effective temperature of the host star.

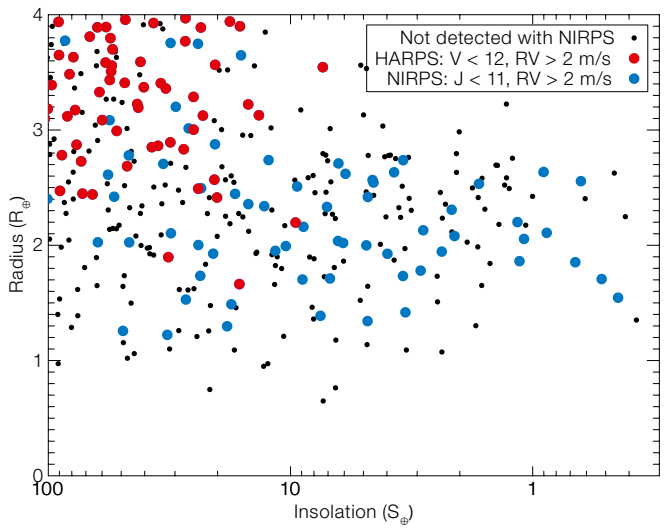

Figure 1. Simulated TESS sample of southern (declination < 20°) planets in an insolation versus radius diagram. Planets amenable to HARPS follow-up are shown in red while those, much more numerous, amenable to NIRPS follow-up are shown in blue. NIRPS will allow the follow-up of numerous planets that are only slightly larger than Earth (1–2.5 $R_\oplus$) and that receive a comparable insolation (0.3–10 $S_\oplus$). Radius, insolation and photometric values are drawn from the simulated set (Sullivan et al., 2015). These planets will be the prime targets for atmospheric characterisation studies with the JWST.

Moreover, the simultaneous use of NIRPS and HARPS will help to disentangle planetary signals from pure stellar jitter; stellar activity shows chromatic dependence whereas the planetary signal, due to the planet's gravitational pull, is known to be achromatic (Figueira et al., 2010). This will enhance the scientific output by filtering out false positives efficiently. Gaia astrometry and direct imaging will complement such studies by detecting planets on wide orbits (> 1000 days).

Atmospheric characterisation of exoplanets

Transiting planets offer a unique opportunity to gather information about the composition and temperature of their atmospheres, as well as the presence of molecular species, including biosignature gases or surface atmospheric features. High-resolution transmission spectroscopy allows the wavelength shift of individual narrow spectral features in the atmosphere to be tracked as the planet orbits the star. As an example, in HARPS observations of the hot Jupiter HD 189733 (Woolf & Wallerstein, 2005) the Na doublet was spectrally resolved, allowing its line contrasts to be measured and the temperature to be derived at two different altitudes.

Thanks to its large spectral coverage, several spectroscopic features are present within the wavelength range of NIRPS, such as CO, CO_2, CH_4, H_2O in the *H*-band, and also Na, H_2O in the visible domain. This plethora of molecules makes NIRPS very competitive in characterising the atmospheres of hot Jupiters and hot Neptunes. In addition, by measuring the spectroscopic transit, the projected spin-orbit alignment can be measured using the Rossiter-McLaughlin effect, providing an important parameter linked to the formation and dynamic evolution of the system. The spin-orbit alignment has never been measured for small planets orbiting M dwarfs and would provide new insights into the dynamical histories of these planets.

Other science cases covered by NIRPS

While exoplanet detection and characterisation will take the lion's share of NIRPS observing time, a number of other significant science niches are foreseen for the instrument. NIRPS is expected to

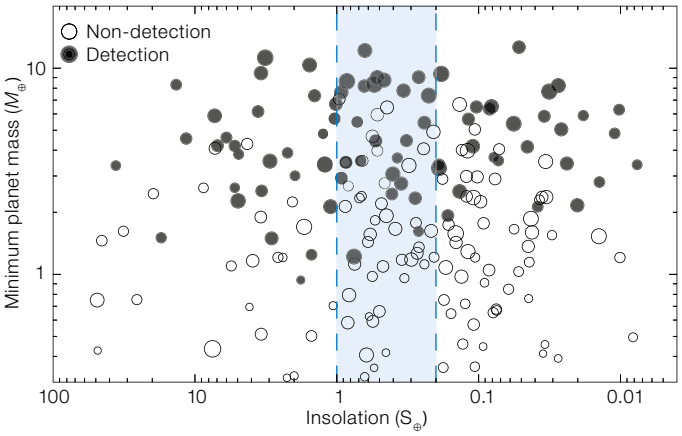

Figure 2. Simulated NIRPS planet survey results in the insolation/minimum planet mass plane. With the predicted NIRPS performances and realistic stellar properties we recovered 79 planets around 100 stars in 150 to 200 visits per star. The detection framework is described in Cloutier et al. (2017). The size of each marker is proportional to the planet's radius. The approximate "maximum greenhouse" and "water-loss" limits of the habitable zone are highlighted in blue ($0.2 \leq S/S_\oplus \leq 1$); (Kopparapu et al., 2013).

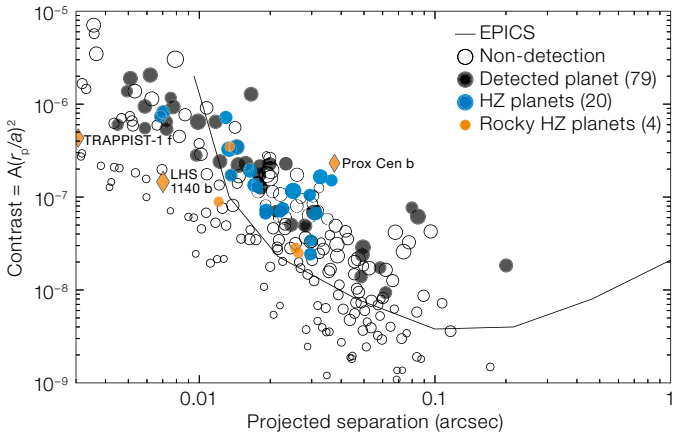

Figure 3. The same simulated NIRPS planet population as shown in Figure 2 in the projected separation/contrast plane. The contrast in reflected light depends on the planet radius (r_p), separation (a) and geometric albedo (A; we have assumed a value of A = 0.3 for all planets). Shaded circles represent planets that would be detected with NIRPS; detected habitable-zone planets are highlighted in blue and detected rocky ($r_p < 1.5\ R_\oplus$) habitable-zone planets are highlighted in red. The planet population is compared to the contrast curve expected to be achieved by the third generation of near-infrared imagers (using the ELT). Orange diamonds show the estimated location of nearby habitable-zone planets around M dwarfs (Anglada-Escudé et al., 2016; Gillon et al., 2016; Dittmann et al., 2017).

contribute to dynamical studies of ultracool dwarfs in young moving groups, enabling RV measurements well into the sub-stellar regime all the way to the deuterium-burning limit. These require kilometre per second accuracy at near-infrared wavelengths. The exquisite line spread function stability required for exoplanet detection will permit stellar variability studies that attempt to measure minute variations in line profiles, such as Doppler imaging of ultracool stars and brown dwarfs.

Simultaneous observations with HARPS and NIRPS will allow a better calibration of stellar activity during RV monitoring of Sun-like stars. Nearby G and K stars are bright enough to allow metre per second-precision measurements in either the optical or near-infrared.

Near-infrared wavelengths are best suited to observations of cool, red M dwarfs, not only because their spectral energy distribution makes them more than an order of magnitude brighter in the NIR than in the visible, but also because near-infrared stellar spectra are significantly less blended than their visible counterparts. This factor is critical in allowing for a more precise line-by-line analysis (Önehag et al., 2012; Wyttenbach et al., 2015) and motivates the expansion of spectroscopic analysis to the near-infrared. The derivation of precise stellar parameters will allow us to move one step further, and obtain precise chemical abundances for key elements (such as alpha and iron-peak elements) in M dwarfs, opening up new avenues for research, such as the chemical evolution of the Galaxy as monitored by its most populous inhabitants.

Specifications, overall design and expected performance

To achieve its science goals, NIRPS must meet a suite of top-level requirements. The spectrograph will operate in the *Y*-, *J*- and *H*-bands with continuous coverage from 0.98 to 1.8 mm. It will ensure high radial velocity precision and high spectral fidelity corresponding to 1 m s^{-1} in less than 30 min for an M3 star with $H = 9$. Its spectral resolution will be 100 000 to best exploit the spectral content. It will be operated simultaneously with HARPS without degrading the HARPS performance. First light is planned for 2019, considering the timeline for space missions such as JWST and TESS.

An adaptive optics fibre-fed spectrograph

NIRPS is part of a new generation of adaptive optics (AO) fibre-fed spectrographs. Its originality resides in the use of a multi-mode fibre that is much less affected by AO correction residuals than a single-mode fibre, while allowing comparatively higher coupling efficiency in degraded seeing and on fainter targets, with relaxed AO specifications.

NIRPS will mainly use a 0.4-arcsecond fibre, half that required for a seeing-limited instrument, allowing a spectrograph design that is half as big as that of HARPS, while meeting the requirements for high throughput and high spectral resolution.

The AO system is designed around a 14 × 14 Shack-Hartmann wavefront sensor (WFS) operating between 700 and 950 nanometres, coupled to a 15 × 15 deformable mirror with a loop frequency of 250 to 1000 Hz. The high density of actuators and the high speed are necessary to correct for high-order wavefront errors and to reach a high coupling efficiency. The AO will lead to a 50 % efficiency for targets as faint as $I = 12$ in median seeing conditions (Woolf & Wallerstein, 2005). A 0.9-arcsecond fibre will be used for fainter targets and degraded seeing conditions. Figure 4 shows the expected overall throughput of NIRPS in the two modes, the High Accu-

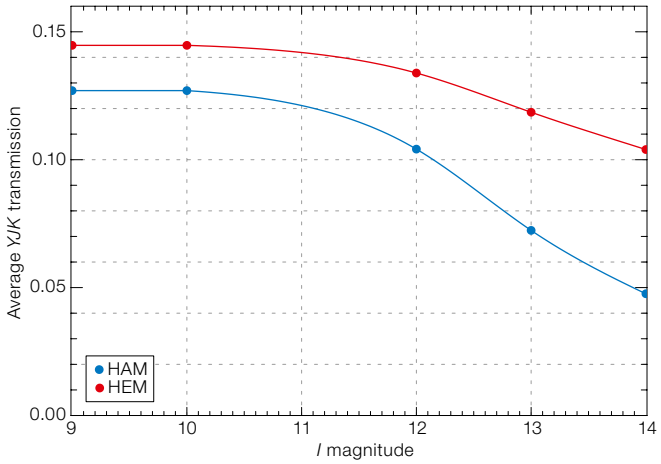

Figure 4. Expected overall throughputs of the NIRPS instrument, including atmosphere and telescope, with AO system as a function of *I*-band magnitude for a median seeing of 0.9 arcseconds for the HAM (0.4-arcsecond fibre) and HEM (0.9-arcsecond fibre) modes.

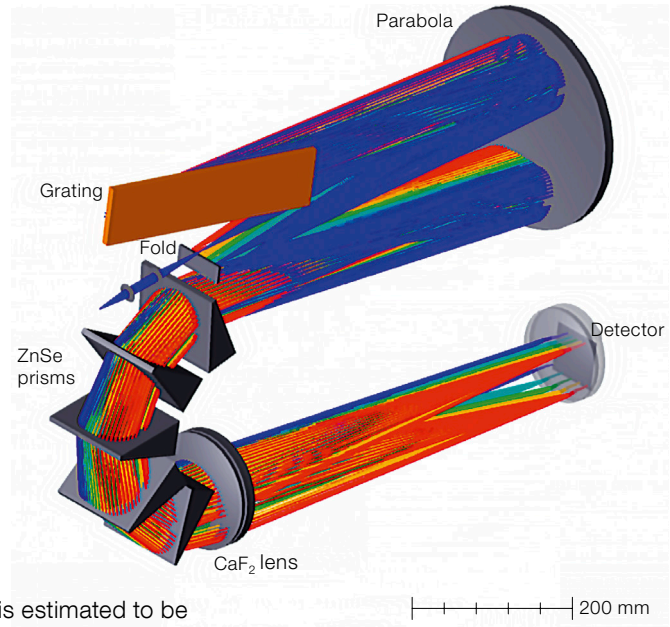

Figure 5. NIRPS optical design layout. The small fibre size enables a much more compact design than other seeing-limited spectrographs with similar resolving power on 4–8-metre telescopes.

racy Mode (HAM) and the High Efficiency Mode (HEM).

While a smaller fibre increases modal noise, NIRPS will use the many degrees of freedom offered by its AO system to properly scramble the stellar flux at the fibre's entrance. This will be used in conjunction with three more scrambling methods: octagonal fibres; a fibre stretcher that modulates the phase between modes; and a double scrambler that exchanges the near and far fields.

A compact cryogenic echelle spectrograph

The entire optical design is oriented to maximise high spectral resolution, long-term spectral stability and overall throughput (Figure 5). Light exiting from both object and calibration fibre links is collimated by a parabolic mirror used in triple pass and is relayed to an R4 echelle grating. The diffracted collimated beam is focused by the parabola on a flat mirror that folds the beam back to the parabola. The cross dispersion is done with a series of five refractive ZnSe prisms that rotate the beam by 180°. A four-lens refractive camera focuses the beam on an a Hawaii 4RG 4096 × 4096 infrared detector. The instrument covers the 0.97 to 1.81 µm domain on 69 spectral orders with a 1 km s^{-1} pixel sampling at a resolution ($\lambda/\Delta\lambda$) of 100 000 (HAM) or 75 000 (HEM). The global throughput of the spectrograph alone is estimated to be 30 % at 0.97 µm and 45 % at 1.81 µm. The spectrograph is installed inside a cylindrical cryostat (1.12-metre diameter, 3.37 metres long) maintained at an operating temperature of 80 K with a stability of 1 mK and an operating pressure of 10^{-5} mbar (Figure 6). The instrument will be installed in the East Coudé Room of the 3.6-metre Telescope.

While some near-infrared radial-velocity instruments have opted to cover the *K*-band (2.0–2.38 µm), the decision was taken not to do so for NIRPS, favouring higher spectral resolution and simplicity. We nevertheless preserved the possibility of adding, at a later time, a *K*-band spectrograph in a separate cryostat. The common path of the NIRPS front-end, including the atmospheric dispersion corrector (ADC), covers the *K*-band.

Two main observing modes combined with HARPS

The HARPS and NIRPS spectrographs can be operated individually or jointly. The default operation mode will see both instruments operating simultaneously, except for high-fidelity polarimetric observations with HARPSpol. NIRPS and HARPS are fed by different fibre links permanently mounted at the Cassegrain focus; each instrument will have two different modes, HEM and HAM. For NIRPS, the HAM and the HEM use 0.4 and 0.9 arcsecond-fibres respectively, leading to spectral resolutions of R = 100 000 and 75 000. The HEM uses a pupil slicer inserted in the double scrambler. Users can switch between modes at any time during the night, and the mode used in one spectrograph does not constrain the mode used in the other spectrograph. Each mode is composed of two fibres, a science channel fed by the stellar beam and a simultaneous calibration channel fed by the background sky light or by a calibration lamp (Hollow-Cathode lamp, Fabry-Pérot, or Laser Frequency Comb). In principle, all the different configurations will be available and are technically possible for HARPS and NIRPS. The new front end shown in Figure 7 includes all the opto-mechanical devices:

1) The VIS/NIR dichroic movable beam splitter to enable HARPS-only and HARPSpol observations.
2) The ADC covering the 700–2400 nm domain.
3) The deformable mirror of the AO system mounted on the tip-tilt plate to compensate for any misalignment with HARPS.
4) The calibration sources injection for both AO wavefront sensor and NIRPS spectrograph.
5) The fibre selector allowing selection between the two modes, HAM and HEM.

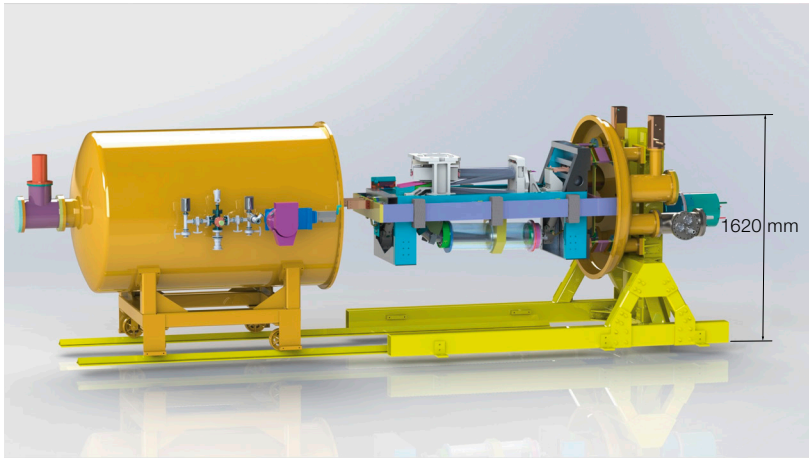

Figure 6. NIRPS optical bench and cryostat design layout.

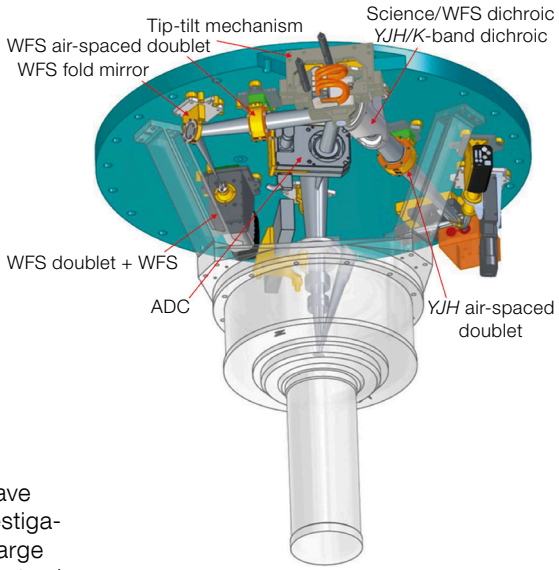

Figure 7. The NIRPS Front End to be installed on the 3.6-metre Telescope focus. The bottom grey part is the existing HARPS Cassegrain fibre adapter.

6) A magnification selector to change the magnification or field of view of the near-infrared acquisition camera.

Operations

In return for the manpower effort and financial contributions of the consortium to design, build, maintain and operate NIRPS for five years, ESO will grant the consortium a period of Guaranteed Time Observation (GTO) on the 3.6-metre Telescope using the combined NIRPS/HARPS instrument. GTO will amount to up to 40 % of the 3.6-metre Telescope time over this period, leaving ample time for community-driven science topics. The GTO will only target M dwarf exoplanet science, leaving room for a broad range of projects in other fields and from other groups.

Once NIRPS is operational in late-2019, the consortium will be in charge of the Science Operations of the 3.6-metre Telescope on behalf of the entire community. This will include the coordination of observations, quality control of the data collected with HARPS and NIRPS and delivery of the reduced data to the ESO archive. The so-called Phase 1, which includes, along with the Call for Proposals, the evaluation and scheduling of the selected projects, is fully organised by ESO.

Since 2009, a substantial fraction of the 3.6-metre Telescope observing runs (about 100 nights per semester) have been coordinated by principal investigators involved in different HARPS Large Programmes in the field of exoplanet science. Scheduled nights and observers are pooled together to optimise the observing sampling — critical to RV monitoring — and to guarantee the presence of competent observers on the mountain, ultimately reducing travel costs. Such coordination is paramount to maximising the science output and the operational efficiency, benefiting a large number of users.

It is foreseen that HARPS+NIRPS open-time programmes will require similar organisation in order to produce the highest scientific return from the 3.6-metre Telescope, optimising the use of available time while continuously adapting the observing queue to external, often unpredictable, observing conditions. Such coordination will be also very important in the context of the community organisation for the follow-up of incoming space missions.

Many of the impressive results obtained with HARPS have been achieved thanks to the intrinsic stability of the hardware. However, its advanced Data Reduction Software (DRS) plays an equally important role. The HARPS DRS delivers quality control indicators on-the-fly enabling the quality of the science frame and the health of the instrument to be assessed in real time. It also produces reduced and science-ready spectra and RV measurements in real time.

NIRPS will follow the same concept. Its DRS will be a fundamental part of the NIRPS system, assessing data quality in real time, and producing reduced spectra. Radial velocities will also be provided by the DRS. However, given the complexity of dealing with the telluric lines, an end-of-night reprocessing might be necessary to produce science-ready radial velocities. NIRPS raw and reduced data will be made available via the ESO archive. In addition, local data centres spread amongst the consortium are under consideration.

The arrival of NIRPS, with its extended near-infrared wavelength coverage and high RV stability, will be the final move towards making the La Silla Paranal Observatory the scientific hub for exoplanet discoveries. NIRPS will complement the scientific capabilities of existing instruments, open up new avenues for a wide range of applications, and provide ground support for future space missions, ensuring ESO's place at the forefront of exoplanet studies for many years to come.

The NIRPS consortium

The NIRPS consortium is jointly led by Université de Montréal and Université de Genève and includes partners from Brazil

(UFRN), France (IPAG, LAM), Portugal (IA, Universidade de Porto and IA, Universidade de Lisboa), Spain (IAC), Switzerland (University of Bern) and Canada (Université Laval, McGill University, Herzberg Institute of Astrophysics, Royal Military College of Canada, York University, University of Toronto, University of Western Ontario, University of British Columbia).

Acknowledgements

Université de Montréal gratefully acknowledges the funding provided by the Canada Foundation for Innovation and the Quebec Ministère de l'Éducation et de l'Enseignement Supérieur. This work is carried out in the framework of the National Centre for Competence in Research "PlanetS" and supported by the Swiss National Science Foundation (SNSF). This work was supported by Fundação para a Ciência e a Tecnologia (FCT, Portugal) through research grants from national funds and by FEDER through COMPETE2020 by grants UID/FIS/04434/2013 & POCI-01-0145-FEDER-007672 and PTDC/FIS-AST/1526/2014 & POCI-01-0145-FEDER-016886. P.F. and N.C.S. acknowledge support from FCT through Investigador FCT contracts nr. IF/01037/2013/CP1191/CT0001 and IF/00169/2012/CP0150/CT0002. P.F. further acknowledges support from Fundação para a Ciência e a Tecnologia (FCT) in the form of an exploratory project of reference IF/01037/2013/CP1191/CT0001.

Dedication

This paper is dedicated to the memory of Leslie Saddlemyer who passed away suddenly in January 2017. Les played a pivotal role in a number of major astronomical instrumentation projects, including recently the Gemini Planet Imager and the SPIRou (CFHT) spectrograph. He was the lead project engineer in the early phases of NIRPS. Les was very enthusiastic about the NIRPS project which he saw as his last major endeavour before retirement.

Table 1. Summary of NIRPS characteristics

Subsystem	Parameters
HAM-mode	Spectral resolution: $\lambda/\Delta\lambda$ = 100 000 0.4 arcsecond object fibre, AO-assisted feed 0.4 arcsecond simultaneous reference fibre
HEM-mode	Spectral resolution: $\lambda/\Delta\lambda$ = 75 000 0.9 arcsecond double slicing in the pupil plane 0.4 arcsecond simultaneous reference fibre
Environment	Vacuum: < 10^{-5} mbar Cryogenic: 80 K with 1 mK stability
Spectral domain	0.97–1.81 μm (*YJH* photometric bandpasses)
Calibration sources	Hollow cathode lamp, Stabilised Fabry-Perot, Laser Frequency Comb
Detector and format	Hawaii-4RG, 4 k × 4 k, 15 μm pixels
Limiting magnitude	1 m s^{-1} in 30 min for an M3 star with H = 9
Stability	< 1 m s^{-1} intrinsic stability over one night Calibration down to < 1 m s^{-1} over the lifetime of the instrument
Sampling	1 km s^{-1} per pixel, 3 pixels per FWHM
Operation	Simultaneous operation with HARPS without degrading HARPS's performance
Schedule	First light in 2019

The NIRPS team will remember him not only for his expertise, but also for his contagious enthusiasm and friendliness.

References

Almenara, J. M. et al. 2015, A&A, 581, 7
Anglada-Escudé, G. et al. 2016, Nature, 536, 437
Astudillo-Defru, N. et al. 2017, A&A, 602, 88
Berta, Z. K. et al. 2013, ApJ, 775, 91
Berta-Thompson, Z. K. et al. 2015, Nature, 527, 204
Bonfils, X. et al. 2005, A&A, 443, L15
Bonfils, X. et al. 2013, A&A, 549, A109
Charbonneau, D. et al. 2009, Nature, 462, 891
Cloutier, R. et al. 2017, AJ, 153, 9
Conod, U. et al. 2016, Proc. SPIE, 9909, 41
Delfosse, X. et al. 2013, A&A, 553, 8
Deshpande, R. et al. 2013, AJ, 146, 156
Dittmann, J. A. et al. 2017, Nature, 544, 333
Dressing, C. D. & Charbonneau, D. 2015, ApJ, 767, 95
Figueira, P. et al. 2010, *Extrasolar Planets in Multi-Body Systems: Theory & observations*, EAS Publications Series, 42, 131
Gillon, M. et al. 2016, Nature, 533, 221
Kopparapu, R. K. et al. 2013, ApJ, 765, 131
Mayor, M. et al. 2014, Nature, 513, 328
Önehag, A. et al. 2012, A&A, 542, 33
Rauer, H. et al. 2014, Experimental Astronomy, 38, 249
Ricker, G. R. et al. 2014, Proc. SPIE, 9143, 20
Snellen, I. et al. 2015, A&A, 576, 59
Sullivan, P. W. et al. 2015, ApJ, 809, 77
Woolf, V. M. & Wallerstein, G. 2005, MNRAS, 356, 963
Wyttenbach, A. et al. 2015, A&A, 577, 62

Links

[1] SOXS spectrograph: http://www.brera.inaf.it/~campana/SOXS/Son_of_X-Shooter.html

ESO/A. Santerne

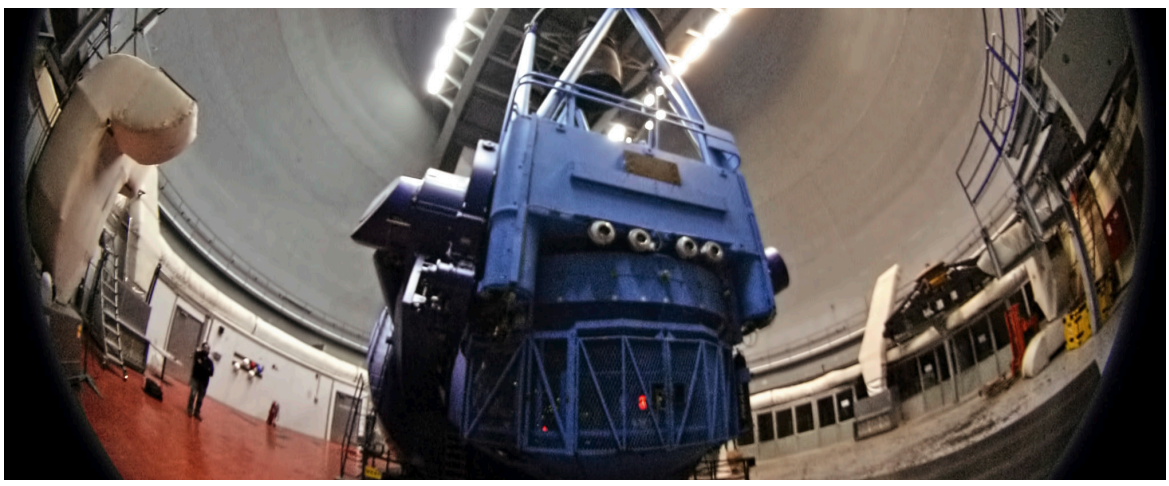

Fish-eye lens view of the inside of the ESO 3.6-metre Telescope dome.

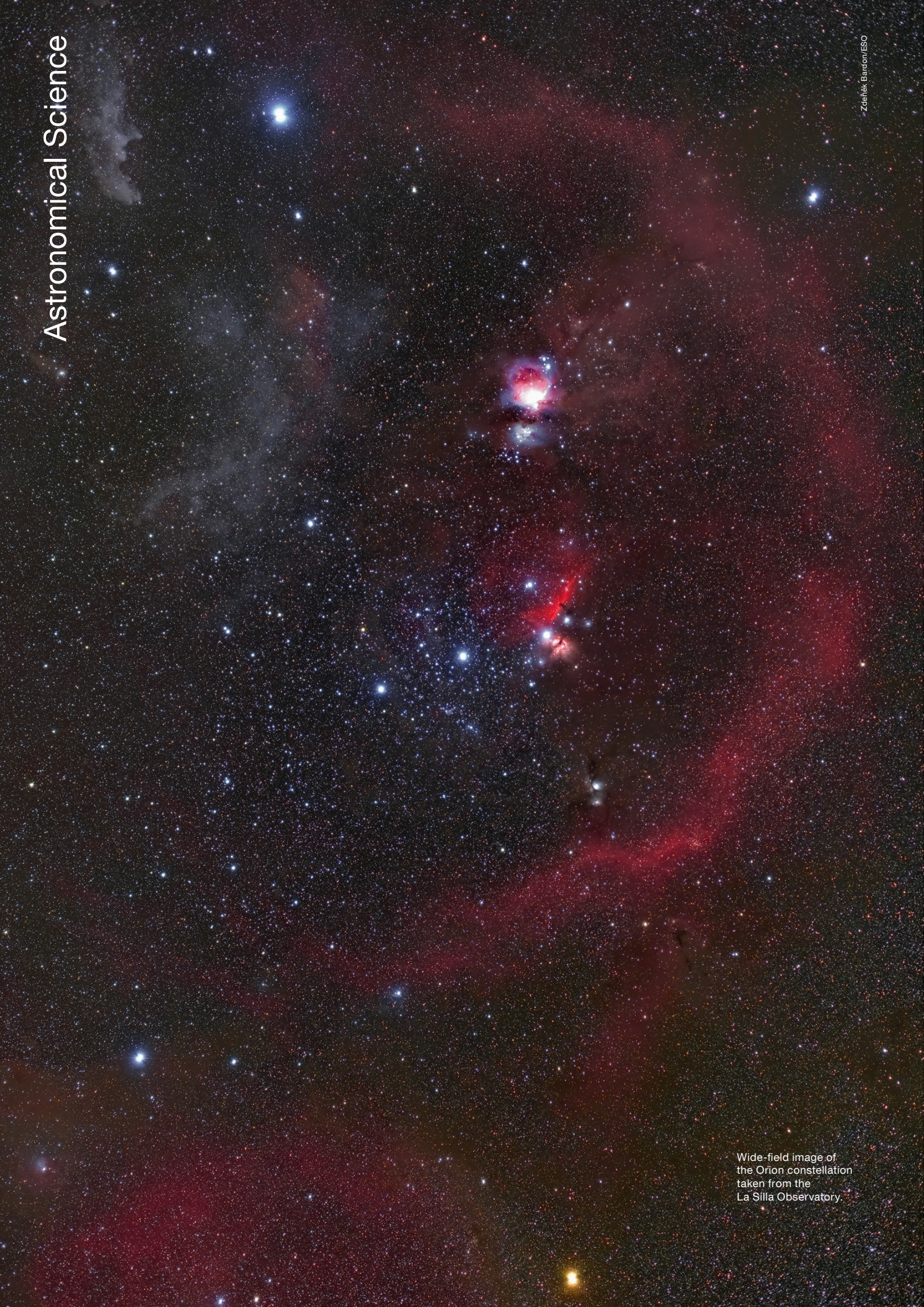

Zdeněk Bardon/ESO

Wide-field image of the Orion constellation taken from the La Silla Observatory.

DOI: 10.18727/0722-6691/5035

SPHERE Sheds New Light on the Collisional History of Main-belt Asteroids

Michaël Marsset[1]
Benoit Carry[2,3]
Myriam Pajuelo[2,3]
Matti Viikinkoski[4]
Josef Hanuš[5]
Pierre Vernazza[6]
Christophe Dumas[7]
Bin Yang[8]

[1] Astrophysics Research Centre, Queen's University Belfast, UK
[2] Université Côte d'Azur, Observatoire de la Côte d'Azur, Laboratoire Lagrange, CNRS, France
[3] IMCCE, Observatoire de Paris, PSL Research University, CNRS, Sorbonne Universités, UPMC Université Paris 06, Université Lille, France
[4] Department of Mathematics, Tampere University of Technology, Tampere, Finland
[5] Astronomical Institute, Faculty of Mathematics and Physics, Charles University, Prague, Czech Republic
[6] Aix Marseille Université, CNRS, Laboratoire d'Astrophysique de Marseille, France
[7] Thirty Meter Telescope (TMT) Observatory, Pasadena, USA
[8] ESO

The Spectro-Polarimetric High-contrast Exoplanet REsearch (SPHERE) instrument has unveiled unprecedented details of the three-dimensional shape, surface topography and cratering record of four medium-sized (~ 200 km) asteroids, opening the prospect of a new era of ground-based exploration of the asteroid belt. Although two of the targets, (130) Elektra and (107) Camilla, have been observed extensively for more than fifteen years by the first-generation adaptive optics imagers, two new moonlets were discovered around these targets, illustrating the unique power of SPHERE. In the next two years SPHERE will continue to collect high-angular-resolution and high-contrast measurements of about 40 asteroids. These observations of a large number of asteroids will provide a unique dataset to better understand the collisional history and multiplicity rate of the asteroid belt.

Context

Disc-resolved imaging is a powerful tool with which to investigate the origin and collisional history of small bodies in the Solar System; for example, the recent *in-situ* visits of the comet 67P/Churyumov-Gerasimenko by the Rosetta mission, the asteroids Vesta and Ceres with the Dawn mission, and the dwarf planet Pluto with New Horizons. However, fly-by and rendezvous space missions are rare and only a very limited number of objects have been visited to date.

In the late 1990s, observations of (4) Vesta with the Hubble Space Telescope (HST) demonstrated the capability of remote observations to spatially resolve impact features on the surface of some of the largest asteroids. Specifically, HST observations led to the discovery of the "Rheasilvia basin" at the south pole of Vesta, and allowed the origin of the V-type asteroids (Vestoids) and howardite-eucrite-diogenite (HED) meteorites to be established as collisional fragments from Vesta (Thomas et al., 1997).

In the 2000s, a new generation of adaptive optics (AO) imagers installed on the largest ground-based telescopes, such as the NAOS-CONICA (NACO) instrument on the Very Large Telescope (VLT), and the Near-InfraRed Camera 2 (NIRC2) on the W. M. Keck II Telescope, made disc-resolved imaging possible from the ground for a large number of medium-sized asteroids (~ 100–200 km in diameter). In turn, these observations triggered the development of methods for modelling the three-dimensional (3D) shapes of these objects (Carry et al., 2010a; Viikinkoski et al., 2015a) which were validated by in situ measurements during the Rosetta fly-by of asteroid (21) Lutetia (Carry et al., 2010b). In parallel, these AO imagers allowed the discovery and study of satellites of asteroids by direct imaging from the ground (see the Asteroids IV chapter of Margot et al., 2015).

More recently, the newly commissioned SPHERE instrument on the VLT (Beuzit et al., 2008) revealed the surfaces of four medium-sized asteroids in even greater detail: (3) Juno; (6) Hebe; and the two binary systems (107) Camilla and (130) Elektra. This remarkable achievement opens the prospect of a new era of exploration of the asteroid belt and its collisional history.

Internal structure and collisional history

High-angular-resolution images were collected with SPHERE at several epochs to provide full longitudinal coverage of the asteroids' silhouettes. Observations were acquired with the InfraRed Dual-band Imager and Spectrograph (IRDIS) in the broad *Y*-band, using the asteroid as a natural guide star for AO corrections. After each asteroid observation, images of a nearby star were acquired under exactly the same AO configuration to estimate the instrumental point spread function (PSF). These stellar calibration images were subsequently used to restore the optimal angular resolution of the asteroid images through image deconvolution techniques.

The IRDIS images of (3) Juno and (6) Hebe are shown in Figure 1, together with the corresponding geometric views of the 3D-shape models derived for these objects. The achieved angular resolution, $\theta = \lambda/D \sim 0.026$ arcseconds, corresponds to a projected distance of only ~ 20–25 km on the asteroid's surface. Compared to earlier images provided by HST and high-contrast imagers on 10-metre telescopes, including NACO and NIRC2 on Keck, SPHERE improves the spatial resolution of the available images of those asteroids by a factor of two to four.

The analysis of the SPHERE images, together with that of optical light curves, allows a precise 3D reconstruction of the asteroid's shape (Figure 2). Combining such measurements with the asteroid's mass estimate returns a highly accurate determination of its density and, therefore, information on its internal structure. Excellent agreement is found for asteroids Juno and Hebe between their measured density and that of their associated meteorites, respectively the ordinary L- and H-type chondrites (~ 3.4–3.5 g cm^{-3}), implying a homogeneous and intact interior for these objects. Camilla and Elektra, on the other hand, have very low densities (~ 1.4–1.7 g cm^{-3}; see Pajuelo et al., 2017 and Hanuš et al., 2017), lower in fact than any known meteorite found on Earth. This result implies either a very

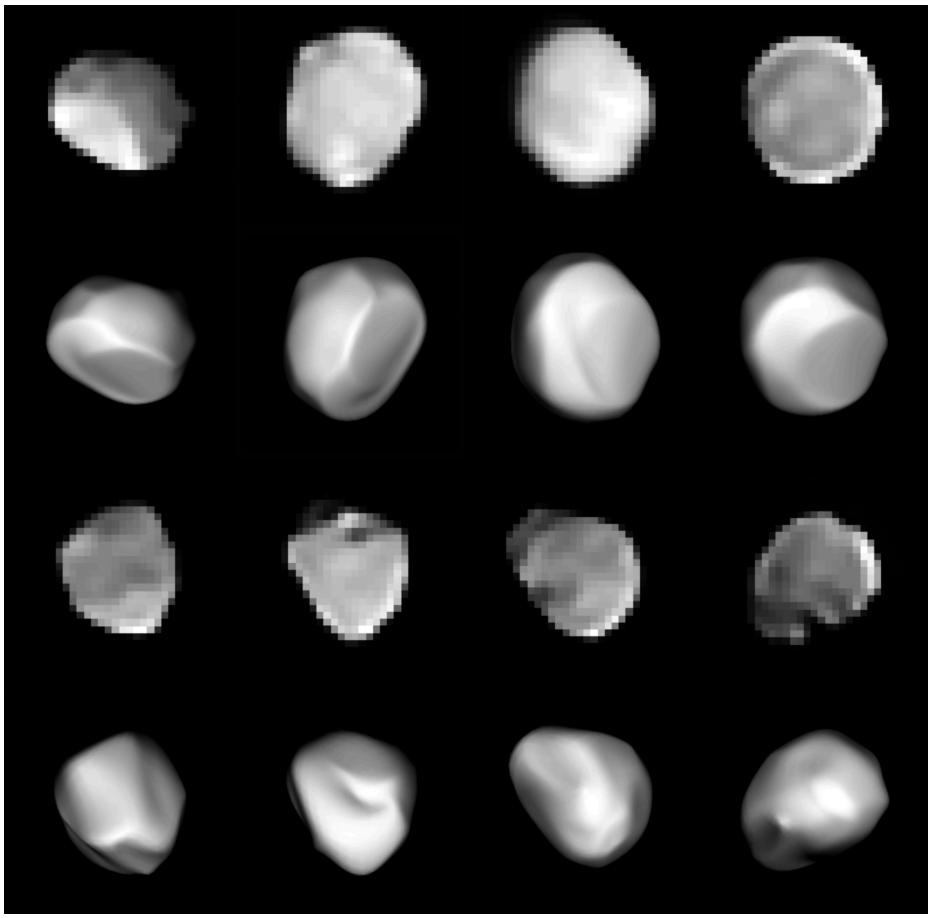

Figure 1. Deconvolved SPHERE images compared with the projections of their corresponding 3D models, for asteroids (3) Juno (top two rows respectively) and (6) Hebe (bottom two rows). Adapted from Viikinkoski et al. (2015b) and Marsset et al. (2017).

porous structure or an interior made from a high fraction of volatiles. Such a discrepancy may also indicate that Juno and Hebe formed in situ, whereas Camilla and Elektra formed in a volatile-rich environment, far from their current location.

A common feature among all four asteroids is the presence of large depressions on their surfaces, likely remnants of large impacts. In the case of Hebe, the largest depression encompasses a volume roughly a fifth of that of nearby asteroid families with similar composition. This could be evidence that Hebe is not the main source of ordinary H chondrites (Marsset et al., 2017), in contrast to some proposed scenarios.

The formation of asteroid binaries through collisional excavation

Simultaneous spectro-imaging observations of the primary and its moon for the two binaries, (107) Camilla and (130) Elektra, were further obtained using the Integral Field Unit (IFU). IFU observations were carried out in the IRDIFS_EXT mode, where the IFU covers 39 spectral channels between 0.95 and 1.65 microns (*YJH*-bands), while IRDIS performs broad-band imaging simultaneously in *K*-band. A solar analogue star was observed after each asteroid observation in order to remove the solar colour from the asteroid's spectrum.

The known satellites of Camilla and Elektra are clearly detected in the IRDIS and IFU images after subtracting the central halo of each of the primaries (Figure 3). The same process also unveiled the presence of a new smaller companion around Elektra (Yang et al., 2016) and also one around Camilla (Marsset et al.,

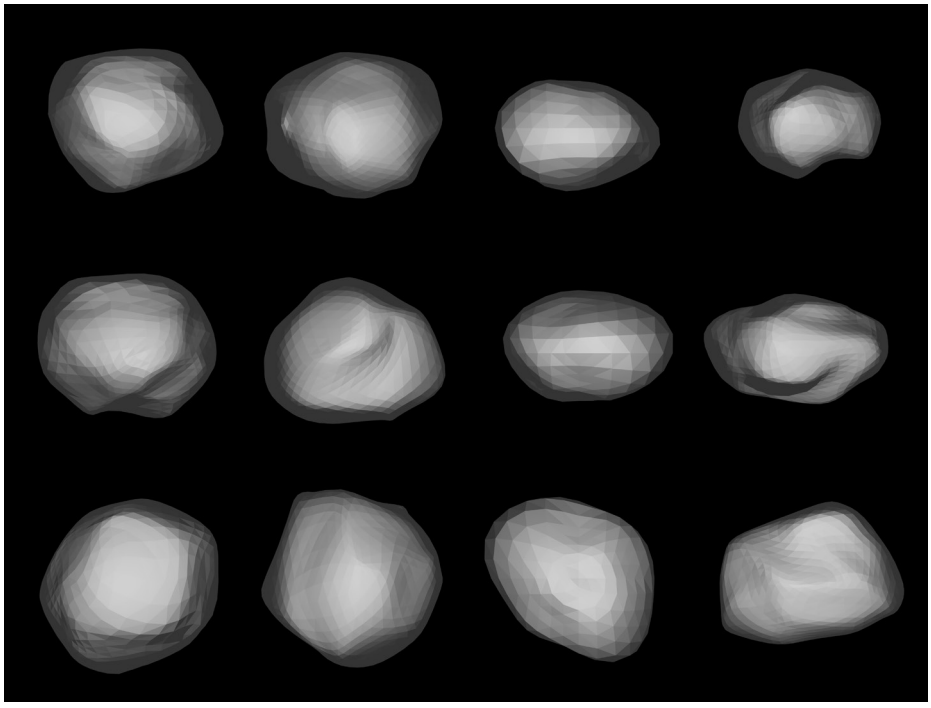

Figure 2. 3D shape models reconstructed from a combination of SPHERE images and optical light curves. Viewing directions are two equator-on views rotated by 90 degrees (first two rows) and a pole-on view (last row). Adapted from: Viikinkoski et al. (2015b); Hanuš et al. (2017); Marsset et al. (2017); and Pajuelo et al. (2017).

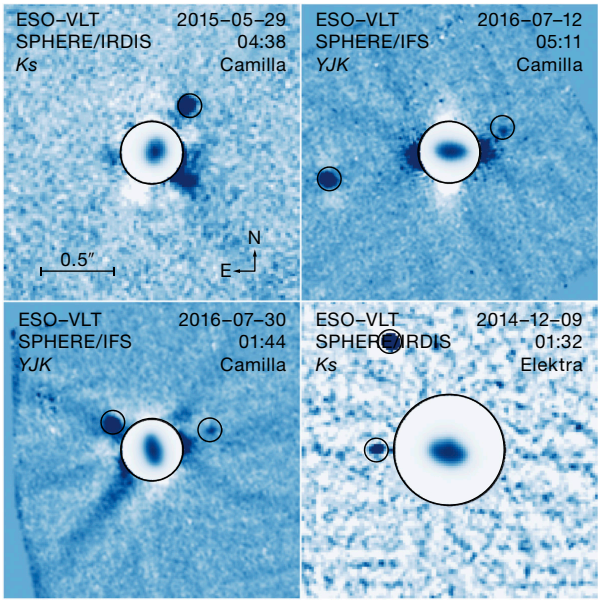

Figure 3. (Left) Halo-removed, SPHERE inverted-colour images of (107) Camilla and (130) Elektra. The small circles highlight the positions of the satellites. The central circle shows the primary. Adapted from Yang et al. (2016) and Pajuelo et al. (2017).

Figure 4. (Lower) SPHERE IFU spatially-resolved near-infrared spectrum of Camilla (orange) and its main moon (light blue). The IFU spectra are compared to a long-slit spectrum obtained with the Infrared Telescope Facility (IRTF), in black, and complemented with publicly available visible data retrieved from the SMASS database (green). The IFU data reveal no colour variation between the two bodies within the accuracy level of our measurements. From Pajuelo et al. (2017).

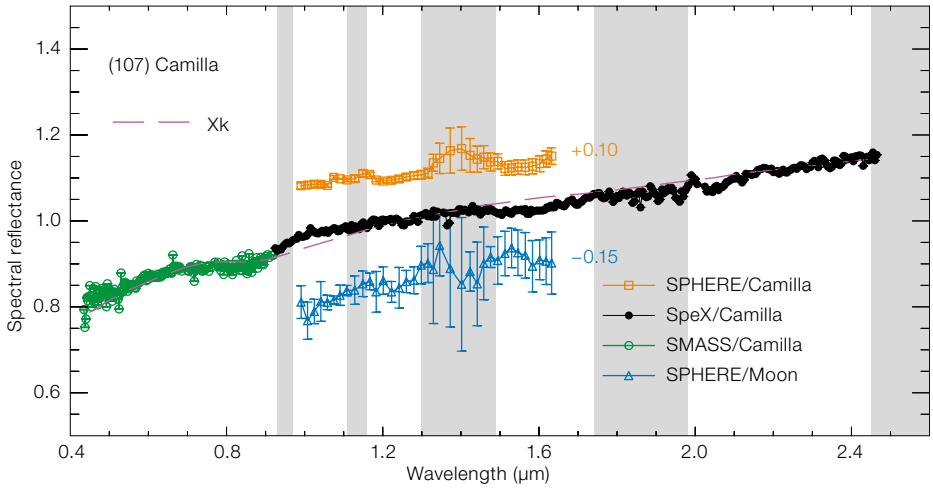

2016), making these two objects the fifth and sixth triple systems discovered in the asteroid belt after (45) Eugenia, (87) Sylvia, (93) Minerva, and (216) Kleopatra.

It is worth noting that both Camilla and Elektra have been extensively studied in the past using the first-generation high-contrast imagers. Specifically, more than 60 observations of Camilla were acquired between 2001 and 2016 with HST, NACO, NIRC2 and the Near-InfraRed Imager and spectrograph (NIRI) at the Gemini Observatory. The discovery by SPHERE of additional companions around these two heavily studied asteroids illustrates its outstanding performance in terms of contrast and angular resolution compared to earlier-generation instruments.

This performance also translates to the spectral data extracted from the IFU cubes. Component-resolved measurements of binaries usually suffer from the scattered light of the primary, which contaminates the photometry of the moon. Using SPHERE, the achieved contrast and resolution allow a clear separation of the two components, which indicate that the primary body and its moons share very similar properties and hence composition in each triple system (see Figure 4 and Yang et al., 2016; Pajuelo et al., 2017). This finding supports the hypothesis that multiple systems in the main asteroid belt formed through collisional processes. This formation scenario is also consistent with the presence of large surface depressions on both Camilla and Elektra. An estimate of their volume shows that these excavations can easily account for the creation of the two satellites of Camilla (Pajuelo et al., 2017) and Elektra (Hanuš et al., 2017).

The future exploration of the asteroid belt

In the next two years, our team will collect a set of volume, shape and topographic measurements for a substantial fraction of all > 100 km diameter main-belt asteroids (approximately 40) sampling the main compositional classes via a large SPHERE programme (ID: 199.C-0074, PI: P. Vernazza). These observations will allow us to determine the bulk density of these objects and hence to characterise their internal structure. In turn, this information will allow us to determine: (a) the nature of the initial building blocks (rock only, or a mixture of ice and rock); and (b) which compositional classes experienced differentiation. Our survey will also provide elements of answers to the following questions:

– What is the diversity in shapes among and within the main compositional classes? Space missions have revealed a variety of shapes among the few visited small bodies (for example, Ceres: spherical; Vesta: ellipsoidal, 67P: bi-lobed). We anticipate that our survey will make new discoveries in this domain.
– What is the multiplicity rate of large asteroids and is it related to their surface composition? It is understood that collisions are at the origin of the existence of multiple (binary and triple) asteroids. Answering this question will provide key constraints on models simulating asteroid collisions. In particular, it will allow us to understand whether rocky bodies have the same response to impacts as the ice-rich ones.

References

Beuzit, J.-L. et al. 2008, Proc. SPIE, 7014, 18
Carry, B. et al. 2010a, Icarus, 205, 460
Carry, B. et al. 2010b, A&A, 523, A94
Hanuš, J. et al. 2017, A&A, 599, A36
Margot, J.-L. et al. 2015, in *Asteroids IV,* (Tucson: University of Arizona Press), 355
Marsset, M. et al. 2016, IAU Circular, 9282
Marsset, M. et al. 2017, A&A, 604, A64
Pajuelo, M. et al. 2017, submitted to Icarus
Thomas, P. C. et al. 1997, Science, 277, 1492
Viikinkoski, M. et al. 2015a, A&A, 576, A8
Viikinkoski, M. et al. 2015b, A&A, 581, L3
Yang, B. et al. 2016, ApJ, 820, L35

DOI: 10.18727/0722-6691/5036

Three years of SPHERE: the latest view of the morphology and evolution of protoplanetary discs

Antonio Garufi[1,2]
Myriam Benisty[3]
Tomas Stolker[4]
Henning Avenhaus[2]
Jos de Boer[5]
Adriana Pohl[6]
Sascha P. Quanz[2]
Carsten Dominik[4]
Christian Ginski[5]
Christian Thalmann[2]
Roy van Boekel[6]
Anthony Boccaletti[7]
Thomas Henning[6]
Markus Janson[6]
Graeme Salter[8]
Hans Martin Schmid[2]
Elena Sissa[9]
Maud Langlois[8]
Jean-Luc Beuzit[3]
Gaël Chauvin[3]
David Mouillet[3]
Jean-Charles Augereau[3]
Andreas Bazzon[2]
Beth Biller[6]
Mickael Bonnefoy[3]
Esther Buenzli[2]
Anthony Cheetham[10]
Sebastian Daemgen[2]
Silvano Desidera[9]
Natalia Engler[2]
Markus Feldt[6]
Julien Girard[3]
Raffaele Gratton[9]
Janis Hagelberg[3]
Christoph Keller[5]
Miriam Keppler[6]
Matthew Kenworthy[5]
Quentin Kral[7]
Bruno Lopez[11]
Anne-Lise Maire[6]
François Menard[3]
Dino Mesa[9]
Sergio Messina[9]
Michael R. Meyer[2]
Julien Milli[3]
Michiel Min[4]
André Muller[6]
Johan Olofsson[6]
Nicole Pawellek[6]
Christophe Pinte[3]
Judit Szulagyi[2]
Arthur Vigan[8]
Zahed Wahhaj[8]
Rens Waters[4]
Alice Zurlo[8]

[1] Universidad Autónoma de Madrid, Departamento de Física Teórica, Madrid, Spain
[2] Institute for Astronomy, ETH Zurich, Switzerland
[3] Université Grenoble Alpes, Institut de Planétologie et d'Astrophysique de Grenoble, France
[4] Anton Pannekoek Institute for Astronomy, University of Amsterdam, the Netherlands
[5] Sterrewacht Leiden, the Netherlands
[6] Max Planck Institute for Astronomy, Heidelberg, Germany
[7] LESIA, Observatoire de Paris, PSL Research Université, CNRS, Université Paris Diderot, Sorbonne Paris Cité, UPMC Paris 6, Sorbonne Universités, France
[8] Aix Marseille Université, CNRS, Laboratoire d'Astrophysique de Marseille, UMR 7326, France
[9] INAF – Osservatorio Astronomico di Padova, Italy
[10] Geneva Observatory, University of Geneva, Versoix, Switzerland
[11] Laboratoire Lagrange, Université Côte d'Azur, Observatoire de la Côte d'Azur, CNRS, Nice, France

Spatially resolving the immediate surroundings of young stars is a key challenge for the planet formation community. SPHERE on the VLT represents an important step forward by increasing the opportunities offered by optical or near-infrared imaging instruments to image protoplanetary discs. The Guaranteed Time Observation Disc team has concentrated much of its efforts on polarimetric differential imaging, a technique that enables the efficient removal of stellar light and thus facilitates the detection of light scattered by the disc within a few au from the central star. These images reveal intriguing complex disc structures and diverse morphological features that are possibly caused by ongoing planet formation in the disc. An overview of the recent advances enabled by SPHERE is presented.

The large number of exoplanets discovered with various techniques (for example, transit, radial velocity, imaging) indicates that planet formation around young stars is very common. The architecture of the observed planetary systems is surprisingly varied and typically does not resemble that of our Solar System. For example, planets with masses intermediate between our terrestrial and gaseous planets are very frequent. Also, orbital distances smaller than that of our innermost planet are well populated, whereas only a few giant planets have also been found in orbits that are much larger than Neptune's (for example, HR 8799b, HIP 65426b).

This variety likely points to a great diversity in the initial conditions of planet formation throughout all evolutionary stages, from dust grain growth to planet-disc interactions and possibly planet migration. However, the mechanisms of planet formation are only partly understood. Different scenarios have been proposed that are not necessarily mutually exclusive and that act over a range of timeframes. A better characterisation of the physical and chemical properties of protoplanetary discs is therefore crucial in understanding planet formation.

The Spectro-Polarimetric High-contrast Exoplanet REsearch instrument (SPHERE), described in Beuzit et al. (2008) began operating on the Very Large Telescope (VLT) in May 2014. Since February 2015, the team responsible for the Guaranteed Time Observation (GTO) programme (principal investigator: Jean-Luc Beuzit) has dedicated substantial effort and observing time to the characterisation of circumstellar discs, with approximately ten complete nights of telescope time dedicated to debris discs (for example, Lagrange et al., 2016) and a similar amount of time dedicated to protoplanetary discs.

Protoplanetary discs with SPHERE

While optical and near-infrared observations of stars at a distance of a few hundred parsecs may naturally guarantee excellent spatial resolution, imaging the circumstellar environments at these wavelengths suffers from the low contrast of the circumstellar emission compared to the stellar flux. The most efficient way to mitigate this effect is to use a form of differential imaging. In particular, extended structures like circumstellar discs at tens of au from the star are best imaged with

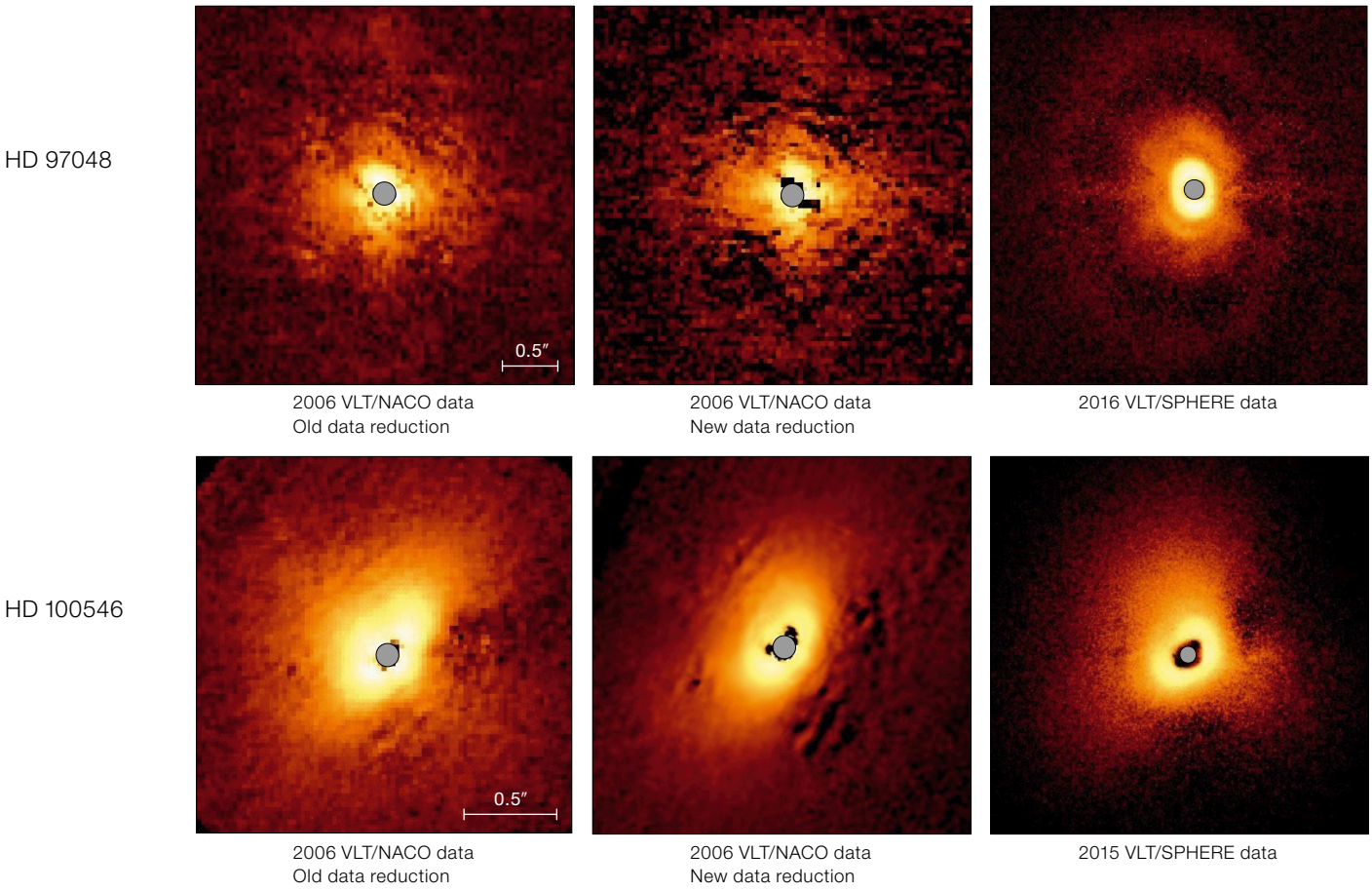

Figure 1. The improving data quality with the new reduction procedures and the impact of SPHERE are illustrated for the two disc systems HD 97048 and HD 100546. The HD 97048 image from NACO old reduction is from Quanz et al. (2012), and the NACO new reduction and SPHERE data are from Ginski et al. (2016). The HD 10056 images are from, left to right, Quanz et al. (2011), Avenhaus et al. (2014) and Garufi et al. (2016).

polarimetric differential imaging (PDI), which exploits the different nature of the stellar (mainly unpolarised) light and scattered (strongly polarised) light from the disc surface. The (quasi-)simultaneous observation of orthogonal polarisation states enables the separation of these two light components, which are then combined to obtain the full set of linear Stokes parameters, as well as the azimuthal component Q_ϕ of the polarised light (see Schmid et al., 2006).

Until five years ago, the NAOS-CONICA (NACO) instrument on the VLT was the only ESO facility offering PDI. Some pioneering work gave us a hint of the morphological diversity of discs (see, for example, the review by Quanz et al., 2011). However, there was no systematic approach to the observation of discs using PDI, with only a handful of objects observed at the time. The performance of PDI has significantly improved over the last five years thanks to: (i) an optimised data reduction, which corrects for the instrumental polarisation and employs the azimuthal Q_ϕ parameter to reduce the noise floor in the image (see Avenhaus et al., 2014a); and (ii) the advent of SPHERE. Figure 1 illustrates the effects of these advances.

SPHERE was mainly designed to provide imaging and spectroscopic characterisation of exoplanets. However, SPHERE's extreme adaptive optics (XAO) module SAXO (Fusco et al., 2006) and the high-precision polarimetry offered by the subsystems — the Zurich IMaging POLarimeter ZIMPOL (Thalmann et al., 2008) and the InfraRed Dual-band Imager and Spectrograph IRDIS (Dohlen et al., 2008) — make SPHERE among the best instruments to perform PDI of circumstellar discs. This combination equips it with an unprecedented combination of excellent sensitivity (more than four orders of magnitude in contrast) and angular resolution (~ 3 au in the visible and ~ 7 au in the near-infrared for sources at 150 pc). Furthermore, it is the only instrument mounted on an AO-assisted 8-metre telescope to perform PDI in the visible.

Imagery of protoplanetary discs

A glimpse of the morphological variety of protoplanetary discs emerging from the GTO programme can be seen in Figure 2. These ten sources represent only a small fraction of the entire sample of discs imaged so far with PDI. Nonetheless, all the morphological elements now routinely discovered in all protoplanetary discs can be appreciated here. Our census, initially biased towards more luminous stars, is

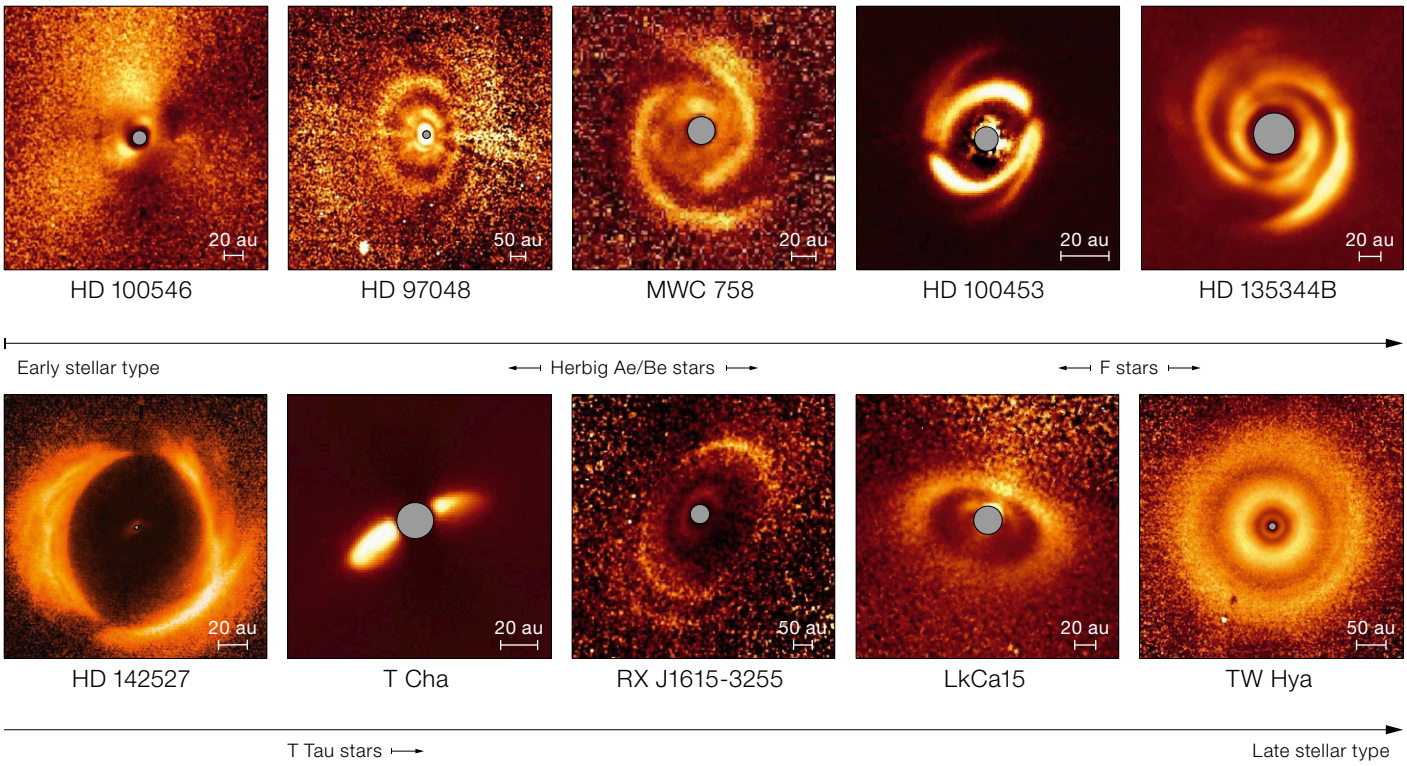

Figure 2. Collection of images of protoplanetary discs observed in PDI with SPHERE. References to the images are: HD 100546, Garufi et al. (2016); HD 97048, Ginski et al. (2016); MWC 758, Benisty et al. (2015); HD 100453, Benisty et al. (2017); HD 135344B, Stolker et al. (2106); HD 145527, Avenhaus et al. (2017); T Cha, Pohl et al. (2017); RX J1615-3255, de Boer et al. (2016); LkCa 15, Thalmann et al. (2016); TW Hya, van Boekel et al. (2017).

now more uniform across all stellar types, with discs around T Tauri stars like LkCa 15 (Thalmann et al., 2016) being as well characterised as the most imaged Herbig Ae/Be systems, like HD 100546 (Garufi et al., 2016).

The clearest finding from an inspection of the available sample is that all discs show morphological features. In the majority of sources, either concentric rings (HD 97048, Ginski et al., 2016; TW Hya, van Boekel et al., 2017) or spiral arms (MWC 758, Benisty et al., 2015; HD 135344B, Stolker et al., 2016a) are revealed. Some discs, predominantly those with spirals, also show radially extended dips that can be interpreted as shadows cast by a misaligned disc at a few au from the central star (Benisty et al., 2017; Avenhaus et al., 2017).

The interpretation of features from inclined discs is less immediate because of the degeneracy between scattering phase function, disc geometry and illumination effects in these sources. This analysis is nonetheless pivotal to constrain the composition of dust grains (Stolker et al., 2016b; Pohl et al., 2017) and the geometry of the disc surface (de Boer et al., 2016), both of which are necessary to understand planet formation.

Comparison with ALMA images

PDI images are sensitive to micron-sized dust grains at the disc surface. These grains are very well coupled to the gas under typical disc conditions. On the other hand, images at (sub-)millimetre wavelengths trace larger grains within the disc. Comparing SPHERE and Atacama Large Millimeter/Submillimeter Array (ALMA) images with comparable angular resolution can potentially reveal the different morphologies of different disc components. In fact, many disc processes (for example, grain growth or dust filtration) are expected to differentiate the distribution of gas and large grains throughout disc evolution, leaving their imprint on the disc structure. This is illustrated in Figure 3 for two prototypical examples from PDI, one showing concentric rings (TW Hya) and another showing spiral arms (HD 135344B).

Similarly to the PDI data, the ALMA images of TW Hya show a number of rings and gaps (Andrews et al., 2016). Van Boekel et al. (2017) performed a detailed comparison of the radial profiles of these two datasets, highlighting both similarities and profound differences. The entire detectable signal from ALMA is located within the second bright ring from PDI at approximately 60 au. The two main millimetre dips seen in both the image and the radial profile in Figure 3 have analogous dips in PDI at 25 au and at 40 au. Similar considerations apply to some rings. In general, large-scale structures have a stronger contrast in SPHERE data, whereas narrow features appear more profound with ALMA. There is no general consensus regarding the origin of these rings, with both planet-disc interactions and dust accumulation in correspondence with ice lines being the most promising explanations.

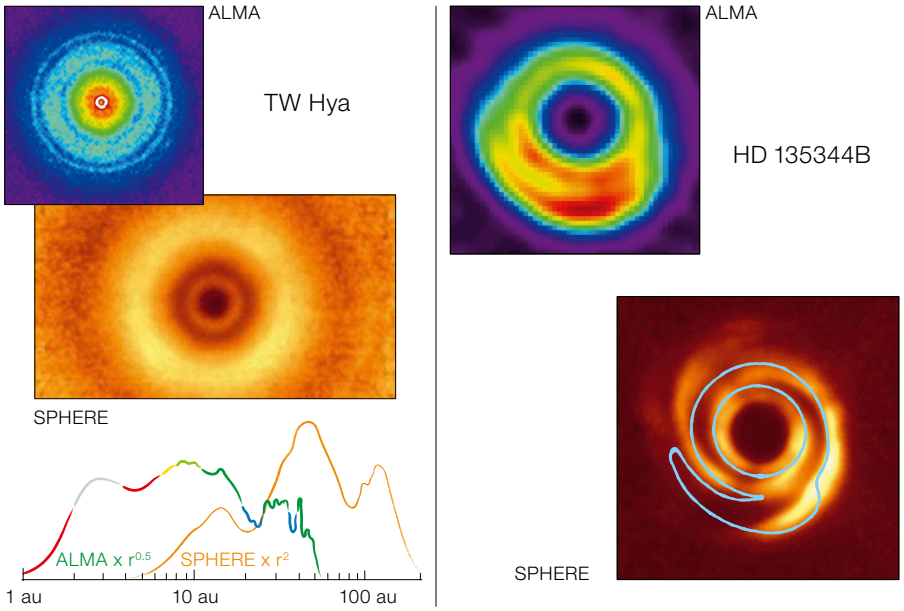

Figure 3. Comparison of ALMA and SPHERE images for two prototypical discs shown at the same spatial scale. For TW Hya, the ALMA image is from Andrews et al. (2016) and the SPHERE image and radial profiles from van Boekel et al. (2017). For HD 135344B, the ALMA image is from van der Marel et al. (2016) and the SPHERE image is from Stolker et al. (2016).

On the other hand, the spiral arms visible in the PDI image of HD 135344B are not detected by ALMA (van der Marel et al., 2016) even though the lower angular resolution of these images still leaves this scenario open. The best available image of this source shows an inner ring at approximately 45 au and an asymmetric feature to the south running parallel to the ring. The inner ring lies at a larger distance than the inner rim in scattered light at 25 au. The southern feature does not match the location of the two spirals but rather seems to follow the trail of the western one, or alternatively to run parallel to the eastern one but at a larger orbital radius. These radial and azimuthal displacements between small and large grains may be speculatively related to the formation history of these features, with a vortex-like structure to the south being generated by an inner dust trap at smaller radii, which is in turn related to the possible presence of planets within the inner cavity (van der Marel et al., 2016).

Disc cavity or no disc cavity

Another fundamental aspect revealed by both near-infrared and millimetre images is the high occurrence of large (> 10 au) central cavities. In many cases, these cavities appear smaller in PDI than in the millimetre images (for example, HD 135344B). In some other cases, they are not detected in PDI down to the instrument coronagraph, even though this is up to four times smaller in size than the millimetre cavity (for example, MWC 758). A systematic study of these differences is fundamental in the context of planet-disc interactions, since the most probable scenario for the formation of these cavities is the dynamical action of orbiting companions.

The high occurrence of cavities in discs surrounding Herbig stars can be appreciated from Figure 4. It can be seen that the long-standing observational dichotomy found by Meeus et al. (2001) between sources with large far-infrared excess (Group I) and small far-infrared excess (Group II) can be understood in terms of the presence or absence of a large disc cavity. From the sample of Herbig stars with available PDI images (covering the vast majority of sources within 200 pc), it is clear that discs with large cavities represent more than half of the total. If we exclude low-mass discs where outer stellar companions at 100s of au are likely truncating the disc from outside (bottom-left of the chart) this fraction increases to ~ 75 %.

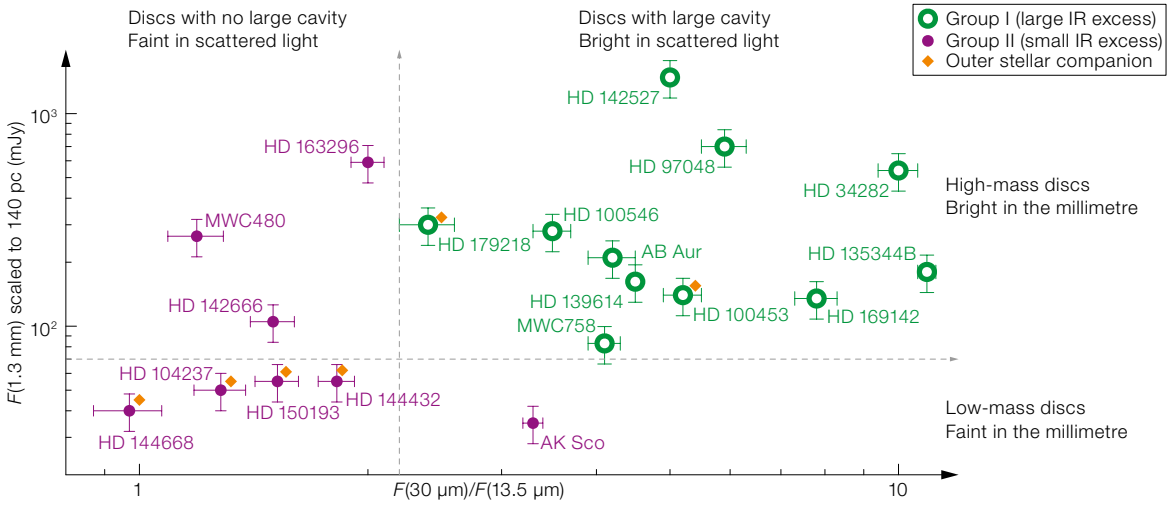

Figure 4. Millimetre to mid-infrared chart (adapted from Garufi et al., 2017). The photometric ratio of 30 μm to the 13.5 μm ratio on the x-axis is a proxy for the amount of scattered light traced by SPHERE. The y-axis indicates the millimetre brightness scaled to the same distance. The brown diamonds denote sources with outer stellar companions.

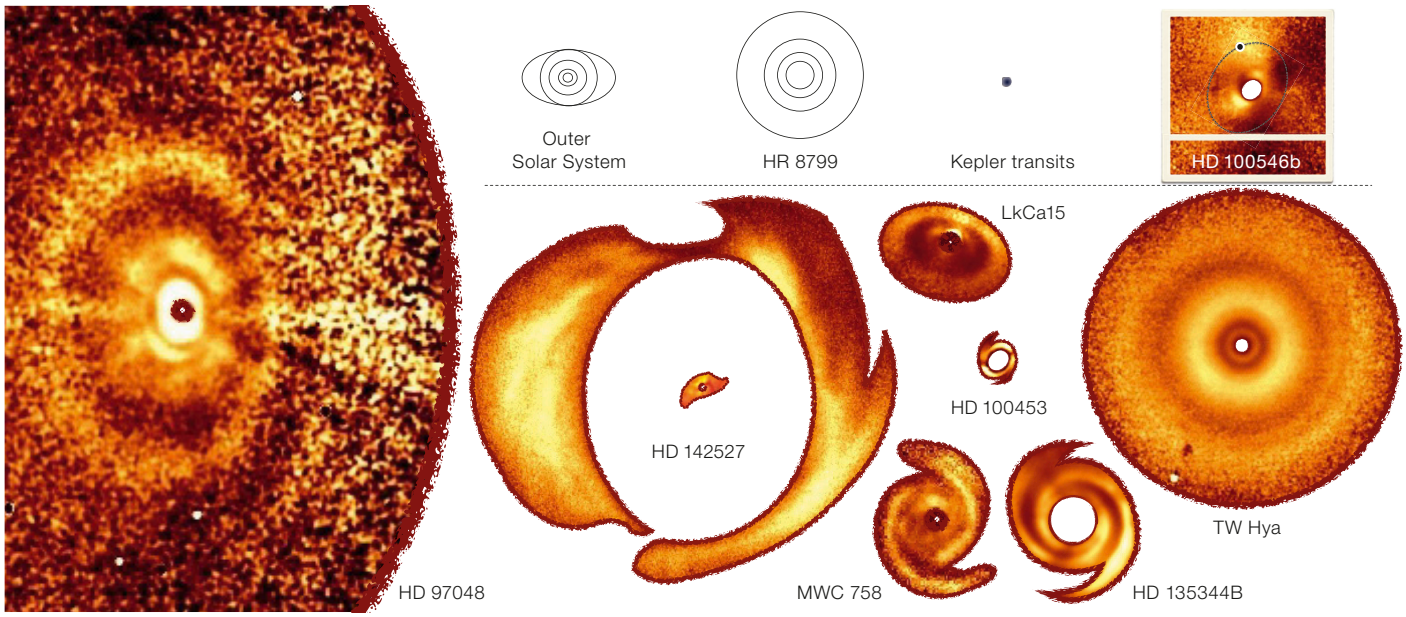

Figure 5. Illustrative protoplanetary discs and planetary systems all shown at the same physical scale.

Figure 4 also shows that discs without a large cavity (Group II) are fainter in scattered light. The photometric ratio of the x-axis is in fact a good proxy for the amount of signal detected in PDI (Garufi et al., 2017) while the millimetre flux along the y-axis gives an approximate measurement of the dust mass. Figure 4 shows that Group II sources can be divided into two sub-categories according to their millimetre flux, likely explaining the elusiveness of Group II sources in scattered light. Millimetre flux observations reveal both discs as massive as Group I, which are likely shadowed by their own inner rim at the (sub-)au scale, and those with low mass and an outer companion, which are probably smaller than (or comparable with) the size of the coronagraph employed for the PDI observations and are thus faint.

Both the presence and the size of the disc cavity, as well as the disc radial extent, may be intimately related to the morphology of the resulting planetary systems. However, a taxonomic approach to the resolved information of the discs

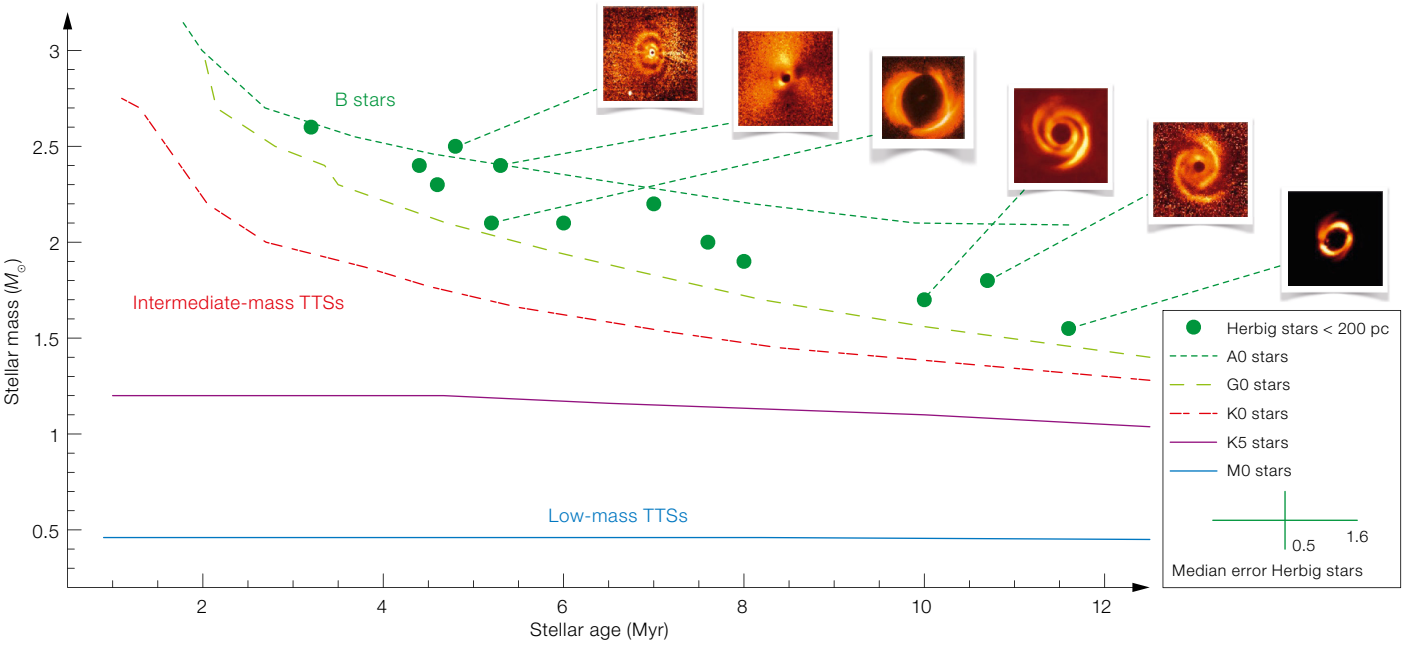

Figure 6. Stellar mass – age diagram for the Herbig stars within 200 pc, compared with the pre-main sequence tracks by Siess et al. (2000), for a given spectral type and varying luminosity.

and the architecture of planetary systems has yet to be attempted.

Link with planetary systems

Unfortunately, the intermediate stages of planet formation cannot be studied observationally because of the lack of detectable emission from metre- to kilometre-sized bodies. Thus, the most obvious approach to establishing a link between protoplanetary discs and planetary systems is the direct comparison of their physical scale, as shown in Figure 5. The planetary orbits in systems like that of HR 8799, or our own Solar System, lie at scales comparable to the locations of some disc features like rings, cavities and spirals.

However, the vast majority of the currently known exoplanets have been discovered by the Kepler space mission with the transit method, which is strongly biased towards planets within a few au of the central star. To date, very few gas giant planets have been imaged beyond 30 au (for example, the SPHERE SHINE survey; Chauvin et al., 2017). In other words, the routinely discovered disc features do not have an obvious counterpart in the exoplanet distribution. This can be explained by one or more of the following considerations:

(a) Planet migration due to disc forces is a very efficient and rapid process;
(b) A large population of as yet unseen low-mass planets exists at large orbits;
(c) The discs that we observe are exceptional, as with HR 8799;
(d) Commonly observed disc features are not due to the interaction with planets.

In any case, the solution to this apparent incongruity is related to the mechanisms of planet formation. Disc fragmentation due to instability is believed to be a possible mechanism in the early evolution of discs (less than 1 Myr old), whereas the stars we observe with discs are much older (see below). Accretion of gas onto planetary embryos as massive as a few Earth masses appears more likely at this stage. In this scenario, disc gaps and cavities may be sculpted by (accreting?) giant planets and/or facilitate the formation of kilometre-sized planetesimals from the intense growth of millimetre-sized particles (through a dust trap).

The most promising observational approach to these questions is the detection and characterisation of forming planets still embedded in the disc, and possibly of their circumplanetary disc. To date, very few such candidates have been found. Among these, HD 100546b is one of the best studied, even though its impact on the disc morphology remains somehow elusive (see for example, Quanz et al., 2013; Garufi et al., 2016).

Evolution of discs (and of our view of it)

Owing to large uncertainties in stellar ages, there have not been conclusive results on the evolution of disc features with time. The new Gaia distances to Herbig stars enable us to refine the stellar properties, as depicted in Figure 6. In this diagram the stellar masses and ages of the nearby (< 200 pc), and therefore most studied, Herbig stars (i.e., with spectral types between F6 and B9), are compared to pre-main sequence tracks of later (cooler) spectral-type stars.

Bearing in mind both the small number of objects and the uncertainty in pre-main sequence models, it is clear that discs showing symmetric double-spiral arms are found around older (i.e., less luminous) stars, like HD 135344B and MWC 758. On the other hand, very extended discs with multiple and more complex structures are found predominantly around younger (more luminous) stars, like HD 97048 and HD 100546.

Another interesting hint from the diagram in Figure 6 is that all well-studied Herbig stars within 200 pc are older than 3 Myr. To find younger stars still more massive than the Sun, we should look for: (i) early B stars, (ii) particularly luminous A and F stars, or (iii) intermediate-mass T Tauri stars (IMTTS; namely T Tauri stars with spectral types between G0 and K5). Unfortunately, no star from the first two categories has been found within 200 pc. This means that to study the younger counterparts of the well-known discs around Herbig stars, we should image the surroundings of IMTTS, especially in the more luminous systems. From the diagram, it is also clear how a larger range of stellar masses is covered with a certain spectral type interval when moving to later spectral types.

All of these considerations motivate us to extend our past successful study of Herbig stars to T Tauri stars. Fortunately, SPHERE performs much better than expected with fainter stars. We have already imaged the circumstellar environment of more than 40 T Tauri stars, both in GTO and in open-time programmes. The next step for the consortium will be the comparison of these newly imaged disc features around T Tauri stars with those known from older and/or more massive systems. Our goal is to compare the physical conditions for planet formation to carry out a complete census of stellar ages and masses.

References

Andrews, S. M. et al. 2016, ApJ, 820, L40
Avenhaus, H. et al. 2014a, ApJ, 790, 56
Avenhaus, H. et al. 2014b, ApJ, 781, 87
Avenhaus, H. et al. 2017, ApJ, 154, 33
Benisty, M. et al. 2015, A&A, 578, L6
Benisty, M. et al. 2017, A&A, 597, A42
Beuzit, J.-L. et al. 2008, SPIE Conf. Ser., 7014, 18
Chauvin, G. et al. 2017, arXiv:1707.01413
de Boer, J. et al. 2016, A&A, 595, A114
Dohlen, K. et al. 2008, SPIE Conf. Ser., 7014, 3
Fusco, T. et al. 2006, SPIE Conf. Ser., 6272, 62720K
Garufi, A. et al. 2016, A&A, 588, A8
Garufi, A. et al. 2017, A&A, 603, A21
Ginski, C. et al. 2016, A&A, 595, A112
Lagrange, A.-M. et al. 2016, A&A, 586, L8
Meeus, G. et al. 2001, A&A, 365, 476
Pohl, A. et al. 2017, A&A, 605, A34
Quanz, S. P. et al. 2011a, The Messenger, 146, 25
Quanz, S. P. et al. 2011b, ApJ, 738, 23
Quanz, S. P. et al. 2012, A&A, 538, A92
Quanz, S. P. et al. 2013, ApJ, 766, L1
Schmid, H. M. et al. 2006, A&A, 452, 657
Siess, L. et al. 2000, A&A, 358, 593
Stolker, T. et al. 2016a, A&A, 595, A113
Stolker, T. et al. 2016b, A&A, 596, A70
Thalmann, C. et al. 2008, SPIE Conf. Ser., 7014, 3
Thalmann, C. et al. 2016, ApJL, 828, L17
van Boekel, R. et al. 2017, ApJ, 837, 132
van der Marel, N. et al. 2016, A&A, 585, 58

DOI: 10.18727/0722-6691/5037

ALLSMOG, the APEX Low-redshift Legacy Survey for MOlecular Gas

Matt Bothwell[1]
Claudia Cicone[2]
Jeff Wagg[3]
Carlos De Breuck[4]

[1] Cavendish Laboratory, University of Cambridge, United Kingdom
[2] INAF Osservatorio di Brera, Milan, Italy
[3] SKA Organisation, Macclesfield, United Kingdom
[4] ESO

We report the completion of the APEX Low-redshift Legacy Survey for MOlecular Gas (ALLSMOG), an ESO Large Programme, carried out with the Atacama Pathfinder EXperiment (APEX) between 2013 and 2016. With a total of 327 hours of APEX observing time, we observed the ^{12}CO(2–1) line in 88 nearby low-mass star-forming galaxies. We briefly outline the ALLSMOG goals and design, and describe a few science highlights that have emerged from the survey so far. We outline future work that will ensure that the ALLSMOG dataset continues to provide scientific value in the coming years. ALLSMOG was designed to be a reference legacy survey and as such all reduced data products are publicly available through the ESO Science Archive Phase 3 interface.

Background: observing molecular gas

The assembly of galaxies, over the past 13.8 billion years of cosmic time, is a complex process governed in large part by the behaviour of gas. From gas inflows pouring into dark matter halos (triggering waves of star formation), and the molecular clouds within galaxies (providing the fuel for future galaxy growth), to galactic outflows (which remove fuel and may suppress future star formation), gas regulates many of the physical processes governing the lives of galaxies. If we want to better understand how galaxies grow and evolve, we need to gain a better understanding of their cold gas content.

Observing this cold gas is challenging, however. While modern optical galaxy surveys boast sample sizes into the millions, there are no more than a few thousand galaxies with measured total gas masses (atomic + molecular). In addition the majority of the galaxies with measured gas masses are massive and metal-rich spirals — fairly unrepresentative of the galaxy population as a whole. This deficit arises from a simple physical problem: direct observations of hydrogen molecules are impractical, since molecular hydrogen (H_2) lacks a permanent dipole moment, and the quadrupole lines have excitation temperatures far higher than those in molecular clouds; and also carbon monoxide (the most commonly used molecular gas tracer molecule) cannot survive in the interstellar medium of galaxies without a dust screen to protect it from the dissociating ultraviolet photons. Low-metallicity environments, such as those in the interstellar medium (ISM) of lower-mass galaxies which lack significant dust content, can therefore contain plenty of invisible H_2, while being deficient in the visible tracer molecule (CO).

There are therefore two significant hurdles to clear if a better understanding of gas in galaxies is to be achieved. Firstly, a significant sample of low-mass galaxies must be assembled, and their gas contents studied. Secondly, the gas-phase metallicity of these galaxies should be well constrained, in order to reliably convert from a CO flux into a mass of molecular hydrogen (via the CO-to-H_2 conversion factor, α_{CO}).

In order to begin to overcome these hurdles, we designed and carried out the ALLSMOG survey. Completed in 2016, ALLSMOG was an ESO Large Programme (awarded 300 hours on APEX over four semesters) designed to observe the CO(2–1) emission line in a sample of local ($z < 0.03$), low mass ($M_* < 10^{10}\,M_\odot$) galaxies. The sample was constructed to have a wide range of available ancillary data (including stellar mass, star formation rate and metallicity). The parent sample, based on the Sloan Digital Sky Survey (SDSS) data release 7 (DR7), provides spectra with the strong optical lines needed to estimate gas-phase metallicity, along with stellar masses and star formation rates. For inclusion in the ALLSMOG survey we also required an archival HI observation, enabling us to measure total (i.e., atomic + molecular) gas masses.

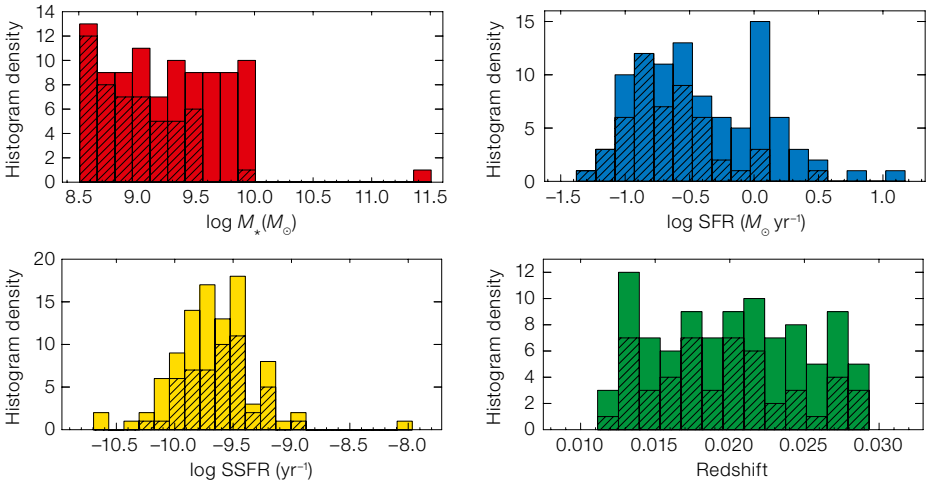

Figure 1. Histograms showing the distribution of parameters in the ALLSMOG sample. Clockwise from top left, the panels show: the distribution of log stellar mass; log star formation rate; redshift; and log specific star formation rate.

The final ALLSMOG survey, completed in 2016, consists of 88 low-mass local galaxies observed in CO(2–1). Histograms of the ALLSMOG parent sample, showing the distribution of various parameters (including stellar mass and redshift), are shown in Figure 1. A halfway-point survey paper was published by Bothwell et al. (2014), in which half of the final sample was made available (and some preliminary analysis was carried out). The full survey paper has now been published (Cicone et al., 2017). We briefly describe some details of the survey design, before giving a selection of scientific results that have emerged so far from the ALLSMOG survey.

Survey details

The ALLSMOG sample is drawn entirely from the Max-Planck-Insitut für Astrophysik – Johns Hopkins University (MPA-JHU) catalogue of spectral measurements and galaxy parameters for the SDSS DR7 (Abazajian et al., 2009). The targets were selected according to the following criteria:

1. Classified as star-forming galaxies (i.e., no evidence of an active galactic nucleus, AGN) according to their location on the diagnostic diagram of Baldwin, Phillips & Terlevich (1981).
2. Stellar masses in the range $8.5 < \log(M_*/M_\odot) < 10$.
3. Redshifts in the range $0.01 < z < 0.03$. The upper bound is due to sensitivity; the lower bound ensures that targets fit within the 27 arcsecond APEX beam.
4. Declinations $\delta < 15$ degrees.
5. Gas-phase metallicity, 12 + log (O/H) $\lesssim 8.5$, according to the calibration by Tremonti et al. (2004). This is intended to exclude sources with very high CO-to-H_2 conversion values for which a detection with APEX would be unfeasible.

The project was initially allocated 300 hours of ESO observing time over the course of four semesters, corresponding to 75 hours per semester throughout periods P92–P95 (October 2013–September 2015). However, during P94 and P95 there was a slowdown in ALLSMOG observations, mainly due to the installation of the APEX visitor instrument Supercam, in combination with better-than-average weather conditions. Due to the resulting ~ 50 % time loss for ALLSMOG during these two semesters, the ESO Observing Programmes Committee (OPC) granted a one-semester extension of the project, hence allowing us to complete the survey in Period 96 (March 2016). The final total APEX observing time dedicated to ALLSMOG amounts to 327 hours.

ALLSMOG is intended to be a CO flux-limited survey, and is also (to first order) a CO luminosity-limited survey, thanks to the narrow redshift distribution of the sample ($0.01 < z < 0.03$). We aimed to reach a line peak-to-rms (root mean square) signal-to-noise (SNR) ratio of ≥ 3 for the detections and a uniform rms for the non-detections, corresponding to rms = 0.8 mK (31.2 mJy) per 50 km s^{-1} channel for the APEX 230 GHz observations.

The ALLSMOG data were processed in the Grenoble Image and Line Data Analysis – Continuum and Line Analysis Single-dish Software (GILDAS-CLASS), using a series of customised scripts based on the statistics of the data, which included a by-eye check of each individual subscan (designed to eliminate scans with baseline ripples or non-Gaussian noise). Examples of final ALLSMOG spectra (presented with archival HI spectra), including non-detections, are shown in Figure 2.

Results (I) — molecular gas scaling relations

Several of the earliest results to come from the ALLSMOG survey concern

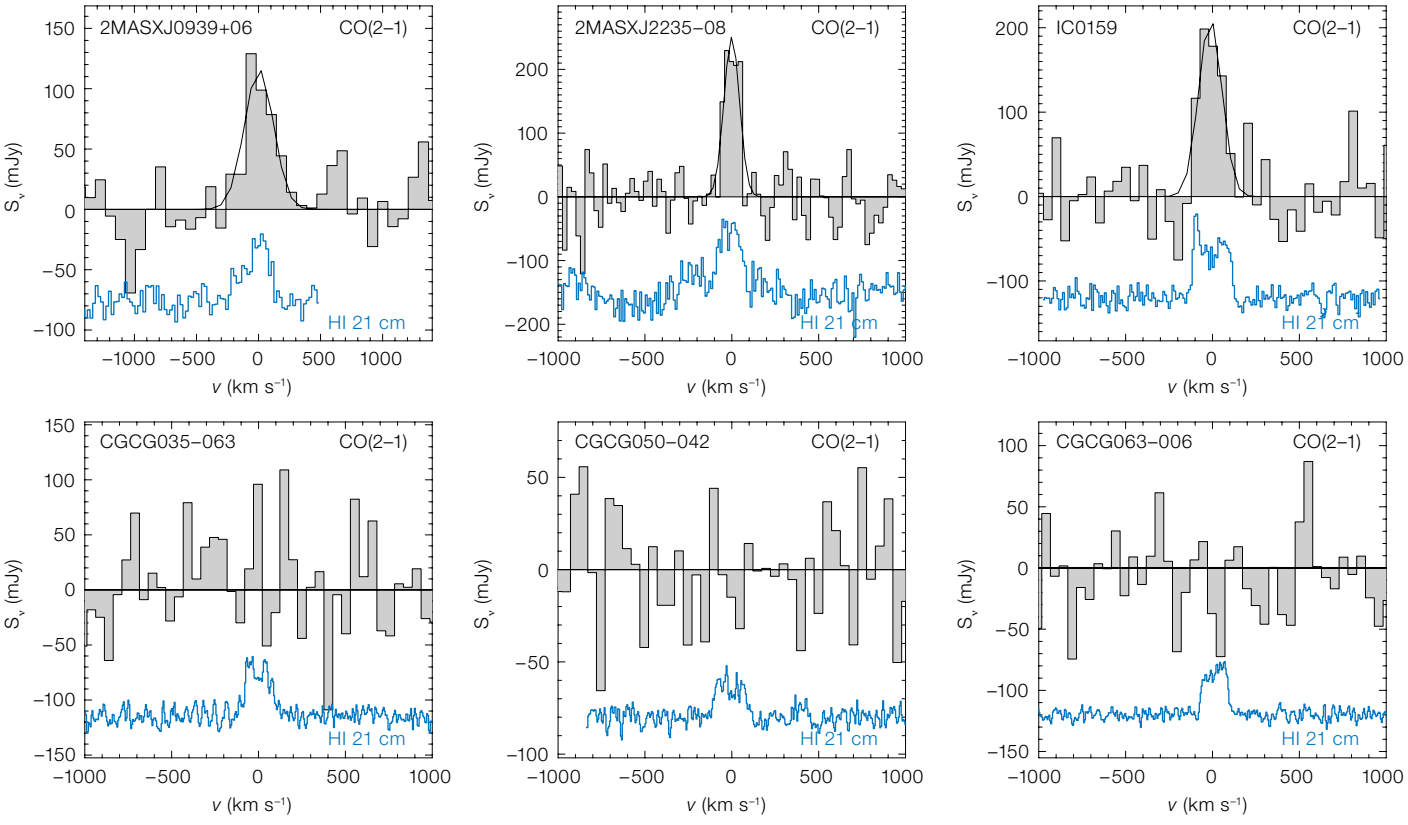

Figure 2. Six example spectra from the ALLSMOG survey, showing CO detections (top row) and non-detections (bottom row). In all panels, the grey upper spectrum is the APEX CO data, and the blue lower one is an archival HI spectrum. Figure adapted from Cicone et al. (2017).

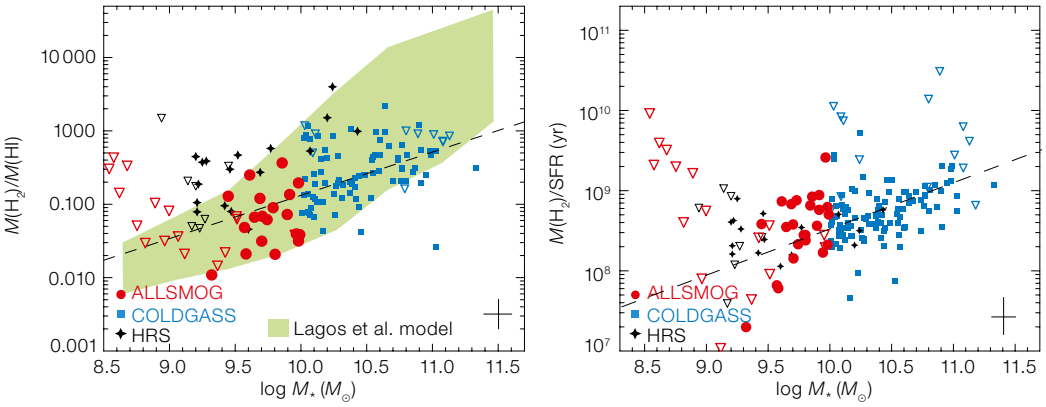

Figure 3. Left panel: H_2/HI ratios for the ALLSMOG sample plotted against stellar mass. Also plotted are the galaxies from the COLDGASS and HRS surveys. The green shaded region shows the semi-analytic model prediction from Lagos et al. (2011); the upper and lower bounds of the coloured region mark the 90th and 10th percentiles of the model distribution. Right panel: gas consumption timescales, plotted against stellar mass, for the ALLSMOG sample. Also plotted are the galaxies from the COLDGASS and HRS surveys. Both panels adapted from Bothwell et al. (2014).

molecular gas scaling relations — the strong trends between the molecular gas masses of galaxies and other large-scale properties (including stellar mass, star formation rate and metallicity). These scaling relations allow insight into the mechanisms underlying galaxy formation by providing simple, quantitative tests that models — both analytical and numerical — are required to match. Indeed, the ability (or otherwise) of a model to reproduce a variety of observed scaling relations has become a critical metric by which a model's success is judged.

The H_2/HI ratio

One scaling relation explored in our first release (Bothwell et al., 2014) is the ratio between the molecular and atomic components of the ISM. The ratio of molecular to atomic gas mass in galaxies is dependent on a range of physical processes, including the interstellar radiation field, the pressure of the ISM, and the abundance of dust (which aids the formation of molecules). Figure 3 (left panel) shows the H_2/HI mass ratio, plotted against stellar mass for the ALLSMOG galaxies and our two comparison samples, the CO Legacy Database for GASS (COLDGASS) and the Herschel Reference Survey (HRS). We overplot in Figure 3 (left panel) the theoretically predicted H_2/HI ratio from Lagos et al. (2011). Our data (which use a Wolfire et al. (2010) CO-to-H_2 conversion factor, which scales with metallicity) produce an H_2/HI ratio distribution in very close accordance with the semi-analytic model data.

Molecular gas consumption times

Another scaling relation explored in Bothwell et al. (2014) was the relationship between molecular gas mass and star formation rate. The ratio between these two quantities is often referred to as the gas consumption timescale, and can be interpreted as the time a galaxy can continue forming stars in the absence of a gas inflow or outflow (i.e., in a closed box). Figure 3 (right panel) shows the gas consumption timescale for ALLSMOG galaxies, and our two comparison samples COLDGASS and HRS, plotted against stellar mass. As above, we have used a Wolfire et al. (2010) CO-to-H_2 conversion factor to calculate molecular gas masses. We confirmed the trend found previously by both Saintonge et al. (2011) and Boselli et al. (2014): that the molecular gas consumption timescale is not constant, but increases with stellar mass over the full mass range of the detected samples (log $M_*/M_\odot > 9$). Molecular gas depletion timescales vary from ~ 2 Gyr at the most massive end of the distribution inhabited by COLDGASS galaxies (log $M_*/M_\odot > 11$), to ~ 100 Myr for the lowest-mass detected galaxies (log $M_*/M_\odot \sim 9$).

Results (II) — fundamental metallicity relations

In recent years, the well-known scaling relations between stellar mass and metallicity (the mass-metallicity relation), and stellar mass and star formation rate (SFR; the main sequence of galaxy evolution) have been extended into a three-dimensional relation, known as the fundamental metallicity relation (FMR; Lara-Lopez et al., 2010; Mannucci et al., 2010). Galaxies out to at least $z \sim 2.5$ lie on the surface defined by the FMR, on which, (a) more massive galaxies have higher metallicities, and (b) at a given stellar mass, galaxies with higher SFRs have systematically lower metallicities. Based on this relation, Bothwell et al. (2013) conducted a study of 4253 local galaxies, finding that the mass-metallicity relation also exhibited a significant secondary dependence on mass of atomic hydrogen (HI), to the extent that the HI-FMR was potentially more fundamental than the correlation with SFR.

Using data from a variety of sources (including the ALLSMOG survey, which provided data on molecular gas masses, along with stellar masses and metallicities), our team was able to demonstrate a strong relationship between gas-phase metallicity and molecular gas content (Bothwell et al., 2016a; 2016b). Using Principle Component Analysis (PCA), we showed that the well-known FMR, describing a close and tight relationship between metallicity and SFR at fixed stellar mass, is entirely a by-product of the underlying physical relationship with molecular gas (see Figure 4).

Summary and future plans

ALLSMOG was an ESO Large Programme, carried out with APEX between 2013 and 2016, which aimed to measure the molecular gas properties of a large sample of low-mass, low-metallicity galaxies in the local Universe. ALLSMOG was designed to be a reference legacy survey, and all reduced data products are publicly available through the ESO Phase 3 archive[1]. In addition, we intend to continue exploiting the ALLSMOG sample in the coming years.

One future project will use the ArTéMiS (*Architectures de bolomètres pour des Télescopes à grand champ de vue dans le domaine sub-Millimétrique au Sol*) bolometer camera on APEX to observe ALLSMOG galaxies at 350 and 450 μm, allowing their dust masses to be constrained via spectral energy distribution (SED) modelling. The ALLSMOG legacy dataset (which provides CO luminosities and metallicities, along with a suite of ancillary parameters), combined with submillimetre-derived dust masses, represents the ideal dataset for launching an investigation into the behaviour of the gas-to-dust ratio as a function of galaxy properties. A small pilot programme has been approved, and will be observed with APEX in late 2017 (principal investigator: Bothwell). The results from this initial study will serve as a proof of concept, guiding the design of future larger ALLSMOG follow-up programmes for far-infrared photometry.

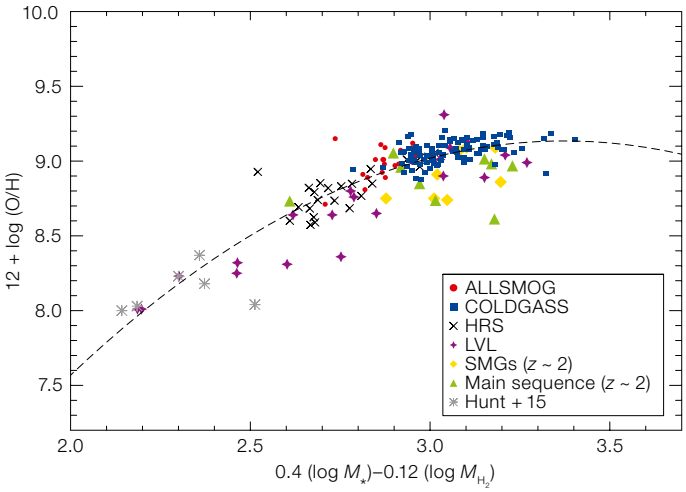

Figure 4. Gas-phase metallicity (12 + log (O/H)) *vs.* the optimum linear combination of stellar mass and molecular gas mass, for a variety of galaxy samples including ALLSMOG. Figure taken from Bothwell et al. (2016a) where further details of the combination of observed parameters can be found.

References

Abazajian, K. N. et al. 2009, ApJS, 182, 543
Baldwin, J. A., Phillips, M. M. & Terlevich, R. 1981, PASP, 93, 5
Boselli, A., Cortesi, L. & Boquien, M. 2014, A&A, 564, 65
Bothwell, M. S. et al. 2014, MNRAS, 445, 2599
Bothwell, M. S. et al. 2016a, MNRAS, 455, 1156
Bothwell, M. S. et al. 2016b, A&A, 595, 48
Cicone, C. et al. 2017, A&A, 604, 53
Lagos, C. Del P. et al. 2011, MNRAS, 418, 1649
Lara-Lopez, M. A. et al. 2010, A&A, 521, 53
Mannucci, F. et al. 2010, MNRAS, 408, 2115
Saintonge, A. et al. 2011, MNRAS, 415, 32
Tremonti, C. A. et al. 2004, ApJ, 613, 898
Wolfire, M. G. et al. 2010, ApJ, 716, 1191

Links

[1] ESO Science Archive Facility Phase 3 access to ALLSMOG: http://archive.eso.org/wdb/wdb/adp/phase3_main/form?collection_name=ALLSMOG

ESO/F. Kamphues

The Atacama Pathfinder EXplorer (APEX) antenna against a backdrop of peaks above the Chajnantor plateau.

DOI: 10.18727/0722-6691/5038

The Close AGN Reference Survey (CARS)

Bernd Husemann[1]
Grant Tremblay[2]
Timothy Davis[3]
Gerold Busch[4]
Rebecca McElroy[5]
Justus Neumann[6,7]
Tanya Urrutia[6]
Mirko Krumpe[6]
Julia Scharwächter[8]
Meredith Powell[9]
Miguel Perez-Torres[10]
The CARS Team*

[1] Max-Planck-Institut für Astronomie, Heidelberg, Germany
[2] Harvard-Smithsonian Center for Astrophysics, Cambridge, USA
[3] School of Physics & Astronomy, Cardiff University, UK
[4] I. Physikalisches Institut, Universität zu Köln, Germany
[5] Sydney Institute for Astronomy, University of Sydney, Australia
[6] Leibniz-Institut für Astrophysik Potsdam, Germany
[7] ESO
[8] Gemini Observatory, Hawaii, USA
[9] Center for Astronomy and Astrophysics, Yale University, USA
[10] Instituto de Astrofísica de Andalucía, Granada, Spain

The role of active galactic nuclei (AGN) in the evolution of galaxies remains a mystery. The energy released by these accreting supermassive black holes can vastly exceed the entire binding energy of their host galaxies, yet it remains unclear how this energy is dissipated throughout the galaxy, and how that might couple to the galaxy's evolution. The Close AGN Reference Survey (CARS) is a multi-wavelength survey of a representative sample of luminous Type I AGN at redshifts $0.01 < z < 0.06$ to help unravel this intimate connection. These AGN are more luminous than very nearby AGN but are still close enough for spatially resolved mapping at sub-kpc scales with various state-of-the art facilities and instruments, such as VLT-MUSE, ALMA, JVLA, Chandra, SOFIA, and many more. In this article we showcase the power of CARS with examples of a multi-phase AGN outflow, diverse views on star formation activity and a unique changing-look AGN. CARS will provide an essential low-redshift reference sample for ongoing and forthcoming AGN surveys at high redshift.

*CARS Team:
Bernd Husemann, MPIA, Germany; Francoise Combes, Obs. de Paris, France; Scott Croom, Univ. Sydney, Australia; Andreas Eckart, Univ. Cologne, Germany; Gerold Busch, Univ. Cologne, Germany; Timothy A. Davis, Cardiff Univ., United Kingdom; Dimitri Gadotti, ESO; Mirko Krumpe, AIP, Potsdam, Germany; Rebecca McElroy, Univ. Sydney, Australia; Justus Neumann, AIP, Potsdam, Germany; Miguel Perez-Tores, IAA, Granada, Spain; Meredith Powell, Yale Univ., USA; Julia Scharwächter, Gemini Observatory, USA; Grant Tremblay, Yale Univ., USA; Tanya Urrutia, AIP, Potsdam, Germany. Phil Appleton, IPAC, USA; Matthieu Bethermin, Aix-Marseille Univ., France; Vardha N. Bennert, California State Univ., USA; Jason Dexter, MPE, Munich, Germany; Jens Dierkes, Univ. Göttingen, Germany; Nastaran Fazeli, Univ. Cologne, Germany; Brent Groves, ANU, Canberra, Australia; Mónica Valencia-S., Univ. Cologne, Germany; Barry Rothberg, LBT, USA; Lutz Wisotzki, AIP, Potsdam, Germany.

Science drivers

The powerful engines of AGN are known to drive very fast winds with speeds of more than 10 000 km s^{-1} based on the detection of very broad absorption lines at rest-frame X-ray and UV wavelengths. Furthermore, systematically blue-shifted wings in high ionisation lines, for example the [O III] 5007 Å emission and Na I D absorption lines, support the notion that those outflows are quite common in AGN and may significantly affect their host galaxies. These gas outflows were resolved with the Hubble Space Telescope (HST) for very nearby AGN host galaxies, and were shown to reach several hundreds of pc in size with a (hollow) biconical geometry (Fischer et al., 2013). It is expected that those outflows become more extended with increasing AGN luminosities and thereby influence the evolution of the entire host galaxies.

Since the interstellar medium (ISM) consists of different gas phases with a large range in temperature (10–10^6 K) and density (0.1–1000 cm^{-3}), it has been difficult to infer the total mass outflow rates and energetics as a function of radius. In particular, the cold molecular gas phase may carry the bulk mass in the outflow (Cicone et al., 2014), despite the ionised gas phase being easier to detect. Hence, multi-wavelength observations are crucial for characterising AGN-driven outflows and to verify whether the winds are either energy- or momentum-driven. In addition, not only the intense and hard radiation field of the AGN may accelerate the gas; radio jets can also directly impact and drive gas far away from the galaxy nucleus. High-resolution radio continuum images are needed to confirm or exclude the presence of extended radio jets in individual objects to discriminate between the different driving mechanisms.

Theorists mainly invoke AGN feedback to suppress star formation during galaxy evolution in order to reproduce the distribution of observed galaxy properties in the present-day Universe. However, a clear causal connection between AGN outflows and the suppression of star formation has not yet been observationally confirmed. Obvious issues that must be overcome to solve this puzzle include the very short timescales of AGN phases with respect to the large dynamical time of the host galaxy, the different timescales probed by star formation indicators, and sample selection effects of AGN and non-AGN control samples (see review by Harrison, 2017).

Many of the current AGN surveys, like the KMOS AGN Survey at High redshift (KASHz; Harrison et al., 2016), the SINFONI Survey for Unveiling the Physics and the Effect of Radiative feedback (SUPER; PI: V. Mainieri) and the WISE/SDSS-selected hyper-luminous quasar survey (WISSH; Bischetti et al., 2017), are focused on luminous AGN at redshifts between 1 and 3 where the peak in cosmic star formation occurs. However, the drawback is a large physical scale of > 7 kpc per arcsecond, which significantly limits the achievable spatial resolution (see Figure 1). For CARS we decided to target a representative sample of the most luminous AGN in the nearby Universe, with redshifts of $0.01 < z < 0.06$. This approach allows us to dissect their host galaxies easily at sub-kpc scales, while still probing an important part of the AGN luminosity function. Thereby, CARS provides a unique reference data set for all high-redshift AGN and bridges the gap between low-luminosity AGN and the rare ultra-luminous AGN.

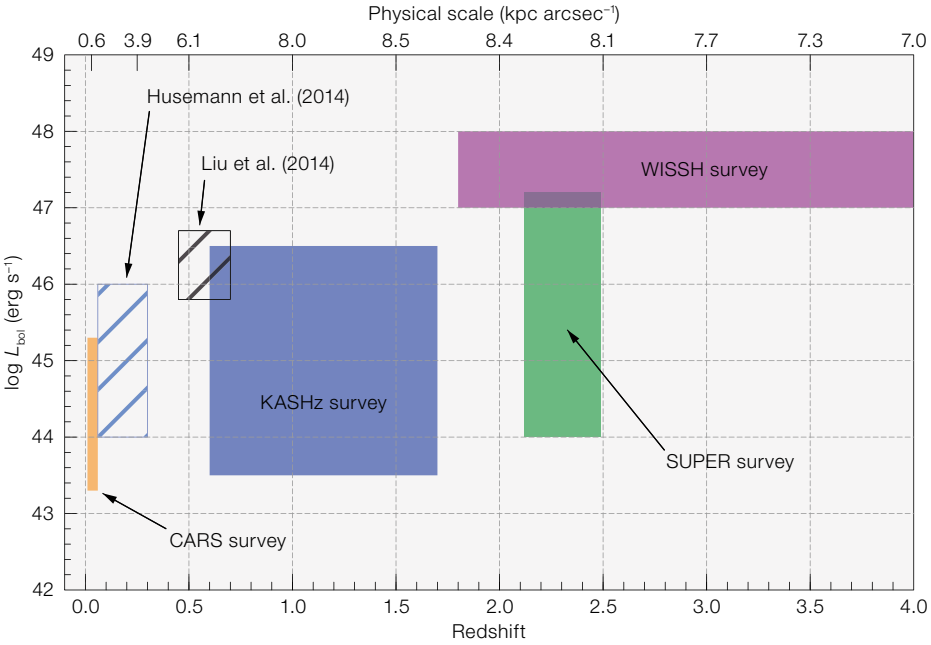

Figure 1. Redshift and AGN luminosity range of various existing and ongoing spatially resolved spectroscopic AGN surveys compared to CARS.

CARS sample and data

CARS is focused on Type I AGN, where the central engine is not blocked by obscuring material. Therefore, the black hole masses can be constrained from the optical spectra, and the point-spread function (PSF) of individual observations can be reconstructed by mapping the intensity of the broad lines from the unresolved nucleus (Jahnke et al., 2004). The largest catalogue of luminous Type I AGN in the southern hemisphere is the Hamburg-ESO Survey (HES; Wisotzki et al., 2000), where objects were selected through *B*-band imaging and slitless spectroscopy. A sub-sample of 99 Type I AGN with $z < 0.06$ has been intensively studied by the group of Andreas Eckart in Cologne (for example, Busch et al., 2014). From this sample, 41 galaxies have already been targeted with single-dish submillimetre telescopes to obtain cold molecular gas masses via the CO(1–0) emission line (Bertram et al., 2007). Since molecular gas content is the prime fuel for star formation in galaxies and an important quantity to study the feedback process in galaxies, the sub-sample of Bertram et al. (2007) serves as the parent sample for CARS.

Our spatially resolved multi-wavelength observations for CARS rely primarily on a snapshot survey with the Multi-Unit Spectroscopic Explorer (MUSE) on the Very Large Telescope (VLT) taken in Periods 94 and 95. Only 15- to 30-minute on-source exposure times are needed, thanks to the unique sensitivity of MUSE and its large field of view that captures the entire AGN host galaxy in one shot. Each MUSE observation obtains 90 000 spectra across a 1 × 1 arcminute field of view, which provides a wealth of physical information at a physical resolution of about ~ 600 pc at 0.8-arcsecond seeing. This is essential to separate the AGN and host galaxy emission and study the stellar and ionised gas components, their respective kinematic fields, ionisation conditions and the distribution of star-forming H II region complexes. The high quality and power of MUSE are shown in Figure 2, where we compare broad-band with pseudo-narrow-band colour images, which already reveal different ISM ionisation conditions in different kinds of host galaxies.

Since the ionised gas represents just one particular phase of the ISM, a large effort has been made by the CARS team to obtain spatially resolved observations of all other important gas phases of the ISM, i.e. atomic, molecular, warm-ionised and hot gas. The cold gas phases are traced by deep Jansky Very Large Array (JVLA) observations of H I at ~ 15-arcsecond resolution and ALMA observations of CO(1–0) at 0.8-arcsecond resolution. Furthermore, we have successfully obtained [C II] observations with the Far-Infrared Field-Imaging Line Spectrometer (FIFI-LS) on board the Stratospheric Observatory For Infrared Astronomy (SOFIA) for eight galaxies, and deep X-ray observations with the Chandra satellite to map the hot gas for two targets as a pilot study. Radio continuum images at C (4–8 GHz) and X (8–12 GHz) bands with 1-arcsecond resolution were also obtained for nearly the entire sample with the JVLA to detect extended radio jets and characterise their luminosity, size and orientation if present. Our follow-up observations do not yet cover the entire AGN sample because of sensitivity constraints and availability of observing time, but the first exciting results are coming out of the survey. Below we highlight some of our ongoing work that demonstrates the power of CARS to recover the individual characteristics of AGN host galaxies.

Tracing the impact of AGN outflows

HE 1353–1917 is fairly unique among the CARS targets because it is an edge-on disc galaxy with a bright unobscured AGN. This means that the usual obscuring torus of the AGN is not lined up with the disc and the ionisation cone of the AGN light directly intercepts the disc of its host galaxy. Indeed, the ionisation cones of the AGN are nicely recovered with MUSE as ionised gas filaments nearly parallel on both sides of the galaxy's disc with a projected extension of 30 kpc (Figure 3). The gas-phase metallicity in the ionisation cones exhibits a radial dependence similar to that of the gas in the disc, indicating that the material was likely lifted off the disc by continuous supernova explosions resulting from ongoing star formation, rather than being blown out by the AGN.

However, looking closer at the heart of the galaxy, the MUSE data reveal a distinct region of ionised gas with very

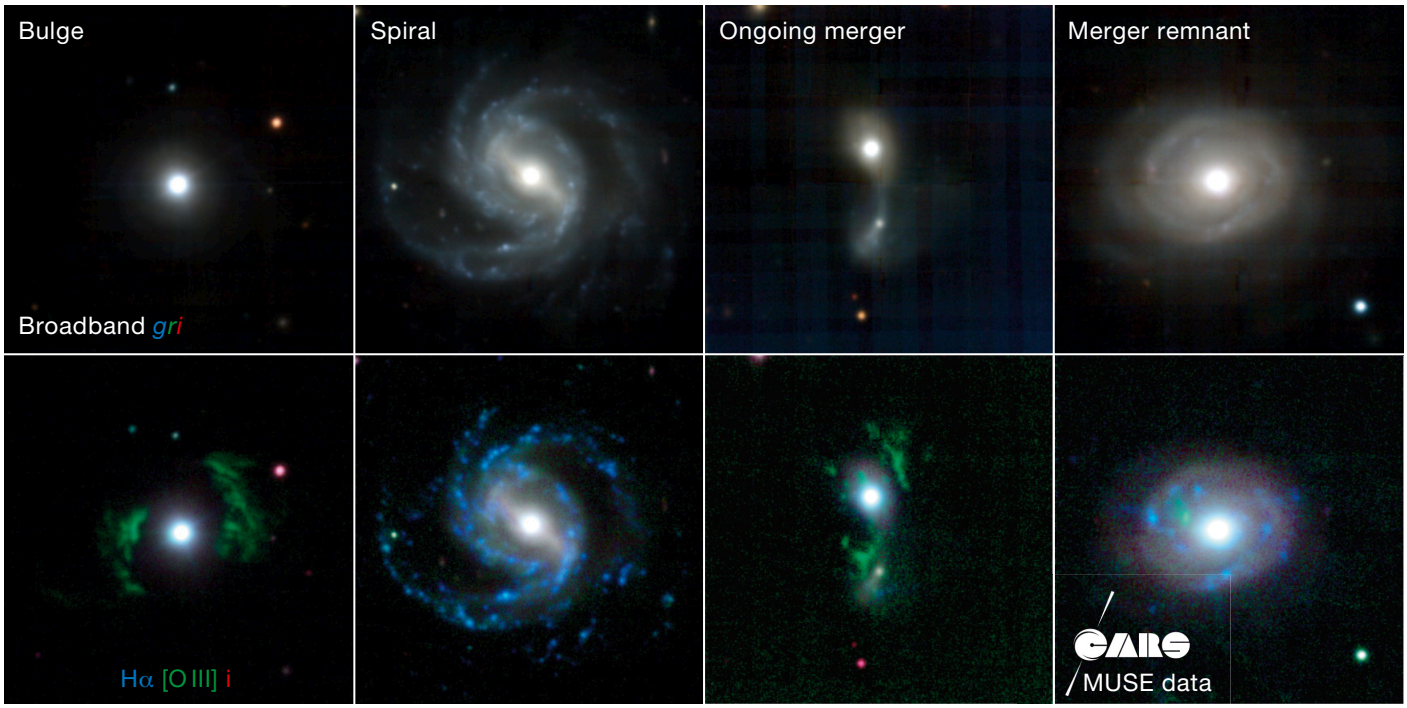

Figure 2 (Above). Broad-band (upper row) and narrow-band (lower row) colour images reconstructed from the MUSE data for four CARS galaxies as examples. Narrow-band images centred on important emission lines reveal very different ISM ionisation states (blue — ongoing star formation, green — AGN photoionisation) and ionised gas distributions on kpc scales reaching beyond the host galaxies in some cases.

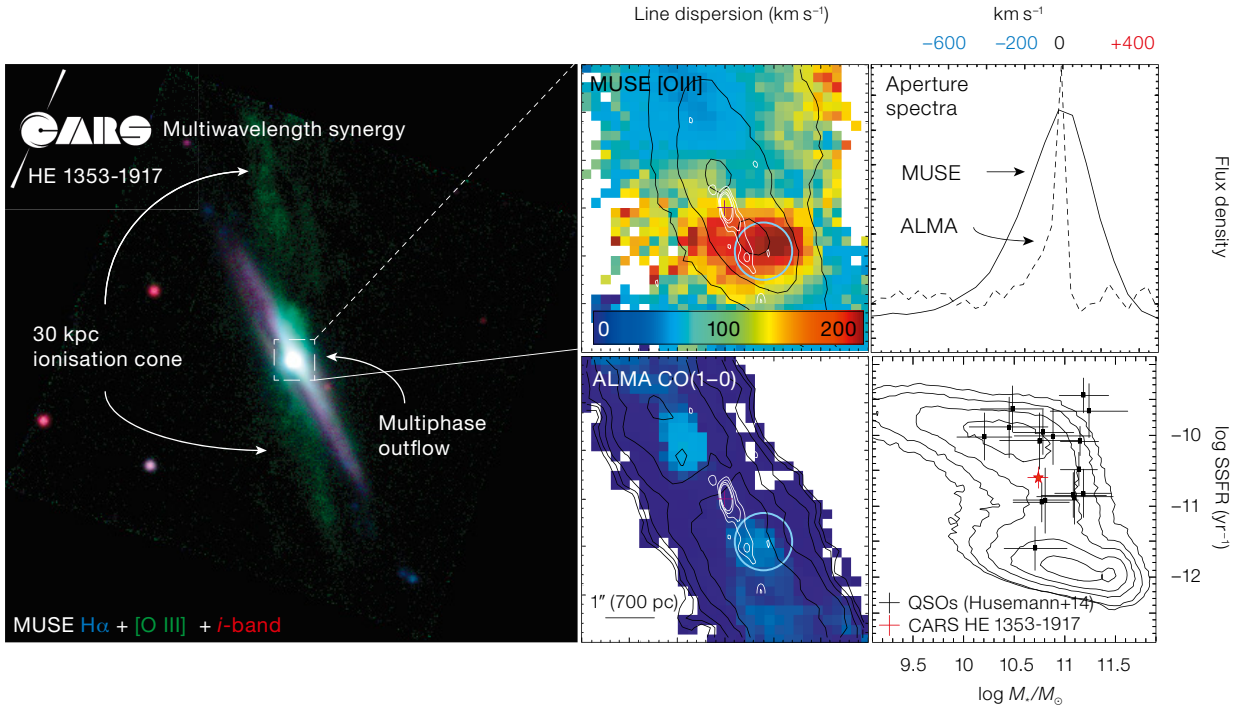

Figure 3 (Below). CARS discovers a spectacular 30 kpc-long ionisation cone (left panel) and a bipolar multi-phase outflow from high velocity dispersion regions (centre panels) in the edge-on CARS galaxy HE 1353–1917. Extended radio emission obtained with the JVLA (white contours, middle panels) is indicative of a low-luminosity radio jet. The different line shapes in the ionised ([O III] from MUSE) and molecular (CO(1–0) from ALMA) gas shown in the upper right panel may be a consequence of the mass and outflow momentum carried in the different gas phases. This galaxy is located in the so-called "green valley" of galaxies with lower specific star formation compared to normal disc galaxies (contours in lower right panel), potentially as a consequence of the outflow's clearing the central kpc of gas.

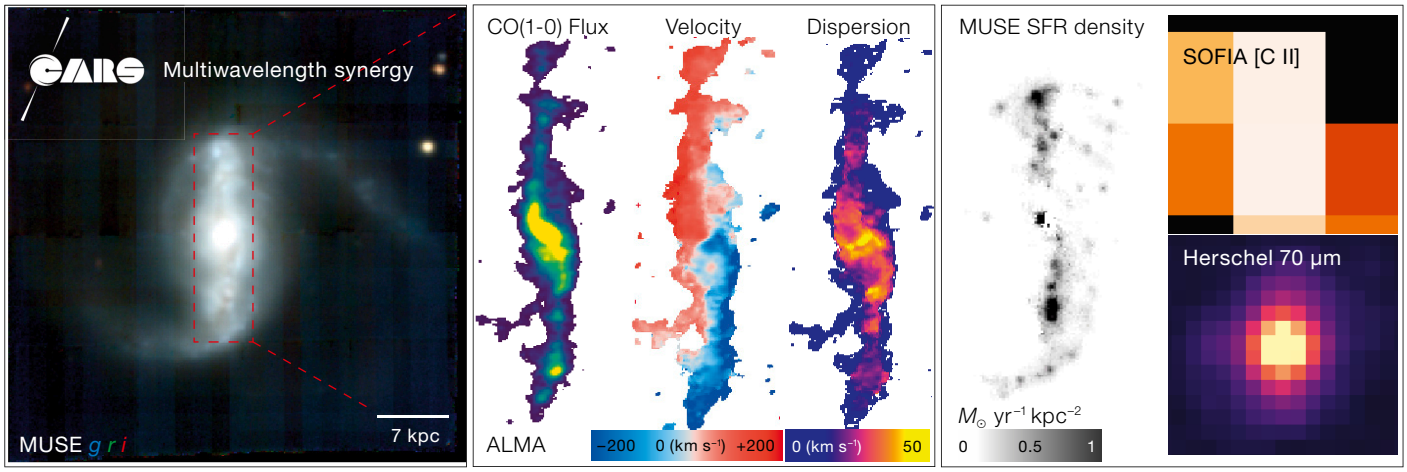

Figure 4. Images of various star formation tracers for the strongly barred CARS galaxy HE 0433–1028 with a luminous AGN at its centre. The left panel shows the *gri*-band composite image from MUSE. The centre panel shows the CO(1–0) emission from the bar, with flux, radial velocity (with a signature of radial motions along the bar), and velocity dispersion. The right panel shows the star formation rate derived from MUSE (Hα) compared to the infrared line ([C II]) and continuum (Herschel 70 μm) appearance.

high velocity dispersion about 1 kpc away from the nucleus. A broad wing in the ionised gas emission lines with an excess in blue-shifted velocities of a few 100 km s^{-1} (Figure 3, upper panels) confirms the presence of a powerful outflow. The JVLA continuum image reveals an extended radio structure terminating at this "hot spot", providing evidence for a possible radio jet. ALMA follow-up observations tracing the molecular gas with the CO(1–0) line also show elevated line dispersion at the same location (Figure 3, lower middle panel), which also occurs on the opposite side of the nucleus at the same distance. The outflow velocities are significantly lower than in the ionised gas, but the wings on the approaching and receding sides are detected as well. Since the molecular gas mass in the outflow is a factor of over 10 more than the ionised gas mass, the lower velocities can be understood in terms of a common momentum carried by the different gas phases, and the changing phase structure of the gas as it flows outwards. Such multi-gas-phase kinematic classifications are therefore important to understanding the physics of AGN-driven outflows. A systematic investigation of AGN-driven outflows in CARS is on the way and will help to understand the incidence, timescales, energetics and driving mechanisms.

One of the big questions for feedback is whether AGN-driven outflows actually cause a suppression of star formation. From the reconstructed broad-band spectral energy distribution of HE 1353–1917 spanning the ultraviolet to the far-infrared, we obtained the stellar mass and specific star formation rate (SSFR). When comparing this to the distribution of galaxies from the Sloan Digital Sky Survey (SDSS), we indeed find a suppression of star formation in HE 1353–1917 compared to that expected for a star-forming disc galaxy at a given stellar mass (lower right panel of Figure 3). This may be explained by a reduced cold gas content and we confirm this for the central circular region of the galaxy with a radius roughly matching the location of the detected shock front. It is tempting to argue for a causal connection between the AGN, the development of an extended outflow in the disc, and the suppressed star formation. However, secular evolution of the galaxy, a bar for example, could lead to a similar reduction of gas and star formation around the centre. Hence, we will have to employ the statistical power of CARS to verify those causal connections in the future.

Star formation in AGN host galaxies

Understanding how star formation and AGN are linked is one of the key aspects of understanding the feedback processes. However, it is notoriously difficult to measure the current SFR in AGN hosts cleanly as the tracers are usually contaminated by the bright AGN light. With CARS we do not want to focus on one measurement, but actually compare various star formation tracers, in order to understand the systematic effects in previous studies and guide future observations at low and high redshift.

An example of how our exquisite multi-wavelength data set can shed light on this issue can be seen in HE 0433–1028, also known as Mrk 618. This galaxy is strongly barred, with intense star formation occurring along the bar. This is already unusual, as star formation is often suppressed along a bar by the high-shear environment. The molecular gas kinematics from ALMA reveal that the gas is apparently funneled inwards, along x_1 orbits at the leading edge of the bar, towards the inner regions where the black hole is being fueled (Figure 4). Gas clouds that are travelling along the x_1 orbits of the bar are subject to a velocity gradient perpendicular to the bar major axis. The resulting shear can disrupt the clouds and prevent them from collapsing and forming stars, which is not the case for HE 0433–1028.

In terms of SFR, we can use MUSE to map the Hα line, which we can verify is dominated by star formation ionisation by employing various emission-line ratio diagnostics, and also correction for dust attenuation as measured from the Balmer decrement. In order to subtract the bright nucleus we employ dedicated PSF-sub-

traction schemes optimised for integral field unit (IFU) data (QDeblend^{3D}; Husemann et al., 2014). Archival far-infrared (FIR) observations are available from the Herschel satellite mission and we also mapped the bright [C II] 158 µm emission line with SOFIA, the only operating FIR observatory in the current post-Herschel era (Figure 4, right panels). Despite the low spatial resolution of SOFIA in the FIR, we can degrade the SFR maps inferred from the MUSE Hα map to test how well all the emission relates to each other in a spatially resolved manner. This has not been done before, but provides important clues for the use of [C II] as a tracer for star formation and/or AGN outflows for high-redshift AGN observed with ALMA.

Mrk 1018 — A unique changing-look AGN

A problem with linking AGN and their host galaxies is the timescale of AGN variability. The CARS team discovered an extreme AGN variability event, which the team is currently monitoring in detail across the electromagnetic spectrum from X-ray to radio. Upon examining the MUSE data for Mrk 1018, we were surprised to find that the typical broad emission lines and continuum emission of a Type I AGN had almost completely disappeared (McElroy et al., 2016). Checking the literature we realised that this was not the first time Mrk 1018 had undergone a dramatic change, as this source also experienced something similar three decades ago. In the 1970s its spectrum also showed weak broad emission lines that then significantly brightened, appearing as a luminous Type I AGN a few years later. The MUSE observation taken by CARS clearly shows that the nucleus has faded significantly. The reconstructed AGN light curve reveals that the dimming started just a few years ago, between 2011 and 2013 (Figure 5).

Although AGN are known to be variable sources at all wavelengths, such dramatic changes in luminosity on short timescales are very unusual. The CARS team obtained rapid follow-up observations with Chandra at X-ray and with HST at far-ultraviolet (FUV) wavelengths. The X-ray spectra do not show any evidence for an increased column density of gas along our line of sight to the AGN, which rules out a temporary obscuration event as an explanation for the dimming (Husemann et al., 2016). A tidal disruption event (TDE) is also excluded because the bright AGN phase was too stable over a long period, which is not predicted by current TDE models. The FUV, which directly probes the accretion disc emission, also fell by a factor of 10–25 in 2016 compared to 2010. This leaves changes in the physical properties of the accretion disc itself as the only option. However, this is difficult to explain with standard accretion disc theory. The viscous timescale of an accretion disc around a black hole of $10^8\,M_\odot$ (as in Mrk 1018) is several thousand years. We therefore speculated that the accretion disc is perturbed via an accretion disc outflow or an interaction with a nearby companion black hole, as highlighted in a recent ESO press release (eso1613).

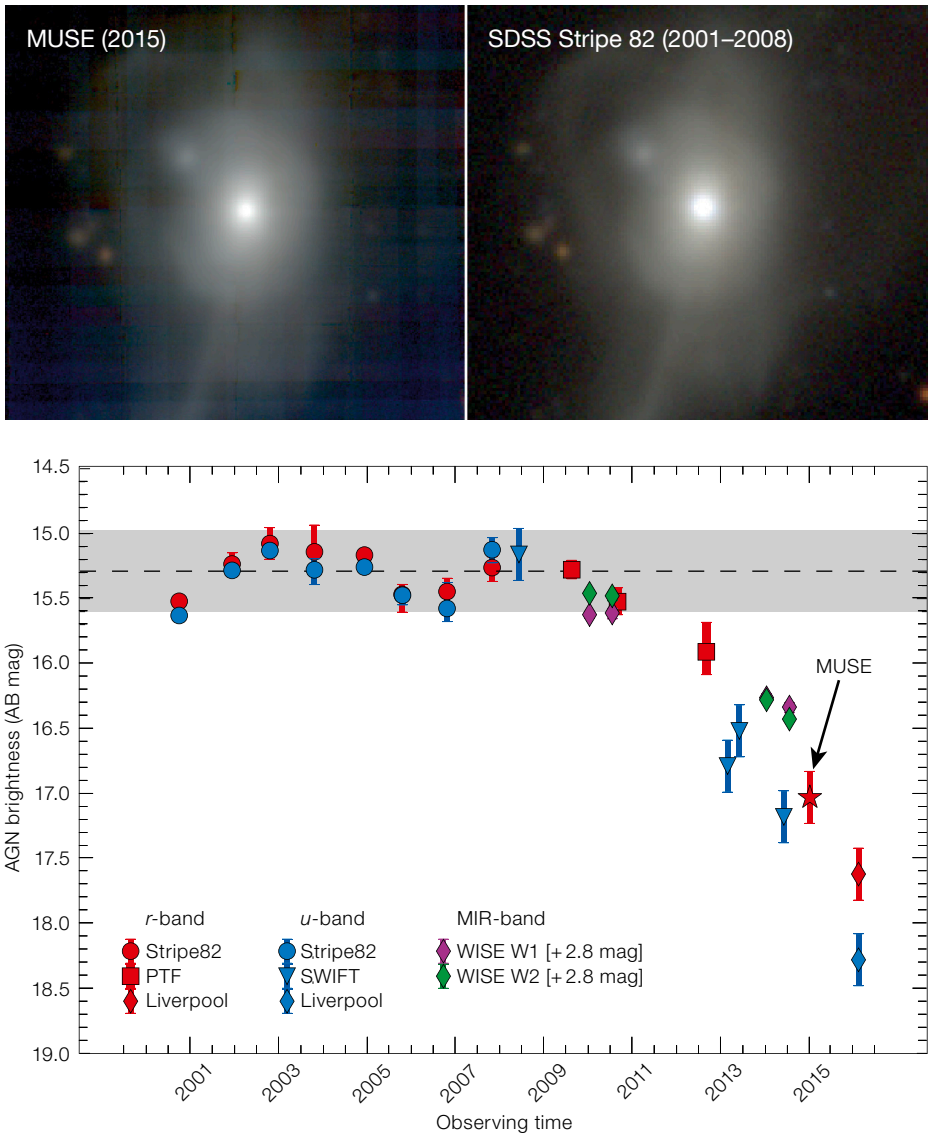

Figure 5. CARS serendipitously discovered an extreme "changing-look" AGN event in Mrk 1018. Upper panels: comparison of reconstructed *r*-band MUSE image with co-added broad-band SDSS Stripe 82 image, revealing a fading nucleus. Lower panel: a 16-year optical lightcurve of the nucleus, highlighting its rapid luminosity drop in recent years and the point of our MUSE discovery.

It is exciting to witness how the accretion disc around a very massive black hole is undergoing a major reconfiguration over just a few years. The CARS team has trig-

gered various ongoing monitoring campaigns in the optical with the VLT VIsible Multi Object Spectrograph (VIMOS), in the FUV with Hubble and in X-rays with Chandra and the X-ray Multi Mirror satellite (XMM-Newton). This will be crucial in understanding the underlying physical mechanism(s) behind the dramatic changes in this archetypical changing-look AGN. More exciting results may therefore be expected from Mrk 1018; stay tuned!

Outlook

The Close AGN Reference Survey (CARS) combines data from several state-of-the-art facilities to establish a spatially resolved multi-wavelength sample and convenes a diverse team with varied expertise. CARS offers a dataset covering a large wavelength range with additional data for selected objects. The combination of such a multi-wavelength dataset for nearby AGN host galaxies with such relatively high AGN luminosities at low redshifts is unique. It opens up a new window to study the link between AGN and their host galaxies via the exchange of energy and baryons.

Even more observations will be taken for CARS in the next year by ALMA to compare molecular and optical emission line diagnostics over the entire host galaxies, spectroscopy with VIMOS IFU in the optical blue wavelength range not covered by MUSE, and wide-field optical and near-infrared imaging to characterise the environment of all CARS AGN host galaxies. In addition, ongoing monitoring of the unique changing-look AGN Mrk 1018 will likely lead to new discoveries that provide important insights into the physics of accretion.

While a first series of CARS papers is currently being prepared by the team, it will clearly be a long-term effort to build up statistical AGN samples. Only with such systematic approaches can the physics of outflows, feedback, fuelling and quenching in AGN host galaxies be revealed. The ultimate aim of CARS is to establish a unique low-redshift reference point for ongoing AGN surveys at high redshift, such as KASHz, SUPER and WISSH, with a long-lasting legacy value.

Acknowledgements

We are grateful to the many Time Allocation and Director's Discretionary Time committees who have enabled CARS to grow into a legacy-class multi-wavelength dataset. We also warmly thank the extraordinary staff at ESO, ALMA, JVLA, SOFIA, and many other observatories, for their tireless work in the preparation and execution of CARS observations, enabling fantastic science for our team and the scientific community as a whole. We feel fortunate and thankful to be advised by a world-class Scientific Advisory Board, led by Francoise Combes, Scott Croom and Andreas Eckart. You can learn more about the CARS survey via the website[1].

References

Bertram, T. et al. 2007, A&A, 470, 571
Bischetti, M. et al. 2017, A&A, 598, A122
Busch, G. et al. 2014, A&A, 561, A140
Cicone, C. et al. 2014, A&A, 562, A21
Fischer, T. C. et al. 2013, ApJS, 209, 1
Harrison, C. M. 2017, Nature Astronomy, 1, 0165
Harrison, C. M. et al. 2016, MNRAS, 456, 1195
Husemann, B. et al. 2014, MNRAS, 443, 755
Husemann, B. et al. 2016, A&A, 593, L9
Jahnke, K. et al. 2004, AN, 325, 128
Liu, G., Zakamska, N. L. & Greene, J. E. 2014, MNRAS, 442, 1303
McElroy, R. et al. 2016, A&A, 593, L8
Wisotzki, L. et al. 2000, A&A, 358, 7

Links

[1] CARS: http://www.cars-survey.org

A. Tudorica/ESO

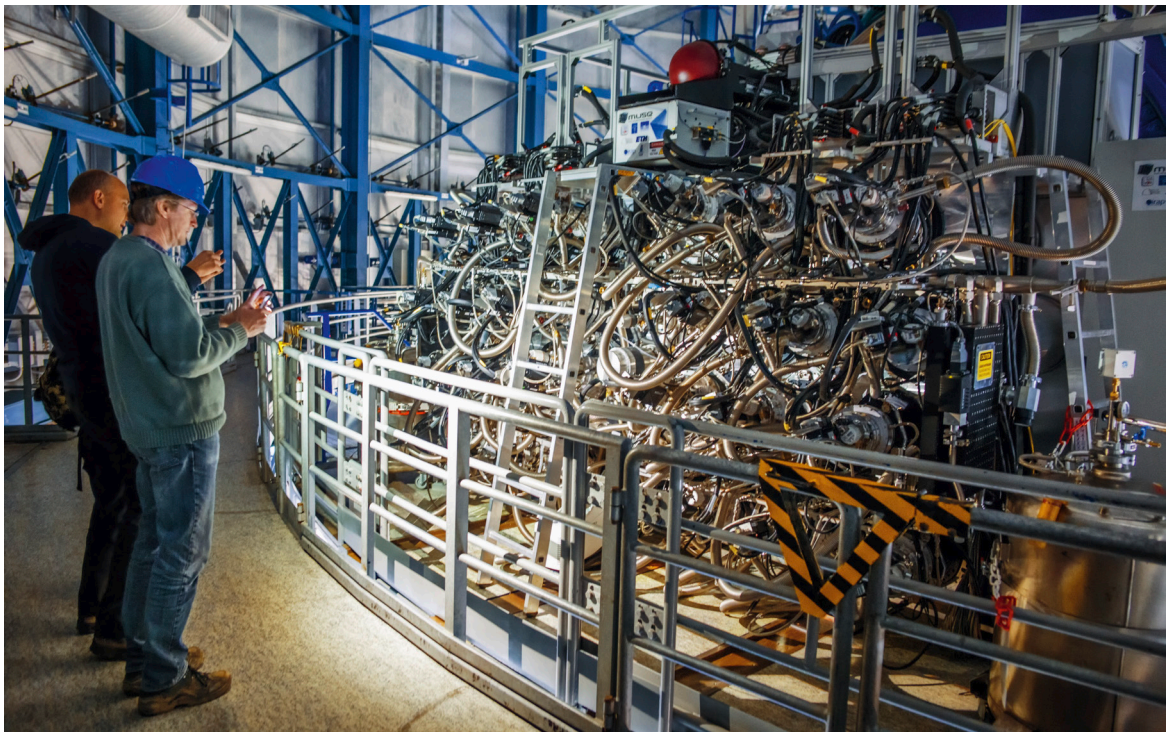

The MUSE instrument, showing the intricate network of pipes surrounding its 24 spectrographs.

DOI: 10.18727/0722-6691/5039

ALMA Observations of $z \sim 7$ Quasar Hosts: Massive Galaxies in Formation

Bram P. Venemans[1]

[1] Max Planck Institute for Astronomy, Heidelberg, Germany

Luminous high-redshift quasars are thought to be hosted by the most massive and luminous galaxies in the early Universe. Over the past few years, we have discovered several quasars at $z \sim 7$ powered by $> 10^9\ M_\odot$ black holes, which allow us to study the formation and evolution of massive galaxies at the highest redshifts. ALMA and PdBI/NOEMA observations have revealed that these $z \sim 7$ quasars are hosted by far-infrared-bright galaxies with far-infrared luminosities $> 10^{12}\ L_\odot$, indicating star formation rates between 100 and 1600 $M_\odot$ year^{-1}. High-resolution ALMA imaging of a quasar host at $z = 7.1$ shows that a high fraction of both the dust continuum and [C II] 158 µm emission comes from a compact region < 2 square kiloparsecs across. Observations of emission from CO and neutral carbon in our $z \sim 7$ hosts provide the first constraints on the properties of the interstellar medium and suggest that the gas heating is dominated by star formation.

Distant quasars: beacons in the early Universe

Among the outstanding important questions in astronomy are when the first galaxies formed, and what their physical properties were. Galaxy candidates have now been identified through deep optical/near-infrared imaging surveys out to redshifts of $z > 10$, only ~ 450 million years after the Big Bang (see, for example, the recent review by Stark, 2016). However, their faintness typically prohibits detailed studies of their nature and characteristics, and, often even their spectroscopic confirmation. Indeed, studying the detailed physical properties of these objects and their contribution to cosmic reionisation is one of the main drivers for the James Webb Space Telescope (JWST) and the next generation of large optical telescopes (in particular the ESO Extremely Large Telescope, ELT).

An effective way to learn more about the constituents of galaxies at the highest redshifts is to study the brightest (and most massive) members of this population. Such luminous galaxies are very rare and not found in the deep, pencil-beam studies that are typically used for high-redshift galaxy searches with, for example, the Hubble Space Telescope (HST).

Quasars are among the most luminous non-transient sources in the Universe. As a result they can be seen out to very high redshift, $z > 7$. Quasars are powered by (supermassive) black holes that accrete matter from their environment. The host galaxies of accreting supermassive black holes at $z > 2$ are among the brightest and most massive galaxies found at these redshifts (for example, Seymour et al., 2007). Therefore, an effective method to pinpoint the most massive and luminous galaxies in the early Universe is to locate bright quasars at the highest redshifts.

A crucial initial step is to find such bright quasars at large cosmological distances. This is extremely difficult as they are very rare (only one luminous quasar is expected at $z \sim 6$ per > 100 square degrees on the sky) and requires large optical/near-infrared surveys that cover a large area. Indeed, the Sloan Digital Sky Survey discovered about 20 bright quasars around $z \sim 6$ (less than 1 Gyr after the Big Bang), which are shown to host supermassive black holes ($> 10^9\ M_\odot$; for example, Jiang et al., 2007; De Rosa et al., 2011). Direct imaging of the stellar light of the galaxies hosting these high redshift quasars via rest-frame ultraviolet/optical studies has proven very difficult, if not impossible. On the other hand, observations of the molecular gas in the host galaxies in the radio and (sub)-millimetre (targeting the rest-frame far-infrared emission) allow the determination of the total gas mass and dynamical mass of the hosts. In the last decade, it has been demonstrated that large reservoirs of metal-enriched atomic and molecular gas and dust can exist in massive quasar host galaxies up to $z \sim 6.4$ (see Carilli & Walter, 2013 for a review). These observations already provide tight constraints on models of galaxy formation and evolution (for example, Kuo & Hirashita, 2012; Valiante et al., 2014).

To further constrain the build up of massive galaxies, it is important to locate and study bright quasars at even higher redshifts. Over the last ten years, with the advent of wide-field near-infrared cameras, large near-infrared surveys started to image the sky to sufficient depth to uncover distant quasars. Using various public surveys, such as the UKIRT Infrared Deep Sky Survey (UKIDSS), the Visible and Infrared Survey Telescope for Astronomy (VISTA) Kilo-degree INfrared Galaxy survey (VIKING), the VISTA Hemisphere Survey (VHS), and the Panoramic Survey Telescope And Rapid Response System survey (Pan-STARRS1), we have discovered more than a dozen luminous quasars with redshifts above $z = 6.5$ (for example, Mortlock et al., 2011; Venemans et al., 2013, 2015).

When compared to the quasars found around $z \sim 6$, the absolute magnitudes, black hole masses (of $\geq 10^9\ M_\odot$) and (metal) emission line strengths of these new $z \sim 7$ quasars are remarkably similar (for example, De Rosa et al., 2014), indicating little evolution in the quasar properties over the 200 Myr between $z = 6$ and $z = 7.1$ (~ 25 % of the Universe's age at that time). Furthermore, not only are these $z > 6.5$ quasars among the most distant sources found today, but they also have luminosities that are about two orders of magnitude larger than those of galaxies found at similar redshifts. These $z > 6.5$ quasars therefore provide a good opportunity to gain crucial insight into the formation and evolution of massive galaxies at the highest redshifts, and to understand the origin of the apparent correlation between bulge mass and black hole mass found in nearby galaxies (for example, Kormendy & Ho, 2013). With the completion of the Atacama Large Millimeter/submillimeter Array (ALMA) we now have a state-of-the-art facility to study the host galaxies of distant quasars in detail.

The host galaxies of $z \sim 7$ quasars

To extend the study of quasar host galaxies to $z \sim 7$, we initiated a programme targeting all quasars discovered at $z > 6.5$ at mm wavelengths, independent of their far-infrared brightness, with the aim of sampling the range of properties of quasar host galaxies and investigating the

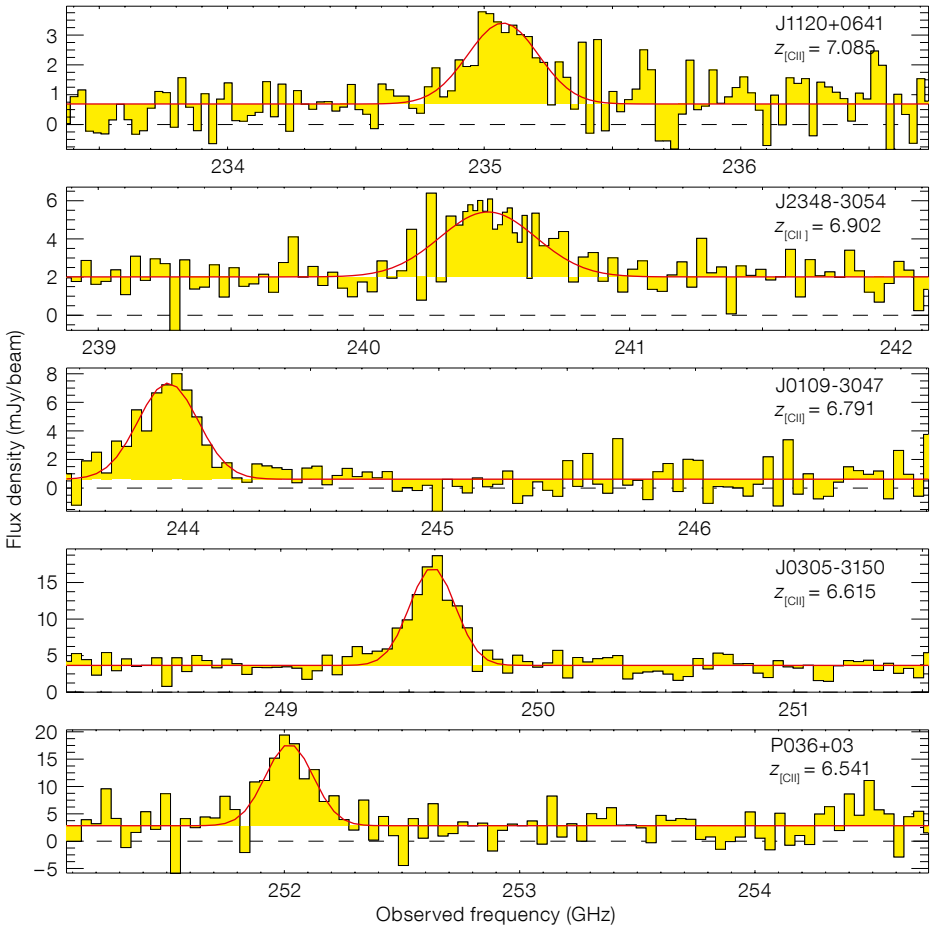

Figure 1. Compilation of [C II] 158 µm observations of five quasars at $z > 6.5$. The top four spectra are from our ALMA Cycle 1 programme (Venemans et al., 2016, 2017a) and the bottom spectrum is from PdBI (Bañados et al., 2015).

relationship between star formation and supermassive black hole growth at $z \sim 7$. Early studies of the host galaxies of $z \sim 6$ quasars, by their nature, concentrated on the far-infrared-bright quasars, and the results from these studies may have introduced a biased view of the characteristics of the typical galaxy hosting a luminous quasar in the early Universe. Using ALMA and the Institut de Radioastronomie Millimétrique (IRAM) Plateau de Bure Interferometer (PdBI), we imaged five $z > 6.5$ quasars, targeting the [C II] emission line (rest-frame wavelength of 158 µm) and the underlying dust continuum in the hosts (Figure 1). An additional seven quasars at $z > 6.5$ have been observed with ALMA and PdBI more recently and in each case the quasar host was detected (for example, Decarli et al., 2017). The host galaxies of $z > 6.5$ quasars show a range of properties, both in the strength and the extent of the far-infrared emission.

The first object in our project was the quasar J1120+0641, at $z = 7.1$ the highest redshift quasar known at that time (Venemans et al., 2012; Figure 1). The host galaxy of this quasar was found to display somewhat different characteristics in its far-infrared (FIR) properties; the far-infrared luminosity of $L_{FIR} = (6–18) \times 10^{11}\,L_{\odot}$ is relatively faint compared to well-studied $z \sim 6$ quasar hosts (which have $L_{FIR} \geq 5 \times 10^{12}\,L_{\odot}$; for example, Wang et al., 2013), and suggests a star formation rate of "only" 100–350 $M_{\odot}\,yr^{-1}$.

Subsequent imaging of four additional $z > 6.5$ quasars revealed a host galaxy population with diverse properties (Figure 1). Both the [C II] emission and the dust continuum vary by a factor up to six among the quasar hosts. The [C II] line fluxes are in the range 1–5 Jy km s^{-1} (corresponding to between $1–6 \times 10^{9}\,L_{\odot}$) and the continuum flux densities range from 0.6 mJy to 3.3 mJy. Despite these variations, all the quasar hosts have far-infrared luminosities of $L_{FIR} \geq 10^{12}\,L_{\odot}$ and can be classified as ultraluminous infrared galaxies (ULIRGs), in contrast to the vast majority of normal galaxies known at these redshifts. The high infrared luminosities indicate that stars formed in these quasar hosts at rates of at least $\sim 100\,M_{\odot}\,yr^{-1}$ and up to $\sim 1600\,M_{\odot}\,yr^{-1}$ (Venemans et al., 2016). Alternatively, using the [C II] luminosity to estimate the star formation rates in the quasar hosts results in very similar values. The far-infrared detections further imply that significant amounts of dust, $M_{Dust} \geq 10^{8}\,M_{\odot}$, have already formed at $z \sim 7$, only 750 Myr after the Big Bang. Such high dust mass requires a very efficient dust production and/or a high stellar mass in the host galaxy (see, for example, Gall et al., 2011).

From the detection of the [C II] emission line, we can start to constrain the dynamical masses of the quasar host galaxies. If we assume that the gas is located in a rotating, thin disc, we can compute the dynamical masses of the hosts from the observed width and spatial extent of the [C II] emission. We estimate that the dynamical masses of the host galaxies at $z > 6.5$ are $10^{10}–10^{11}\,M_{\odot}$. If we compare the host galaxy mass to that of the central black hole, we find a ratio that is higher by a factor 3–4 than found locally (Figure 2; Venemans et al., 2016).

We find that the ratio of black hole mass to galaxy mass evolves with redshift as $(1 + z)^{0.5–0.7}$, indicating that black holes grow faster than their host galaxies in the early Universe. This is supported by the relative growth rates; by computing the growth rate of the black holes (derived from the bolometric luminosities of the quasars) and that of the host galaxies (based on the measured star formation rates), we find that, on average, the black holes are growing at least as fast as their host galaxies.

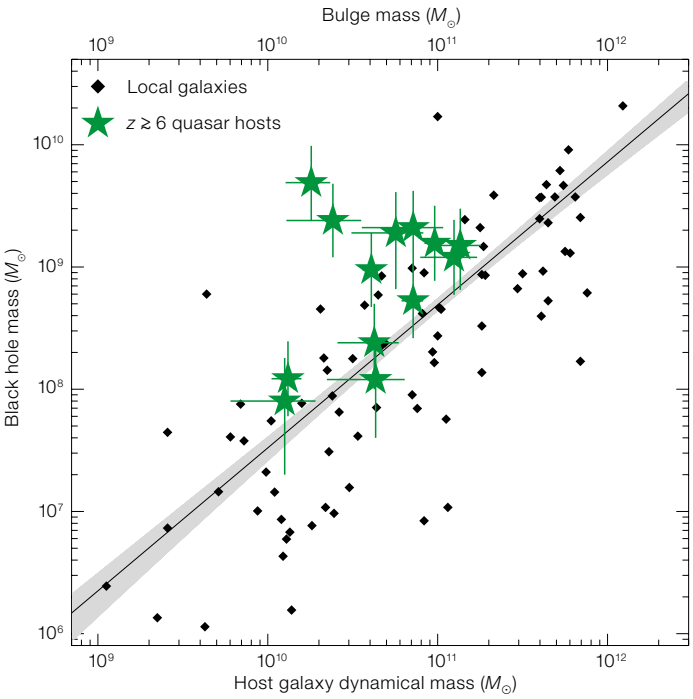

Figure 2. Black hole mass plotted against dynamical mass estimates of $z \geq 6$ quasar host galaxies (filled stars) and the bulge masses of local galaxies (black diamonds, from Kormendy & Ho, 2013). The solid line and grey area show the local black hole to bulge mass relation as derived by Kormendy & Ho (2013). Figure adapted from Venemans et al. (2016).

The crucial assumption in deriving the dynamical masses is that the [C II] emitting gas is distributed in a thin disc. However, our initial observations of the [C II] emission are barely resolved at best. To learn about the spatial distribution and the kinematics of the gas and dust in the quasar host galaxies, higher spatial resolution imaging is essential. We have an ongoing ALMA programme to image the host galaxies of our $z > 6.5$ quasars at high, sub-kiloparsec, resolution (one kiloparsec at $z = 7$ corresponds to an extent of ~ 0.2 arcseconds on the sky). The first source for which we obtained ALMA imaging at a resolution of 1 kiloparsec is the $z = 7.1$ quasar host J1120+0641; the only $z > 7$ quasar known so far.

ALMA high spatial resolution imaging of a $z = 7.1$ quasar host

The host galaxy of the quasar J1120+0641 was initially detected with the PdBI, but the galaxy remained unresolved in the 2 arcsecond beam (~ 10 kpc at the redshift of the quasars; Venemans et al., 2012). As a result, the dynamical mass and the morphology of the line-emitting gas could not be constrained. With ALMA we obtained [C II] imaging at a resolution of 0.23 arcseconds (~ 1 kpc). Surprisingly, the dust continuum and [C II] emission regions are very compact and only marginally resolved in the ALMA data (Figure 3; Venemans et al., 2017a). The majority (80 %) of the emission is associated with a very compact region of size 1.2 × 0.8 square kiloparsecs. Also shown in Figure 3 are the red and blue sides of the emission line: the red contours show emission centred on +265 km s^{-1} and the blue contours the emission centred on −265 km s^{-1}. The red, white and blue crosses indicate the location of the peak of the redshifted, central and blueshifted [C II] emission, respectively. It is clear that there is no evidence for ordered motion at the current resolution.

Applying the virial theorem to these [C II] data yields a dynamical mass for the host galaxy of $(4.3 \pm 0.9) \times 10^{10}\,M_\odot$, only ~ 20 times that of the central supermassive black hole. In the very central region, the dynamical mass of the host is only five times that of the central black hole. In this region, the mass of the black hole and that of the implied dust and gas are able to explain the dynamical mass. In other words, there is not much room for a massive stellar component in the very central region.

The ALMA observations of J1120+0641 begin to spatially resolve the host galaxy of a $z > 7$ quasar. With the even longer baselines available at ALMA, significantly higher-resolution imaging (down to scales of 100s of parsecs) of such distant quasar hosts is now possible, which will start to spatially resolve the sphere of influence of the central supermassive black hole.

The interstellar medium in $z \sim 7$ quasar host galaxies

By measuring the FIR continuum of the $z > 6.5$ quasar host galaxies at different frequencies and observing additional molecular or atomic lines, we can constrain the physical properties of the interstellar medium (ISM) in these galaxies. We therefore obtained additional millimetre and radio observations with ALMA, the PdBI and the US National Radio Astronomy Observatory (NRAO) Karl G. Jansky Very Large Array (VLA) targeting the CO(2–1), CO(6–5), CO(7–6) and [C I] 370 μm emission lines in the $z > 6.5$ quasar hosts (Venemans et al., 2017a,b). An example of ALMA observations of the CO(6–5), CO(7–6), [C I] and underlying continuum emission in a quasar host at $z = 6.9018$ is shown in Figure 4.

We detected CO emission in all of the $z > 6.5$ quasars we targeted, except for J1120+0641. The [C I] emission line was detected in only one quasar host (Figure 4) and was generally found to be significantly fainter than the [C II] line. The derived [C II]/[C I] luminosity ratio was greater than 13 in all cases. From the CO detections, we can determine the mass of the molecular gas reservoirs. Based on the CO line strength, we estimate that the quasar host galaxies contain a molecular gas mass of $(1–3) \times 10^{10}\,M_\odot$. This is approximately ten times the mass of the central supermassive black hole. In all quasar hosts, the (limit on the) strength of the CO emission, in comparison to that of [C II], is very similar to the [C II]/CO line ratio measured in local starburst galaxies and star-forming regions in the Milky Way.

Finally, we can compare the [C II]/[C I] and CO/[C II] line ratios to models to

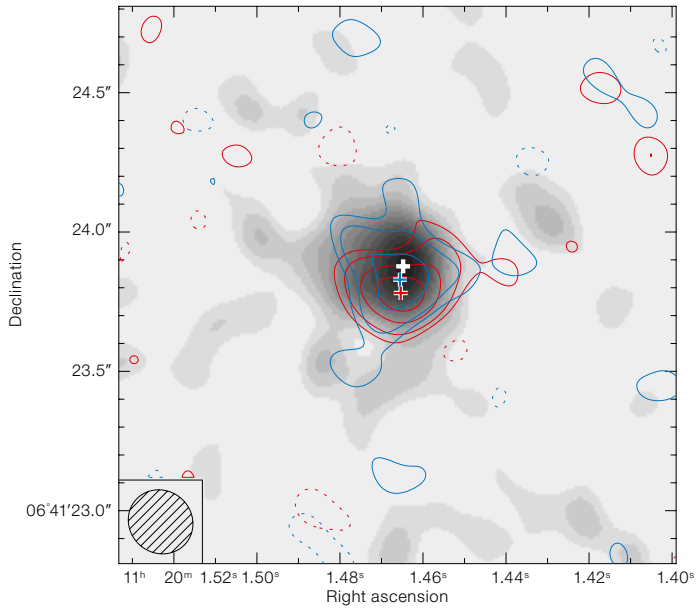

Figure 3. Map of the [C II] emission in J1120+0641 at z = 7.1, averaged over the central 265 km s^{-1} (corresponding to 2/3 × the line full width at half maximium), in greyscale. The red and blue contours show emission centred on 256 km s^{-1} and −265 km s^{-1} respectively. The size of the beam (0.23 × 0.22 arcseconds) is shown in the bottom left corner. Figure adapted from Venemans et al. (2017a).

constrain the physical parameters of the emitting gas. For example, the [C II]/[C I] line ratio can be used to determine the dominant source of radiation (Meijerink et al., 2007): ultraviolet radiation from hot, young stars (a photodissociation region, PDR) or hard X–ray radiation from a central, accreting supermassive black hole (an X-ray-dominated region). The measured (limits on the) [C II]/[C I] line ratio in the z ~ 7 quasar hosts are inconsistent with excitation by an X-ray dominated region. This implies that the heating in the quasar host galaxies is dominated by star formation, and not by the accreting supermassive black hole (Venemans et al., 2017b).

Our observations of CO and [C I] emission lines have enabled us, for the first time, to characterise the physical properties of the ISM in z ~ 7 quasar hosts. By targeting other far-infrared emission lines, such as [O I] 146 µm, [N II] 122 µm, and [O III] 88 µm (all of which are observable with ALMA), we will be able to put further constraints on the properties and metallicity of the interstellar medium in these forming massive galaxies in the early Universe.

Acknowledgements

The work presented here was performed in collaboration with F. Walter, E. Bañados, R. Decarli, E. Farina, C. Ferkinhoff, J. Findlay, P. Hewett, J. Hodge, R. McMahon, R. Meijerink, D. Mortlock, C. Simpson, W. Sutherland, S. Warren, A. Weiß and L. Zschaechner.

References

Bañados, E. et al. 2015, ApJL, 805, L8
Carilli, C. L. & Walter, F. 2013, ARA&A, 51, 105
Decarli, R. et al. 2017, Nature, 545, 457
De Rosa, G. et al. 2011, ApJ, 739, 56
De Rosa, G. et al. 2014, ApJ, 790, 145
Gall, C. et al. 2011, A&ARv, 19, 43
Jiang, L. et al. 2007, AJ, 134, 1150
Kormendy, J. & Ho, L. C. 2013, ARA&A, 51, 511
Kuo, T.-M. & Hirashita, H. 2012, MNRAS, 424, L34
Meijerink, R. et al. 2007, A&A, 461, 793
Mortlock, D. J. et al. 2011, Nature, 474, 616
Seymour, N. et al. 2007, ApJS, 171, 353
Stark, D. P. 2016, ARA&A, 54, 761
Valiante, R. et al. 2014, MNRAS, 444, 2442
Venemans, B. P. et al. 2012, ApJL, 751, L25
Venemans, B. P. et al. 2013, ApJ, 779, 24
Venemans, B. P. et al. 2015, ApJL, 801, L11
Venemans, B. P. et al. 2016, ApJ, 816, 37
Venemans, B. P. et al. 2017a, ApJ, 837, 146
Venemans, B. P. et al. 2017b, ApJ, 845, 154

Figure 4. Maps showing (left to right) the CO(6–5), CO(7–6), [CI] 370 µm and continuum emission at an observed wavelength of 3 mm in the host galaxy of quasar J2348-3054 at z = 6.9018. These ALMA measurements constitute the highest-redshift CO detections to date. Figure adapted from Venemans et al. (2017b).

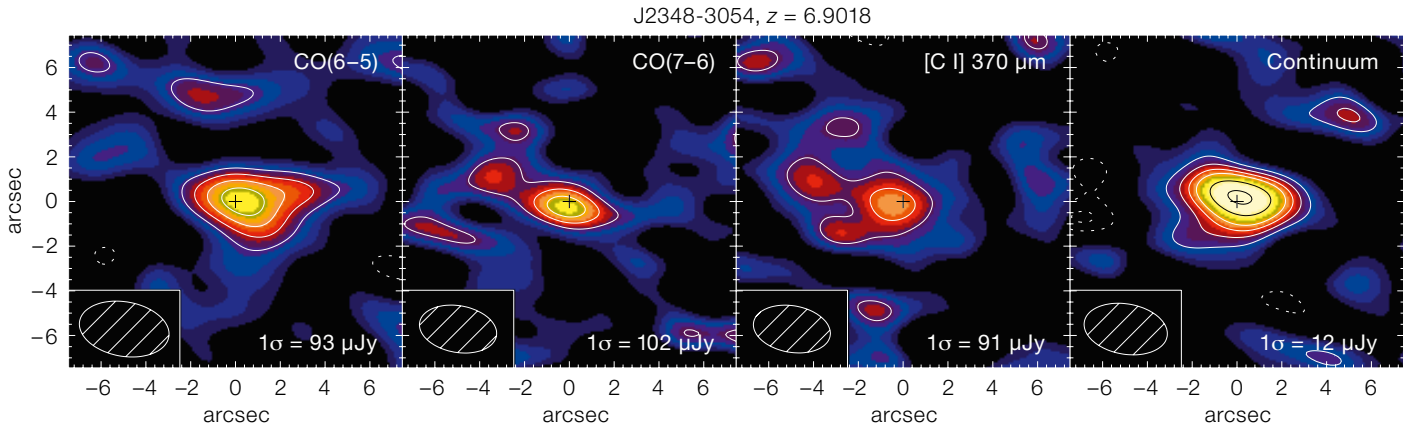

ESO/P. Horálek

Upper: ESO staff testing the new planetarium at the ESO Supernova and Visitor Centre.

Lower: An Australian delegation visited ESO Headquarters on 20 July 2017.

DOI: 10.18727/0722-6691/5040

The Deadline Flurry Formula

Felix Stoehr[1]

[1] ESO

When having to deliver work to a fixed deadline people often wait until the very last minute, in part, because they procrastinate. While procrastination has been studied extensively in the psychology literature, few direct measures of human behaviour leading up to a deadline exist. Here we use metadata from the ALMA proposal submission process over the last five years and find that collective human behaviour for submitting work before a deadline can be described spectacularly well by a simple "universal" law. We also analyse this behaviour as a function of several other factors, such as gender, age, proposal size, number of co-authors and the subsequent success of a submitted proposal.

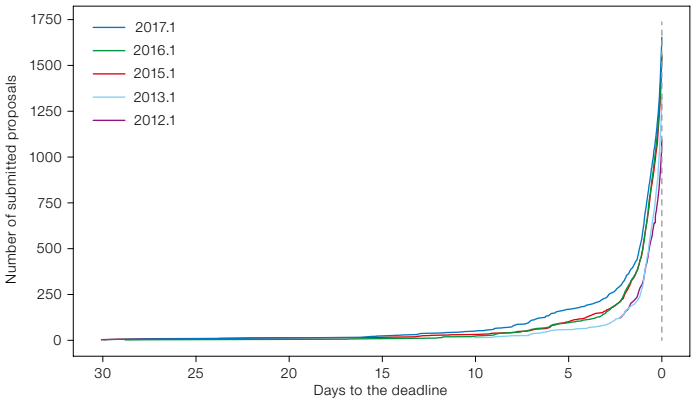

Figure 1. Evolution of the number of proposals submitted to ALMA as a function of the time remaining until the proposal deadline (since the first submission of the proposal) for the different ALMA proposal cycles (see legend). The vertical grey dashed line indicates the proposal deadline.

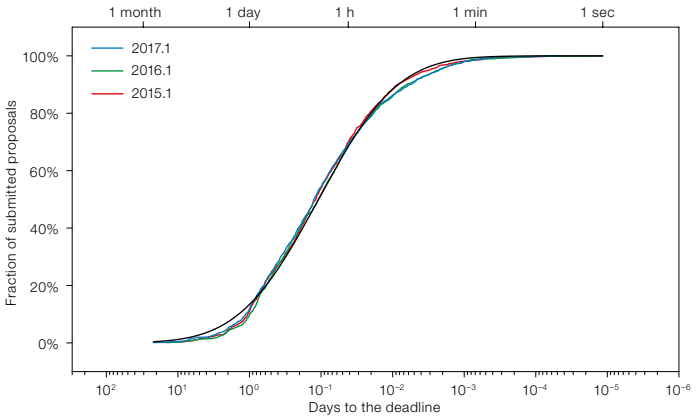

Figure 2. Fraction of submitted proposals as a function of log time to the deadline using the moments of last submission of the proposals for the last three ALMA proposal cycles (3–5). The black line shows the lognormal distribution with $\mu^* = 2h\ 36m$ and $\sigma^* = 0.1349$, explaining 99.87 % of the signal.

Introduction

It is deeply rooted in human nature that work which needs to be delivered by a fixed deadline is often delivered only at the very last moment. Together with factors like a large overall workload and the fact that the delivery itself is the culmination of a long period of work, one reason is certainly procrastination, i.e. the act of delaying a task that must be done. Procrastination was probably first mentioned by Hesiod around 700 BC (Evelyn-White, 1936). Steel (2006) compiled a large meta-study of the state of research on the nature of procrastination. Such psychological studies often focus on the causes (for example, task aversiveness, task delay, self-efficacy, active *vs.* passive procrastination) and the effects on performance. In most cases, these studies rely on questionnaires filled out by test persons (using, for example, the Tuckman Procrastination Scale [Tuckman, 1991]). The correlation between self-reported and actual procrastination, however, is relatively low (Tice & Baumeister, 1997).

In this study, we use the metadata from the Atacama Large Millimeter/Submillimeter Array (ALMA) observing proposal submission process since 2012. ALMA conducts essentially yearly calls for proposals, of one month's duration, with the particularity that users can modify their proposals as often as they wish before the deadline. The number of proposals received in the latest cycles is larger than that of any other single telescope proposal process worldwide.

The metadata are ideally suited to such an analysis. In particular the data are fully objective; the amount of work a Principal Investigator (PI) needs to deliver is fixed by the maximum length of the proposal of four pages (five pages in Cycle 5), which is strictly enforced; the proposals are received well distributed over all time zones; the proposal deadline is strict; additional metadata on the proposals are available (for example, whether the proposal is a student proposal and whether or not it was awarded observing time); and, finally, the incentive to work for a very significant amount of time on a proposal is very high. Indeed, with a single highly competitive call for ALMA proposals per year, the award of observing time can have an enormous positive impact on the career of an astronomer.

The precise timestamps of the proposal submissions not only allow us to measure the median time people submit before the deadline, but also allow us to study the entire cumulative proposal submission evolution. The only similar effort of which we are aware (Durakiewicz, 2016), is for proposal submission to the National Science Foundation (NSF).

Results

Figure 1 shows the cumulative number of submitted proposals for five ALMA proposal cycles as a function of the initial time they have been submitted to the ALMA Observing Tool. Given that proposal submission is a random process, one might have expected the curve to be a (cumulative) Gaussian distribution, where a few PIs submit early, a few very late and the bulk a certain time before the deadline. The actual distribution is, however, radically different. The submis-

sion rate is highest just before the deadline, with about 78 % of all proposals being submitted within the last 12 hours and 32 % submitted within the last hour.

Applying three transformations to these data — normalising, using the instant of the last time at which a PI has submitted a proposal, and using a log-time scale — we find a spectacular result (Figure 2). The proposal submission evolution curves fall nearly exactly on top of each other with a mean standard deviation from the average curve of only 0.02 %; however, note that the ultimate submission time was only available for the last three proposal cycles. More importantly, however, the evolution can be fitted by a simple Gaussian distribution. The black line shows the best-fit cumulative distribution function (CDF) of a Gaussian probability distribution function with mean $\mu^* = 2$h 36m and standard deviation $\sigma^* = 0.1349$ using logarithmic time as random variable. Mathematically this function is the lognormal distribution with

$$\text{Lognormal CDF}\,(t|\mu^*,\sigma^*) = \frac{1}{2}\,erfc\left(-\frac{\ln(t)-\ln(\mu^*)}{\ln(\sigma^*)\sqrt{2}}\right)$$

where t denotes the time to the deadline in days and $\mu^* = e^{\mu}$ and $\sigma^* = e^{\sigma}$ (all dimensionless, expressed in units of days) are the median and the multiplicative standard deviation, respectively, and *erfc* is the complementary error function. μ^* and σ^* are also the mean and standard deviation of the normal distribution with $\chi = \ln(t)$. We will refer to this distribution as the deadline flurry formula (DFF).

This very simple model fits the average evolution of the three proposal cycles extremely well, explaining 99.87 % of the signal (coefficient of determination, r^2) and is valid over at least five decades in time to the deadline. Moreover, the DFF is "universal" in the sense that it can accurately describe the global evolution, can also describe the evolution of subsets of the data (see below) and requires only two parameters which have well known meaning.

Since the evolution of proposal submission over the three submission cycles is almost identical, the statistics suggest that the moment at which the possible improvement of a proposal in the remaining time is perceived not to be worth the effort is a very precise and distinct moment for all proposers, thus leading to the very small scatter. This finding is even more remarkable since there is a much larger scatter in the evolution when using the times of the first proposal submission. Even if PIs start earlier or later, due to external factors like attendance at ALMA proposal preparation community days, the moment at which more work is not considered worth it any more is an intrinsic value for every person. This can be seen as indirect support of theories of motivation, like the Time Motivational Theory (TMT; Steel & König, 2006).

Analysis of sub-samples

Our statistical sample is large enough that we can split it in various ways and study the submission behaviour of subsets; see Figures 3 and 4 as well as Table 1. We use bootstrapping to estimate the 95 % confidence interval of μ^* to be typically +/– 12 minutes, which allows us to assess the statistical significance of our results. We find that PIs from East Asia (EA) submit later ($\mu^* = 1$h 52m) than their colleagues from Europe (EU) (2h 31m) or North America (NA) (3h 41m). As the proposal deadline, which is always set at 15:00 UT, corresponds to very different local times in the different regions (i.e., very late evening for EA, late afternoon for EU and (very) early morning for NA), our data do not allow us to determine whether or not the effect is due only to the different local deadline times or also to actual cultural differences. The fact that there is indeed an influence due to the local deadline time can clearly be seen in Figure 3. The short, flatter parts of the NA and EU curves correspond roughly to midnight until 09:00 local time.

In accord with earlier studies (Rotenstein et al., 2009; Kim & Seo, 2015), we find that PIs of proposals that were awarded observing time, and thus are those with the best performance (roughly 20 % of all proposals), typically submitted earlier (2h 57m). We also find that, in all cases, PI groups which submit the final version later also have started later (based on the time of first submission).

In the literature, stronger procrastination is found to be correlated with younger age (for example, Steel, 2006 and references therein); this coincides with our findings as proposals marked "student project" form the group that submits latest (1h 42m). However, it should be noted that the tag does not necessarily mean that the proposal was submitted by a PhD student as any proposal would bear that tag if the data are to be used for a student project. We use the Python package *sexmachine*[1] to estimate gender from first names; while the algorithm is less effective for EA we find similar fractions of female PIs among the different regions and so judge the subsequent analysis to be reflective of the missing or incorrectly identified population. We find that female PIs submit slightly later than their male colleagues, which is in contrast with earlier findings based on self-reporting of the test persons (for example, Mandap, 2016). Our finding is true globally, but also for each of the three regions separately, thus excluding any possible cultural influence. However, it should be noted that there may be multiple factors at play as, given the demographics of astronomers, the proportion of senior proposers among the male PIs is likely to be higher than that among female PIs.

Finally, we split the full sample into two halves by the amount of observing time requested, as well as by the number of co-authors, and find in both cases that the difference in μ^* between the two halves is larger than the 95 % confidence limit (see Table 1). It seems plausible that it takes more time to agree on and finalise a proposal if a larger number of co-authors is involved (2h 24m *vs.* 2h 52m) and that it takes more time to finish a complicated proposal asking for a lot of observing time (2h 27m *vs.* 2h 48m).

Durakiewicz (2016) studied the submission evolution of proposals to the NSF, finding a good fit using a modified hyperbolic function. The fitted function has only one fixed parameter, the length of the submission window D (days). For $D = 30$, as in our case, their function has an equivalent DFF μ^*-value of 21h 2m for the (final) submission, which is much larger than the 2h 36m of ALMA proposals (it is even larger than the value of ALMA's first submissions) and thus not a good fit to

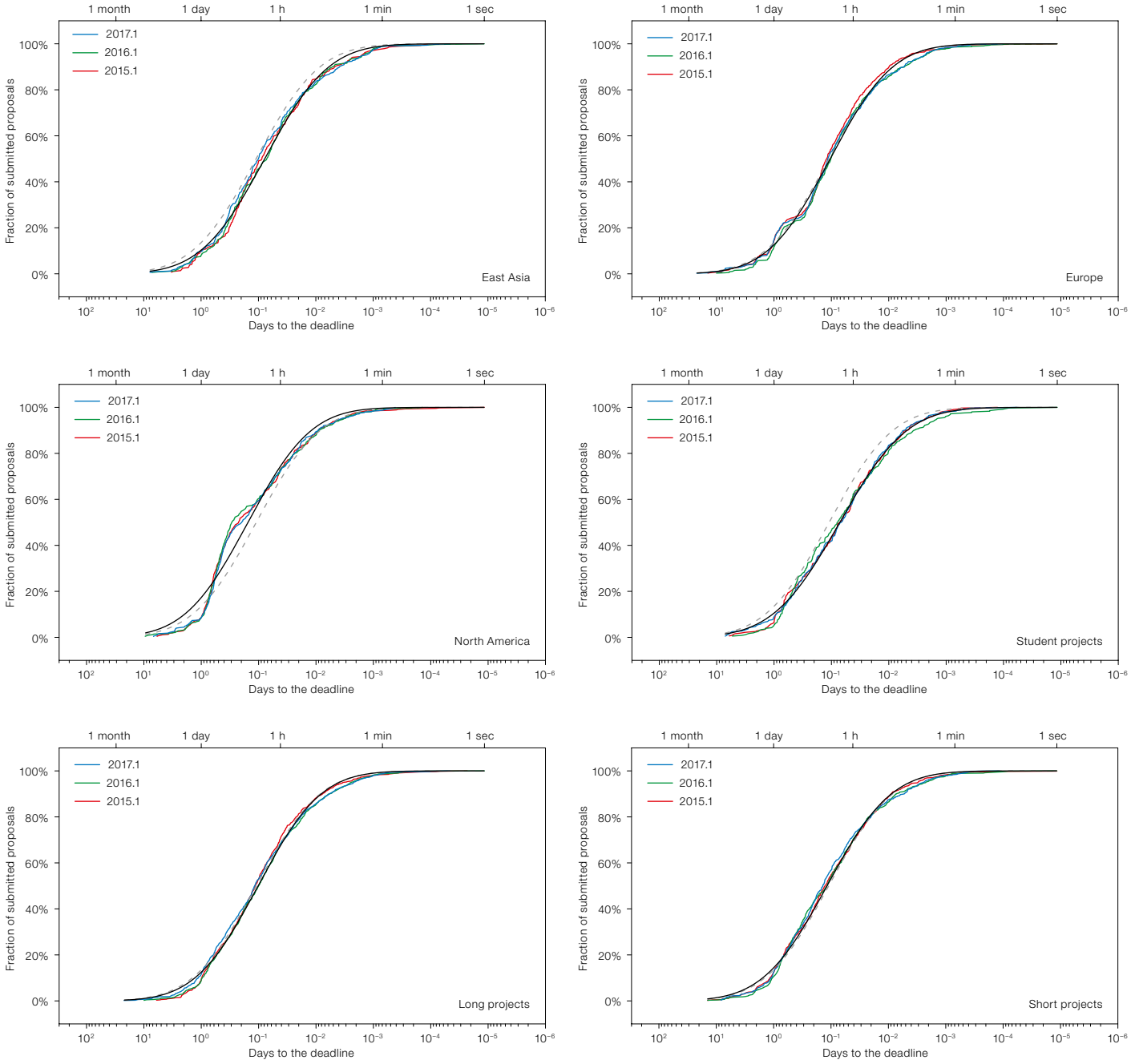

Figure 3. Distributions of the (last) proposal submission times of (from top left to bottom right) East Asia, Europe, North America, student projects, long projects and short projects. The best DFF fit is shown with a black solid line and, for reference, the best DFF fit for the global distribution is shown as a grey dashed line. In the North American PI plot, the effect of the early-morning proposal deadline in North America can be seen. This curve is responsible for the slight deviations of the global curve from the lognormal distribution.

our data. The very different timescales are probably due to the very different proposal processes. Indeed, NSF proposals are not submitted by the PIs directly but by the Sponsored Research office which also has to approve the requested budget.

Context

The study of proposal submission behaviour to a deadline in this work fits into a vast body of scientific quantities that follow a lognormal distribution: from the latency periods of diseases, to the amount of rainfall, the number of words in sentences, the age of marriage and the ratio of income to the size of people (Limpert, Staehl & Abbt, 2001).

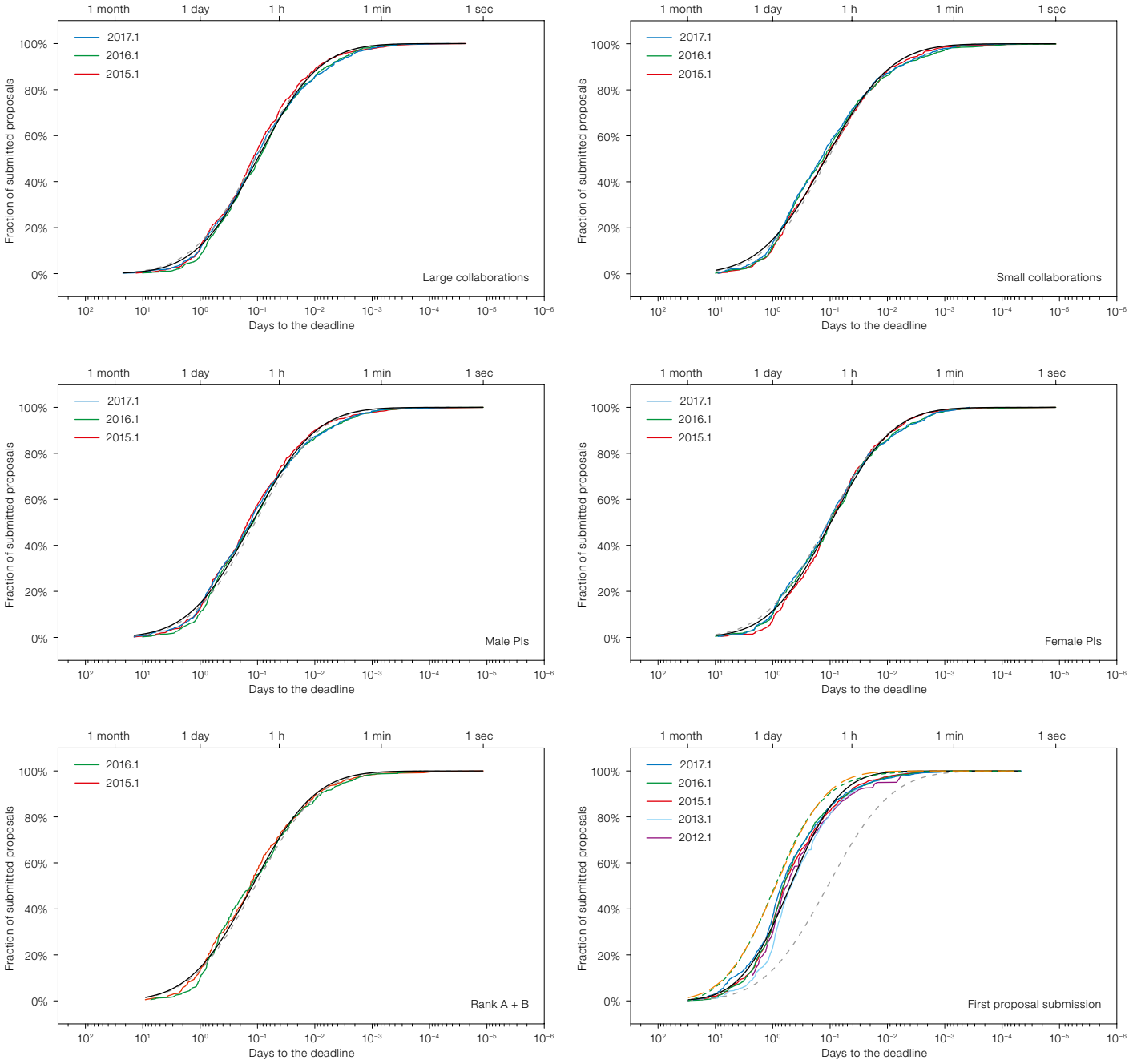

Figure 4. As Figure 3 for the sub groups: large collaborations; small collaborations; male PIs; female PIs; and successful proposals (rank A and B). The best DFF fit is shown with a black solid line and, for reference, the best DFF fit for the global distribution is shown as a grey dashed line. The lower right plot is the time of first proposal submission over all cycles; the modified hyperbolic with D = 30 days proposed by Durakiewicz (2016) has also been added (green dashed line) and fitted with a DFF (orange dashed line). In the plot of successful proposals, only two cycles are shown, as the accepted proposals of the last cycle (2017.1) were not known at the time of writing.

Lognormal distributions arise naturally in random processes when the random variable is a product of random variables; while the sum of the faces when rolling a number of dice repeatedly results in a normal distribution, their product will be lognormally distributed. The self-regulatory behaviour of human motivation is often modelled as the product of influencing factors (for example, in the TMT), so a lognormal distribution of an ensemble is a direct consequence. On account of the above considerations, and because there is no minimum time limit imposed (Mitzemmacher, 2004), we chose the lognormal distribution over multi-power-law distributions, noting that even four-parameter multi-power-law models have been suggested in the literature (Reed & Jorgensen, 2004).

	μ* (days)		σ* (days)	1-σ* interval	2-σ* interval
Last	0.1086	(2h 36m)	0.1349	19h 19m–21m 5s	5d 23h–2m 50s
EA	0.0779	(1h 52m)	0.1334	14h 40m–14m 57s	4d 9m–1m 59s
EU	0.1051	(2h 31m)	0.1399	18h 1m–21m 9s	5d 8h–2m 57s
NA	0.1535	(3h 41m)	0.1369	1d 2h–30m 16s	8d 4h–4m 8s
Student project	0.0715	(1h 42m)	0.1215	14h 7m–12m 30s	4d 20h–1m 31s
Long projects	0.1023	(2h 27m)	0.1382	17h 45m–20m 20s	5d 8h–2m 48s
Short projects	0.1173	(2h 48m)	0.1333	21h 7m–22m 31s	6d 14h–3m 0s
Large collaborations	0.1002	(2h 24m)	0.1409	17h 4m–20m 20s	5d 1h–2m 51s
Small collaborations	0.1195	(2h 52m)	0.1291	22h 12m–22m 13s	7d 3h–2m 52s
Successful	0.1230	(2h 57m)	0.1381	21h 22m–24m 27s	6d 10h–3m 22s
Female	0.0974	(2h 20m)	0.1432	16h 19m–20m 5s	4d 17h–2m 52s
Male	0.1233	(2h 57m)	0.1343	22h 1m–23m 50s	6d 19h–3m 12s
First submission	0.4931	(11h 50m)	0.2073	2d 9h–2h 27m	11d 11h–30m 30s
NSF	0.8769	(21h 2m)	0.2013	4d 8h–4h 14m	21d 15h–51m 9s

Table 1. μ* (median) and σ* (multiplicative standard deviation) values for the various PI sub-groups. The one- and two-σ* boundaries are very asymmetric owing to the log-time distribution and are given by [μ*/σ* .. μ* σ*] and [μ*/σ*^{2} .. μ* σ*^{2}], respectively. The 95% confidence interval on μ* is of the order of +/– 12 minutes.

For future research, it would be interesting to analyse the submission behaviour towards a fixed deadline for different amounts of work to be submitted and for longer and shorter time intervals in which the proposals can be submitted. This might allow prediction of the two free parameters of the DFF given that the behaviour of the PIs appears to be so universal and time-invariant. Practically, our analysis could also be useful for the design of future proposal submission systems, like the new system which is currently being developed for ESO.

As the time just before the proposal deadline is often associated with stress for ALMA PIs, they should be encouraged to make even more use of the possibility of submitting a draft version of the proposal well before the deadline.

Conclusions

We have analysed the behaviour of people submitting work before a deadline using metadata from the ALMA proposal submission process since 2011. We find that the proposal submission evolution is nearly perfectly identical over the years, which suggests it is linked to an intrinsic property of human nature. We also find that this evolution can be extremely well described by a simple lognormal distribution with the time-to-deadline as random variable; the deadline flurry formula.

With the large sample to hand we have also studied the very small deviations from the general submission behaviour for subgroups of PIs. While our result that male PIs submit slightly earlier than female PIs is opposite to the findings published in the literature, we cannot exclude that it is at least in part caused by different age demographics within these subgroups. Our results with respect to PI age and the success of a proposal are consistent with earlier findings.

Acknowledgements

We are indebted to the creators of the ALMA Observing Tool for having the foresight to record the precise timestamps of the proposal submissions. We thank Gautier Mathys, Tomasz Durakiewicz, Wolfgang Kerzendorf, Martin Zwaan, John Carpenter and Gaitee Hussain for very helpful comments. ALMA is a partnership of ESO (representing its Member States), NSF (USA) and NINS (Japan), together with NRC (Canada), MOST and ASIAA (Taiwan), and KASI (Republic of Korea), in cooperation with the Republic of Chile. The Joint ALMA Observatory is operated by ESO, AUI/NRAO and NAOJ.

References

Durakiewicz, T. 2016, Physics Today, 69, 11

Evelyn-White, H. G. 1936, *Hesiod, the Homeric Hymns, and Homerica*, 3rd rev. ed., (Cambridge, USA: Loeb Classical Library), lines 405–413

Kim, K. & Seo, E. 2015, Personality and Individual Differences, 82, 26

Limpert, E., Stahel, W. A. & Abbt, M. 2001, BioScience, 51, 341

Madap, C. 2016, International Journal of Education and Research, 4, No. 4

Mitzenmacher, M. 2004, Internet Mathematics, 1, 485

Reed, W. J. & Jorgensen, M. 2004, Commun. Stat.-Theory & Methods, 33, 1733

Rotenstein, A., Davis, H. Z. & Tatum, L. 2009, Journal of Accounting Education, 27, 223

Steel, P. & König, C. J. 2006, Academy of Management Review, 31, 889

Tice, D. M. & Baumeister, R. F. 1997, Psychological Science, 8

Tuckman, B. W. 1999, Educational and Psychological Measurement, 51, 473

Links

[1] Python name gender resolver: https://pypi.python.org/pypi/SexMachine

DOI: 10.18727/0722-6691/5041

Report on the ESO Workshop

Star Formation from Cores to Clusters

held at ESO Vitacura, Santiago, Chile, 6–9 March 2017

Adele Plunkett[1]
Fernando Comerón[1]
Leonardo Testi[1]

[1] ESO

This conference on star formation explored the synergies between observations and theory and was timed to facilitate collaborations to prepare observing proposals to use ALMA and ESO facilities. The aim of the conference was to review recent progress and to identify how to advance the field over the coming years with observations and numerical simulations.

Conference organisation

The workshop Science Organising Committee was composed for the most part of members of the SOLA (Soul Of Lupus with ALMA) collaboration, which was originally based at the Joint Atacama Large Millimetre/sub-millimetre Array (ALMA) Observatory but now has members around the world (Principal Investigator: I. De Gregorio-Monsalvo, ESO/JAO – Joint ALMA Observatory).

The scientific programme[1] was organised into the following six sessions:
- Session 1: Molecular clouds and star-forming regions (formation, evolution, chemistry, structure);
- Session 2: Outflows, envelopes, first conditions of disc formation;
- Session 3: Pre- and proto-stellar cores;
- Session 4: Earliest stages of the sub-stellar regime;
- Session 5: Multiplicity at early stages of star formation, small clusters;
- Session 6: Star formation at larger scales, surveys.

The first five sessions were chosen to progress from large to small spatial scales in order to address the following question: "What constitutes a prototypical low-mass star-forming region from cluster to core scales?" The last session was added to reflect the content of submitted abstracts and concerned larger scales, including extragalactic star formation.

Figure 1. Conference photo.

Eighty two participants from 20 countries attended and there were 11 invited speakers. There were 4–6 contributed talks in each session as well as "flash" poster talks (with poster viewings held throughout the week). The SOC awarded the poster prize to Vianey Camacho, who presented a poster entitled "Energy Budget of Forming Clumps in Numerical Simulations of Collapsing Clouds".

John Carpenter (JAO) and Willem-Jan de Wit (ESO) summarised existing and new capabilities at ALMA and the Very Large Telescope (VLT), respectively. In addition there were two discussion sessions, which allowed participants to explore topics in smaller groups, and finally Diego Mardones and Leonardo Testi teamed up for the conference summary. Proceedings based on the conference contributions are available through Zenodo[2] and linked on the programme webpage, which is also searchable via the ADS (SAO/NASA Astrophysics Data System).

Scientific summary

Filamentary structures are ubiquitous in star-forming regions. However, the exact terminology used to describe these structures and their characteristics (for example, characteristic widths) was a frequent topic of discussion and it was felt that a more robust way to interpret and characterise structures is needed. Some suggested that the projection of the filament on the plane of the sky could affect its appearance, suggesting, controversially, that some cores may actually be pole-on filaments. Simulations are progressing and enable systematic comparison with observations using statistical metrics. However, they are still lacking some physics (for example, the effects of magnetic fields, chemistry and feedback).

The core mass function (CMF) and its relation to the stellar initial mass function (IMF) were shown in a number of presentations and were a topic of much discussion. In particular, a plot showing the CMF with an arrow pointing to the IMF was subsequently named the "most abused figure" in the conference summary, with many expressing doubts about the direct connection between the CMF and the IMF.

The SOC commended those brave astronomers who tackled the complex topics of magnetic field, angular momentum, and chemistry. It seems likely that significant observational advances will soon be made towards constraining the role of magnetic fields in many aspects of star formation, from clouds and cores, to disc-star interaction, and in driving jets and outflows. Understanding the chemistry may take more time, and discussions revealed the need for caution when analysing observational data for a specific species before more general conclusions can be drawn.

A number of interesting results on the formation and early evolution of brown dwarfs were presented, with ALMA's sensitivity driving progress in this area. The particular challenges posed by the recent

discovery of the planetary system around TRAPPIST-1, were a source of discussion.

The role of the environment needs to be established before extrapolating star formation to different regions, such as galactic centres, spiral arms, and massive complexes compared to smaller clouds. Open questions remain about observed environmental differences; it remains unclear whether these differences are significant or simply due to our lack of understanding of the star formation process. Progress has been made with constraining radiative feedback and dynamical effects in star formation, but we still lack an understanding of the global implications. Despite much debate and healthy discussion, the main question that prompted the conference still remains unanswered: "What constitutes a prototypical low-mass star-forming region from cluster to core scales?"

Post-conference survey

Following the conference, we conducted an online survey to evaluate the success of the conference and identify areas for improvement. The results are summarised in a report which is available as a resource for organisers of future ESO workshops[3]. The results of the survey indicate that the participants found the poster flash talks and discussion sessions useful and offered several suggestions on how to improve their impact.

Figure 2. A photo taken during the tour of ALMA antennae at Chajnantor, at an altitude of 5000 metres.

Social

The conference dinner included an excursion to the beautiful Roan Jasé Astronomical Observatory in the Cajón del Maipo, about an hour outside Santiago. Our hosts Manuela and Leopoldo treated the astronomers to a traditional Chilean family-style barbecue, bilingual presentations about astronomy from the perspective of the indigenous Mapuche culture, and stargazing using small telescopes. Following the conference, some participants travelled to San Pedro de Atacama and the ALMA Observatory (Figure 2), hosted by star-formation enthusiast Al Wootten (NRAO).

Acknowledgements

We would like to thank the SOC and LOC, in particular María Eugenia Gómez and Paulina Jirón for their support in organising the conference. Additionally, we thank the IT support and facilities team who made the daily operations of the conference possible. Special efforts were made to accommodate travel costs and registration for students and postdoctoral researchers, and we thank ESO and NRAO for providing the necessary funding.

Links

[1] Conference website: http://www.eso.org/sci/meetings/2017/star-formation2017.html
[2] Zenodo: https://zenodo.org/
[3] Conference report based on the participants survey: http://www.eso.org/sci/meetings/2017/StarFormation2017/Report_SF2017.pdf

Report on the EWASS Workshop

DOI: 10.18727/0722-6691/5042

EWASS 2017 Special Session SS18: The ELT Project Status and Plans for Early Science

held at Charles University, Prague, Czech Republic, 29 June 2017

Chris Evans[1]
Isobel Hook[2]
Giuseppe Bono[3]
Suzanne Ramsay[4]

[1] UK Astronomy Technology Centre, Edinburgh, United Kingdom
[2] Department of Physics, Lancaster University, United Kingdom
[3] Department of Physics, University of Rome "Tor Vergata", Italy
[4] ESO

A special session was organised at the 2017 European Week of Astronomy and Space Science (EWASS 2017) this summer. The twin aims of highlighting progress on the ELT Programme to the whole European community and of engaging early-stage researchers

in this exciting project were met. A lively programme of talks was presented to a packed room.

Session summary

EWASS 2017 took place in Prague from 26 to 30 June 2017. One of the parallel sessions was Session 18: "The European ELT Project Status and Plans for Early Science". This afternoon session was organised jointly by the four authors of this report. The session attracted a sizeable audience, turning into a "standing room only" event for late-arriving attendees.

The main goal of the session was to highlight recent progress on this exciting and important project to the wider astronomical community in Europe. Since previous EWASS (and formerly JENAM) sessions in 2012 and 2008, the Extremely Large Telescope (ELT) programme has been approved and is now well into its construction phase. Many key contracts are already in place, including agreements to build the first set of instruments. The "First Stone" ceremony took place shortly before this meeting (see de Zeeuw et al., 2017). A particularly strong motivation for this session was to engage with early-stage researchers from across the whole of Europe, since the ELT will be the premier facility available to them as they move into their mid-careers. The session aimed to strengthen their knowledge of the ELT programme and to harness their ideas and expertise. The organisers also wanted to interest the community in undertaking the comprehensive end-to-end simulations of ELT observations, which will be essential to predict how this facility will meet the ESO community's scientific objectives.

The session started with an invited talk from the ELT Programme Scientist, Michele Cirasuolo. He provided an overview of the science cases, instrument concepts[1] and programme status. The rest of the session was given over to contributed talks. As anticipated, the scope of the speakers' scientific goals was broad, ranging from Leen Decin's talk on detailed dust chemistry in stellar winds with METIS (the Mid-infrared ELT Imager and Spectrograph) to Karen Disseau's studies of the high-redshift Universe with the multi-object spectrograph, MOSAIC. Observations of massive stars and stellar populations were discussed by Artemio Herrero and Oscar Gonzalez respectively, while Kieran Leschinski used simulations to demonstrate the potential for determining variations in the stellar initial mass function using the Multi-AO Imaging CAmera for Deep Observations, MICADO, fed by the adaptive optics Multi-conjugate Adaptive Optics RelaY module, MAORY.

Simulations of observations with HARMONI, the High Angular Resolution Monolithic Optical and Near-infrared Integral field spectrograph (by Mark Richardson) and METIS (by Michael Mach) showed how each of these instruments would advance our understanding of galaxies. Two speakers presented the future of observations at high spectral resolving power, with Nicoletta Sanna talking about the plans for the ELT's high-resolution spectrograph, HIRES, and Giuseppe Bono (standing in for Davide Magurno) showing the results from WINERED, a warm near-infrared high-resolution spectrograph that is currently a visitor instrument on the New Technology Telescope (NTT).

Quite apart from the scientific goals of researchers participating in the session, two nice talks highlighted the future of software and hardware with the new generation of instruments: Rainer Köhler gave a flavour of the ongoing work on the METIS data pipeline; and Robert Harris talked about a novel 3D printing technique for manufacturing microlenses for fibre spectrographs.

Acknowledgements

The organisers of this session would like to thank all the presenters for their contributions. We are also very grateful to the organisers of EWASS 2017 for the opportunity to meet together in Prague to share this exciting vision of the future with the ELT.

References

de Zeeuw, T., Comerón, F. & Tamai, R. 2017, The Messenger, 168, 2

Links

[1] For details of the ELT instruments currently in development, see the links at http://www.eso.org/public/teles-instr/elt/

ESO/L. Calçada

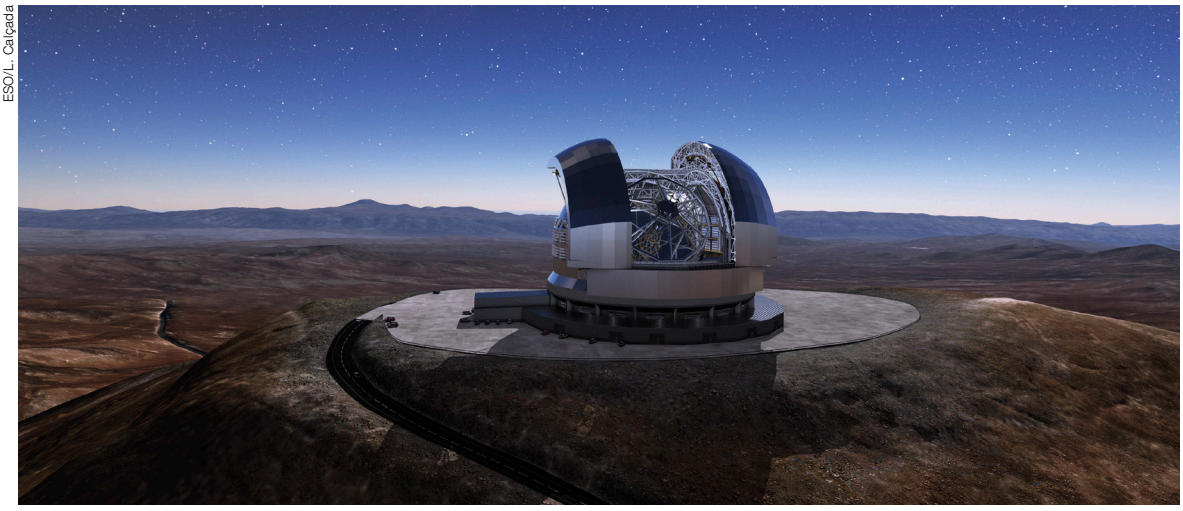

Figure 1. An artist's rendering of the ELT as it will look upon completion in 2024.

DOI: 10.18727/0722-6691/5043

Report on the ESO Workshop

The Impact of Binaries on Stellar Evolution

held at ESO Headquarters, Garching, Germany, 3–7 July 2017

Henri M. J. Boffin[1]
Giacomo Beccari[1]
Monika G. Petr-Gotzens[1]

[1] ESO

The majority of stars have at least one companion and many will interact during their lifetimes, leading to significant changes in their structure, their further evolution and their chemical composition. One can therefore be sure that almost any kind of important or interesting class of objects has been influenced by binary evolution. This workshop aimed to address these important issues, and attracted 170 registered participants. The main conclusion of the workshop is that the textbooks need to be rewritten to account for the role of binarity in many areas of stellar evolution.

Binarity and stellar evolution

The last few decades have seen a paradigm shift following the realisation that most stars are found in binary and multiple systems, with at least 50% of all Sun-like stars having companions — a fraction that most likely goes up to 100% for the most massive stars. Moreover, a large fraction of them will interact in some way or another: at least half of the binary systems containing Sun-like stars (especially when the primary evolves onto the Asymptotic Giant Branch, AGB) and at least three quarters of all massive stars. Such interactions will often alter the structure and evolution of both components in the system. They will, in turn, lead to the production of exotic objects (for example, Algols, Blue Stragglers and other chemically peculiar stars) whose existence cannot be explained by the standard stellar evolution models. They may also lead to outcomes such as non-spherical planetary nebulae, or supernovae and gamma-ray bursts.

It should also be noted that one of the most luminous stars in our Galaxy, Eta Carinae, is a binary, and that the most massive stars may be the result of mergers. Moreover, the first ever gravitational wave detection, announced in 2016, arose from the merger of a binary black hole. As Ed van den Heuvel noted in the conference summary talk, three Nobel prizes have been awarded for work on binary stars (in 1993, 2002 and 2011), further illustrating the importance of binaries. Indeed, 2017 may bring another one for the detection of gravitational waves. In contrast, only two have been given for work on single stars, in 1967 and 1983.

Figure 1. Group photo of the participants at the workshop.

The motivations for this meeting were therefore to examine in detail the impact of binaries on stellar evolution in both resolved and unresolved populations. In particular, Gaia will soon bring a wealth of new data in this area and the community needs to be ready to interpret them. This workshop on “The Impact of Binaries on Stellar Evolution” was therefore organised to discuss all of these issues in detail. The timeliness of the workshop was further highlighted by the attendance of 170 registered participants and many additional day visitors, filling up the ESO auditorium and taking in 23 invited talks and about 40 contributed talks. 98 posters were also discussed during two dedicated sessions, with poster viewings during the various breaks. It was a very busy week indeed!

Getting to know binaries

The workshop was introduced by Henri Boffin, who demonstrated the ubiquity of binary stars in the sky, from our closest neighbour Alpha Centauri to the brightest star in the sky Sirius, and including Alcor and Mizar in the Great Bear as well as the stars of the Trapezium in Orion. He also reviewed the various classes of binary stars and their importance in explaining many astrophysical phenomena.

Max Moe presented the latest analysis of the statistical properties of binary stars. He showed the latest number of companions as a function of primary mass; solar-like stars have on average 0.5 companions, while O stars have 2.1 companions. He also confirmed the most recent results showing that if only 15% of Sun-like primaries will interact through Roche lobe overflow in the course of their lives, this fraction reaches an amazing 80–90% for O-type primaries. He stressed the importance of the dependence of the mass ratio distribution on other parameters, particularly the mass of the primary star and the orbital period. The common use of a uniform mass ratio distribution in population synthesis models is thus a dangerous simplification that is no longer justified given the wealth of available data. An example of this was the survey presented by Jennifer Winters of 1125 M-type dwarfs closer than 25 pc; 26% of the sample had companions. As the survey is limited to separations greater than 2 arcseconds, this is only a lower limit to the real binary fraction.

An important question is how binary stars form. Cathie Clarke showed that the formation of multiple stars is an integral part of star formation, with recent observations by the Atacama Large Millimeter/

NASA, ESA, and The Hubble Heritage Team (STScI/AURA)

Figure 2. Planetary nebulae, some examples of which are shown here, are now in the majority thought to be the result of binary interactions.

Submillimeter Array (ALMA) and the Jansky Very Large Array (VLA) demonstrating that small clusters and non-hierarchical multiples are common in deeply embedded, very young protostars. Christine Ackerl illustrated this with a large survey of multiplicity among 3500 young stellar objects in Orion A using the VLT Infrared Survey Telescope for Astronomy (VISTA). Although such a survey is limited to the most distant (> 229 au) and luminous companions, they found a companion fraction of almost 8 % in the less dense parts of the star forming region. Pavel Kroupa stressed, however, that the binary fraction will decrease with time; interactions in the clusters where stars form will disrupt the widest systems as well as those with the most extreme mass ratios. While the initial binary fraction (i.e., for the youngest stars) is independent of primary mass, dynamical evolution removes binary companions from lower mass stars, leading to the observed difference in companion fractions between M, G and O stars.

Stars do not occur only in binary systems, but also in multiple systems. Triple systems, as Silvia Toonen explained, are not that rare; the fraction of low-mass stars in triple systems is 10–15 %, and this doubles for massive stars. The presence of the third component can have dramatic effects, leading to shrinkage of the inner binary or an increase in its eccentricity, thereby making mass transfer between the components easier.

Low-mass stars and mass transfer

Moving on to low- and intermediate-mass stars, Maurizio Salaris reminded the audience of the current challenges that face stellar evolution models, stressing the many parameters (sometimes with *ad hoc* values) that are in use. Here, as Paul Beck showed, the combination of astroseismology and binarity could come to the rescue, as illustrated by the example of an “Asterix & Obelix system”: a binary system consisting of two red giants of almost the same mass (just a 1% difference) but quite different effective temperatures. Understanding how such small differences in mass lead to such a drastic effect should help to constrain stellar models.

Another key example of the effect of binary interaction in low- and intermediate-mass stars is represented by chemically polluted binaries, comprising such families as Barium, CH, S, or carbon-enhanced metal poor (CEMP-s) stars. Onno Pols gave an overview highlighting our lack of understanding of these stars. Each of these systems contains a white dwarf (WD) companion that produced the s-process elements which polluted the companion; they have orbital periods between 100 and 10 000 days, and are substantially eccentric, placing them in a region of the parameter space that should be empty according to the majority of theoretical models. More observational data, such as high-resolution spectroscopy combined with distances from Gaia, may help to solve this long-standing puzzle, as shown by Ana Escorza and Drisya Karinkuzhi.

There is no doubt that during their mass transfer, these stars also showed the characteristics of symbiotic stars, which are among the widest interacting binaries and contain a red giant and a hot companion, as reviewed by Jennifer Sokoloski. The cause of the enhanced mass loss from the giant in these systems is still unknown, as is the nature of the mass transfer itself. Understanding these objects — as well as their actual numbers — is important as they are sometimes considered to be a possible channel by which Type Ia supernovae are formed (see below). Similarly, cataclysmic variables are also important; they are the shorter-period analogues of symbiotic stars, in which a main sequence star is transferring mass to a WD. Anna Pala presented a 122-orbit HST programme to study such stars; the resulting findings also contradict theoretical expectations. Large surveys to better characterise such stars are clearly called for.

Moving further along the evolutionary sequence, Hans Van Winckel presented the latest results on post-asymptotic giant branch binaries (post-AGBs), which all have orbital periods between 100 and about 2000 days (another unexpected result!). Each pair appears to be surrounded by a circumbinary disc while the secondary also seems to possess a disc and most likely some kind of jet-like outflow, the origin of which is unknown.

The family of such puzzling stars was recently enlarged with the discovery of dusty post-red giant branch (post-RGB) stars, as Devika Kamath told us. These stars are not luminous enough to have an AGB progenitor and so must correspond to systems where the evolution of the primary was cut short on the RGB as a result of mass transfer. Several hundred such systems are now known in the Magellanic Clouds, so they cannot be easily dismissed.

Perhaps the most striking examples of binary interactions are planetary nebulae (PNe). These beautiful cosmic bubbles (Figure 2) are traditionally thought of as being the swansongs of low- and intermediate-mass stars before they end their lives as WDs. However, as David Jones explained, the fact that most PNe are now known to be axisymmetric with quite intricate shapes is most likely an indication of some type of binary processes. Of course, some of the central stars of PNe may not be a binary any more, as they could also be the result of the merger of the two stars from the original binary systems. In fact, some examples of mergers exist. Tomek Kaminski presented evidence of the badly named red novae, likely caused by merging stars.

Stellar clusters

In stellar evolution, the study of stars in clusters is advantageous as many parameters (for example, ages, distances and chemical compositions) can be considered fixed when comparing the stars. They are also a rich field in which to study binary stars. Robert Mathieu reviewed the many alternative pathways of stellar evolution that are present in open clusters. The colour-magnitude diagram clearly does not resemble a textbook example of a single population of stars, having as it does outliers such as photometric binaries, blue straggler stars, yellow stragglers, sub-subgiants and yellow giants, all of which are explained by binarity. He showed that at least a quarter of all stars in a cluster are not on single-star evolutionary paths. Francesco Ferraro reminded us in his review that blue straggler stars represented the first evidence of binaries in globular clusters and have since been used to probe the dynamical processes in such clusters. But Michela Mapelli explained that binaries themselves have a huge impact on the dynamics of clusters. Interactions inside a cluster could also explain the formation of binary black holes that would eventually merge.

Massive stars

Moving on to massive stars, Norbert Langer presented the many challenges to modelling massive stars, stating that "when mass increases, our ignorance also increases!" As most massive stars are members of binary pairs, many of them are interacting systems, one needs to address binarity to understand many processes. Note that if a star is not in a binary system now, it may have been in the past; either the companion having been ejected (explaining runaway stars) or the two stars merging (as could happen in the case of about a quarter of all massive stars!). Hugues Sana presented some of the most recent surveys of binarity in massive stars, showing that O stars in binaries have an apparently flat mass ratio distribution but a tendency to be in short-period systems, with little variation seen as a function of the environment or metallicity, thereby suggesting that these are relatively universal results arising from the physics of the formation process itself.

Nathan Smith explained that perhaps the most obvious result of binary interactions in massive stars are luminous blue variable stars (LBVs). Indeed, the single-star paradigm within which LBVs are a short transition phase between normal O stars and Wolf-Rayet stars is encountering numerous problems, including the fact that some supernova progenitors are now thought to have been LBVs — something that can't be reconciled with the standard paradigm. A binary model for LBVs would provide a much more natural explanation of all the observed characteristics. Observing such LBVs, and in particular the most dramatic example, Eta Carinae, requires the use of interferometric techniques and Joel Sanchez Bermudez showed how the Gravity instrument on the Very Large Telescope Interferometer is leading to a better understanding of this important object.

Exploding stars and black holes

A likely contender for this year's Nobel Prize in Physics is the detection of gravitational waves by the Laser Interferometer Gravitational-Wave Observatory (LIGO) instruments. Gravitational waves were shown to be the tell-tale signature of the merger of two massive black holes. Gijs Nelemans provided an overview of the challenges faced when doing such measurements and of the current theories that aim to explain how such binaries form. He also predicted a bright future for this new area of astronomy; from 2019 on, we shall be able to detect massive systems up to several Gpc away, and this limit will later be pushed to a redshift of 10, i.e., basically all of the visible Universe. Coen Neijssel also showed that we need a rather low metallicity to explain the observed events, as at solar metallicity the mass loss from massive stars would be too high to produce the kind of binary black holes that have been observed.

This was a natural point at which to discuss other explosive events in the Universe that are, unsurprisingly, also linked to binary stars. Nando Patat first reviewed our current knowledge of Type Ia supernovae. Showing some "back of the envelope" calculations — that were literally done on the back of an envelope (Figure 3) — he described how the double degenerate model (in which a supernova is the result of the merging of two WDs) went from being the underdog to being the most favoured theory, even though the problem is still far from being fully solved. Perhaps the most worrying aspect is that we are still unsure whether these supernovae are indeed the "standard candles" that astronomers think they are when measuring distances in the Universe.

That the double degenerate model is now in great favour was also illustrated in talks by Chris Pritchet and Na'ama Hallakoun. The latter presented an analysis of the SPY (ESO SN Ia Progenitor surveY) sample, which took about 2200 UVES spectra of about 800 WDs, measuring radial velocities with a precision of 1–2 km s^{-1}. Analysing a clean sample of 439 WDs for which they have multi-epoch spectra with high signal-to-noise ratio, they found that 10 % consist of double degenerate

systems with separations smaller than 4 au. The estimated merger rate is therefore more than enough to explain all observed Type Ia supernovae.

Moving further up in mass, Nial Tanvir discussed gamma-ray bursts (GRBs). It has long been known that the short GRBs originate from merging neutron stars, but evidence is now also mounting that even for long GRBs, binaries may be needed!

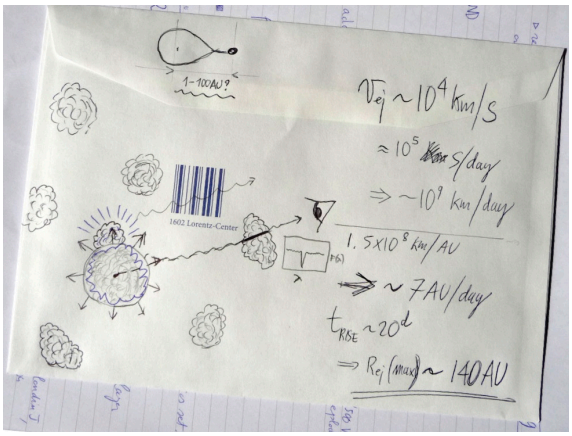

Figure 3. Nando Patat's "back of the envelope" calculation for the double degenerate model, showing how the merging of two WDs can lead to a Type Ia supernova.

A legacy

Else Starkenburg opened the last session of the conference, pointing to the fact that the lowest-metallicity stars that still exist today probably carry the imprint of very few supernovae in the early Universe. This turns out to be one of the key science goals of Pristine, a survey at the Canada-France-Hawaii telescope devoted to the search for the most metal-poor stars. Along the same lines, Sara Lucatello reviewed the present-day results on binary fractions at low metallicity. Evidence seems to suggest that CEMP stars likely originate from binaries. Moreover, preliminary data from the Lick Extremely Metal Poor (EMP) binary survey indicate a higher binary fraction at higher ([Fe/H] ≈ –2) metallicity. Putting it all together, Rob Izzard reviewed why we need to perform binary population synthesis, and how it is currently done. There are now more and more sophisticated codes that address many problems, although one needs to be sure that the correct physics is used. JJ Eldridge showed also how stellar models may be used in population and spectral analysis, while Laurent Eyer and Nami Mowlavi highlighted the observational side, stressing the fact that, with Gaia and the future Large Synoptic Survey Telescope (LSST), we are now entering a data-driven era and we need to prepare for it. Gaia will find and characterise tens of millions of binaries of various sorts, and is therefore bound to revolutionise the field – if we are ready to address the data flow.

We hope that this workshop will have a strong legacy and we have therefore assembled PDF files of most presentations via the programme webpage[1], as well as many of the posters[2]. We also prepared videos of the presentations that are also linked from this page. However, perhaps the most obvious outcome of the meeting is that textbooks need to be rewritten to take into account the importance of binarity in stellar evolution. We have therefore also embarked on producing a textbook that will comprise edited versions of most of the invited talks at the workshop. The book will be published by Cambridge University Press next year.

Acknowledgements

We would like to thank the members of the SOC for their hard work in putting together a very interesting and diverse scientific programme. It is a pleasure to thank Stella-Maria Chasiotis-Klingner for her dedicated support with all the logistics, as well as Tereza Jerabkova, Viktor Zivkov, Na'ama Hallakoun, Fabio Herz, Anna Vucovic, Jürgen Riesel and the ESO logistics staff for their invaluable help in making the workshop run smoothly. Many thanks also to Ed van den Heuvel for providing an enlightening summary talk of this very dense workshop.

Links

[1] Programme with links to presentations: http://www.eso.org/sci/meetings/2017/lmbase2017/program.html
[2] List of poster PDFs as well as poster abstract booklet: http://www.eso.org/sci/meetings/2017/lmbase2017/posters.html

DOI: 10.18727/0722-6691/5044

Forty Years at ESO — Bernard Delabre and Optical Designs

Tim de Zeeuw[1]
Samuel Lévêque[1]
Luca Pasquini[1]
Michèle Péron[1]
Jason Spyromilio[1]

[1] ESO

The optical designer Bernard Delabre has retired from ESO after 40 years at the forefront of telescope and instrument optics. A short overview of his achievements and his legacy of astronomical telescopes and instrumentation is presented. Bernard Delabre was

awarded the 2017 Tycho Brahe Prize by the European Astronomical Society.

Bernard-Alexis Delabre received his diploma in optics in 1974 at the École d'Optique de Morez in France. He worked for a few years at the Société SEIMA (now Valeo) designing car headlights before joining ESO, then in Geneva, in 1977 and he has been at ESO ever since.

During his 40 years of service, Bernard has made profound contributions to optical and infrared ground-based astronomy, which have benefited the entire astronomical community. His genius has been in the optimisation of instrument designs. He brought a clear vision of what astronomers need and how the details of an optical design can be merged with the mechanical constraints to provide optimal performance. It was normal to find astronomers, mechanical engineers, control engineers and system analysts all sitting with Bernard in his office discussing, negotiating and evolving designs.

Bernard was the chief optical designer of a number of telescopes, including the New Technology Telescope (NTT) on La Silla and the Extremely Large Telescope (ELT). While the NTT and the Very Large Telescope (VLT) are classical Ritchey-Chrétien designs, for the ELT Bernard invented a beautiful five-mirror design that provides an aberration-free field, telecentric without a corrector, with an adaptive mirror conjugated close to the ground and an intermediate focus (Delabre, 2008). Recently Bernard has worked on a novel design for a telescope 12–15 metres in diameter suitable for massively multiplexed spectroscopy (Ellis et al., 2016; Pasquini et al., 2016).

Bernard designed the optics of nearly all ESO instruments built in the past 35 years. He was a true innovator in optical design for instrumentation during the fundamental transition to large-format two-dimensional digital detectors. As the telescopes and detectors increased in size and improved in performance, the challenge was for the optical design to ensure that the best image quality was delivered with the fewest elements. Bernard exemplifies the ESO tradition of working at the forefront of technological evolution, applying novel technologies to enable new capabilities for astronomy.

Instrumentation developments

The ESO Faint Object Spectrograph and Camera (EFOSC) was the first focal reducer and spectrograph combination (Buzzoni et al., 1984). The innovative optical design included the creation of a parallel beam space between the collimator and the camera, which allowed for the insertion of a multitude of different optical elements, such as filters, grisms and Wollaston prisms for polarimetry. EFOSC was made possible thanks to a new glass, FK54, and flexible cements that enabled an efficient and broad-band achromatisation. It was one of a series of optical developments made by Bernard, working closely with optical manufacturers to broaden the scope of instrumentation for astronomy.

Many copies of EFOSC are in operation at observatories around the world, including the ARIES Devasthal Faint Object Spectrograph Camera (ADFOSC) at the Aryabhatta Research Institute of Observational Sciences (ARIES) telescope in India, the Danish Faint Object Spectrograph and Camera (DFOSC) at the 1.5-metre Danish telescope on La Silla, the AndaLucia Faint Object Spectrograph and Camera (ALFOSC) at the Nordic Optical Telescope on La Palma, and the Asiago Faint Object Spectrograph and Camera (AFOSC) at the 1.82-metre telescope on Mount Ekar, to name but a few. Derivatives of the design were the Low Dispersion Survey Spectrograph (LDSS) at the Australian Astronomical Observatory, the William Herschel Telescope and the Magellan telescopes, the Faint Object Camera And Spectrograph (FOCAS) at Subaru, the Gemini Multi Object Spectrograph (GMOS), and, last but not least, the FOcal Reducer and low dispersion Spectrograph (FORS1 and 2) at the VLT.

With the ESO Multi-Mode Instrument (EMMI) on the NTT, Bernard designed the first truly multimode instrument to combine low and intermediate resolution and cross-dispersed echelle spectroscopy

Bernard Delabre

with imaging. As with EFOSC the incoming wide-field focal plane could be combined with a slit mask that provided multi-object spectroscopy using grisms. Using the same camera to image, take grism spectra and deliver the cross dispersion for the echelle grating is quite remarkable.

The next step in Bernard's use of evolving technology to improve optical performance came with the Infrared Spectrometer And Array Camera (ISAAC), the first-generation infrared camera spectrograph for the VLT. Diamond turning to generate optical surfaces was becoming viable in the 1990s. Bernard realised that this created an absolute mechanical reference for the optical surface. Three-mirror anastigmats, which previously had been considered too difficult to align and keep aligned, could now be employed. They provided a wide corrected field of view, free from bulky transmission optics which are temperamental and difficult to model for a cryogenic instrument. Three-mirror anastigmats are now very popular for instrumentation, and also for some telescopes.

The white pupil concept introduced by André Baranne in 1972 was further developed by Bernard for the UV-Visual Echelle Spectrograph (UVES) for the VLT. This new configuration eliminates vignetting and aberrations by delivering a sec-

ond white-light pupil, where the cross disperser and the camera are located. With a few added optical elements, resulting in the loss of only a few percent of the light, the vignetting typical of traditional designs is removed and the image quality and overall luminosity substantially enhanced. This new design was again adopted by several instrument builders in Europe and overseas.

Bernard also developed the 4C concept, which enables camera chromaticism to be compensated through the chromatic effect introduced by the collimator. It was used in several VLT instruments including X-shooter and the VIsible Multi Object Spectrograph (VIMOS) and inspired the design of instrument concepts overseas, such as the Gemini Montreal-Ohio-VIctoria Echelle Spectrograph (MOVIES; Delabre et al., 1989). Bernard also developed a new "pupil slicing" technique for one of the early instrument concepts for the ELT and worked on the optical design of the Echelle SPectrograph for Rocky Exoplanet and Stable Spectroscopic Observations (ESPRESSO). This instrument combines pupil slicing with anamorphism and slanted volume phase holographic (VPH) gratings to achieve high resolving power.

Recently, Bernard also took a leading role in the development of optical designs for instruments using curved detectors, where no optical design with an affordable number of lenses can be found with identical transmission and identical field of view. This work is paving the way for future massively multiplexed spectrographs (Iwert & Delabre, 2010). All the ESO spectrographs under construction — the near-infrared Enhanced Resolution Imager and Spectrograph (ERIS) and the Multi-Object Optical and Near-infrared Spectrograph (MOONS) on the VLT, and the 4-metre Multi-Object Spectrograph Telescope (4MOST) on VISTA — are also benefitting from Bernard's incomparable expertise.

Award and retirement

Nearly all astronomers in Europe, and many outside, have used or will use a Delabre optical system for their science, be it at ESO or elsewhere. Three of the ten pioneering spectrographs of the twentieth century are attributed to Bernard (Hearnshaw, 2009). His genius and dedication were acknowledged in the award of the Tycho Brahe Prize for 2017 by the European Astronomical Society which was presented to Bernard at the meeting in Prague in July[1,2].

A retirement party was held in Bernard's honour on 28 July 2017 at ESO Headquarters and was attended by many friends and colleagues who have worked closely with him. Speeches were given by the ESO Director General Tim de Zeeuw, Gerald Hechenblaikner of the Directorate of Engineering and his colleagues Samuel Lévêque and Jason Spyromilio. At the party, it was announced that Bernard was to be made Emeritus Engineer at ESO in appreciation of his many achievements, and in anticipation of many more ingenious optical designs.

References

Buzzoni, B. et al. 1984, The Messenger, 38, 9
Delabre, B. et al. 1989, SPIE, 1055, 340
Delabre, B. 2008, A&A, 487, 389
Ellis, R. S. 2016, *The Future of Multi-Object Spectroscopy: a ESO Working Group Report*, arXiv:1701.01976
Hearnshaw, J. 2009, *Astronomical Spectrographs and Their History*, (Cambridge: Cambridge University Press)
Iwert, O. & Delabre, B. 2010, SPIE, 7742, 774227
Pasquini, L. et al. 2016, SPIE, 9906, 99063C

Links

[1] Tycho Brahe Prize award 2017: http://eas.unige.ch/tycho_brahe_prize.jsp
[2] ESO Announcement of Tycho Brahe Prize: http://www.eso.org/public/announcements/ann17018/

Departure of Patrick Geeraert, Director of Administration

Tim de Zeeuw[1]

[1] ESO

Patrick Geeraert was appointed Head of Administration at ESO in 2008, initially on a one-year secondment from the European Organization for Nuclear Research (CERN) in Geneva. One year became three, three became five, five became seven, and seven became nine. He has now returned to CERN.

When he arrived at ESO the then Administration division consisted of two nearly independent units, one in Chile and the other in Garching, and the Human Resources (HR) department also needed to return to Administration. In the context of the unification of ESO's structures, and in order to increase the links between the sites in Chile and Germany, Patrick oversaw the evolution of Administration towards a much more inte-grated structure. After a while it became clear that HR also needed to be inside the Administration division and the title was changed to the Directorate of Administration, with Patrick as its Director.

Patrick played a key role in leading the last two collective bargaining rounds in Chile. The recent one in 2016 was particularly challenging as it involved the

Paranal Union, the La Silla Union and the group of non-unionised Local Staff Members. A single three-year agreement was concluded with all sides happy with the outcome. He also initiated a drive to raise external funding for non-core ESO business. This led to the donation, by the Klaus Tschira Foundation, of the building for the ESO Supernova Planetarium & Visitor Centre, due to open in April 2018.

Patrick was also instrumental in convincing the Finance Committee and ESO Council to fund the expansion of the programme required by the Extremely Large Telescope (ELT). This meant developing the unusual funding model and helping to convince Brazil to sign the Accession Agreement with ESO. Alongside this, Patrick's other achievements included streamlining ESO spending, staying on budget with construction of the Atacama Large Millimeter/submillimeter Array (ALMA), establishing the tools for medium and short term borrowing, hedging of the Chilean Peso, working on the Polish accession and, last but not least, securing the Strategic Partnership with Australia (see Comendador-Frutos, de Zeeuw & Geeraert, p. 2).

Patrick left ESO at the end of August to return to CERN. Farewell parties were held in Chile and Garching in August and Figure 1 shows a photograph from the one held at the ESO Vitacura premises in Santiago. We wish Patrick every success "back home" at CERN.

Figure 1. Patrick Geeraert being fêted at his farewell party in Chile.

DOI: 10.18727/0722-6691/5045

Jerry Nelson — An Appreciation of his Pioneering Telescope Work

Jason Spyromilio[1]
Philippe Dierickx[1]

[1] ESO

Jerry Nelson, the intellectual, technical and spiritual father of the Keck telescope project passed away in Santa Cruz on 10 June 2017. The telescope world has lost one of its true masters. At the 4th conference on Large Telescopes held at ESO in Geneva in 1977, Jerry presented the work of astronomers at the University of California who had "looked seriously at the possibility of constructing a large, 10-metre-class, optical telescope […] which would match superlative seeing" with "modern area detectors (CCD arrays, photographic emulsion)". Although in 1977 Jerry was leaving open the possibility that the primary might be monolithic, it is clear in that publication that segmentation was the solution that he considered best. Jerry was at least two decades ahead of the field.

The cost of a telescope is largely connected to its kinematic volume and its weight, driven by the mass needed to support the optics. Heavier optics implied more expensive telescopes. Telescope mirrors have to keep their shape and relative positions if the instruments are to receive an acceptably sharp focal plane. The stiffness of the optics is related to their thickness-to-diameter ratio; the 4-metre-class mirrors in the late 1970s were monsters, expensive, difficult to produce and slow to reach thermal equilibrium. Either a thin meniscus or a sandwich would be needed to increase the aperture using a monolithic mirror. Segmentation of the primary mirror results in stiffness of the local optical surface, while the overall shape is determined by the control system, at a much more manageable weight budget. As for kinematic volume, containing the length of the telescope — hence the size of its dome — drives the system design towards a fast primary mirror.

Figuring off-axis aspheres and cutting them to hexagonal shape is a daunting challenge. The steeper the primary mirror, the more difficult this task becomes. Everything had to be developed and Jerry was at the heart of all of these efforts. With Jacob Lubliner, Jerry developed stress mirror polishing, converting the problem from an aspherical one to one of spheres. Jerry was active in the development of the edge sensors that measured the positions of the mirrors with nanometric precision and the actuators that moved the mirrors with similar precision. All of this was done without the power of the tools that we now have at hand and without the prior knowledge that it can be made to work.

Philippe Dierickx

Jerry Nelson seen through an uncoated mirror segment of the Keck Telescope in 1994.

Jerry's plethora of TMT (Ten Meter Telescope, before it became Keck) technical notes, in areas ranging from optics, mechanics, electronics and control are a treasure trove for all telescope builders. Jerry had a long collaboration with Terry Mast and Gary Chanan as well as with the large and dedicated team of engineers and scientists who made Keck the success that it has undoubtedly been. In addition to the many honours that the astronomical community bestowed upon him, Jerry shared the Kavli prize in astrophysics (with Roger Angel and Ray Wilson) and was awarded the Benjamin Franklin Medal in Electrical Engineering, the André Lallemande Prize of the French Academy of Sciences, and the Dannie Heineman Prize for Astrophysics of the American Astronomical Society.

Jerry followed his Keck success by leading the adaptive optics efforts at the University of California and being the project scientist for the 30-metre CELT (California Extremely Large Telescope, later merged with the Very Large Optical Telescope [VLOT] and the Giant Segmented Mirror Telescope [GSMT] into his second TMT — the Thirty Meter Telescope).

As ESO proceeds with the construction of its 39-metre segmented mirror telescope, we acknowledge an enormous debt of gratitude to Jerry for the transformational success of his endeavours, and for giving astronomy a path to ever bigger telescopes.

Jerry was gifted with insatiable curiosity, armed with a beautiful mind, and endowed with endless enthusiasm. The telescope world will sorely miss his leadership and his willingness to help and advise, as well as his perennial smile.

DOI: 10.18727/0722-6691/5046

Fellows at ESO

Adele Plunkett

My story does not begin with "Since I was a child, I looked at the sky and wanted to be an astronomer." Instead, when I was a child growing up in Texas (USA), I was looking in a million directions and I had no idea what I wanted to be when I grew up. Admittedly, I still don't know. When I was a child, I knew that I liked maths and science. I also liked languages and travelling. I didn't know how I could fit these "likes" together, but I've found that the coincidences of life bring them together naturally.

My journey to become an astronomer has made several stops in Chile, from where I write this piece today nearly 10 years after I first heard about it in 2008. In 2008, during the third year of my physics undergraduate programme, I spent seven months as an exchange student in La Serena, in the *norte chico* (small north) of Chile. I enrolled in the Universidad de La Serena, with three diverse courses on archaeo-astronomy, electrical circuits, and Chilean economics. I did not know that Chile hosted some of the most important telescopes in the world, but I soon learned as I participated in an undergraduate research programme hosted at the Cerro Tololo Inter-American Observatory (CTIO) and funded by the US National Science Foundation.

My first astronomy research project at CTIO studied chemical abundances of Pleiades stars, with Simon Schuler. I was fascinated when someone pointed out the Pleiades cluster that I could see with my naked eye one night, and the next day I was analysing spectra of those stars on the computer. The same semester, I

Gabriel M. Gallegos, Public Affairs Intern, US Embassy Santiago

Adele Plunkett

was fortunate to be invited to observe at CTIO with Frank Winkler from Middlebury College, my home university in Vermont (USA). Frank was an observer in the purest sense of the term, and during long integrations at the telescope he oriented me to the night sky by eye. The data obtained during those observing runs sparked the plan for my undergraduate thesis project — a study of supernova remnants — which I would complete the following year upon return to Middlebury.

At the CTIO library, I devoured books about the first telescopes in Chile, intrigued by the adventures of site testing, arriving by donkey, and camping on virgin mountaintops. Since the beginning, astronomy in Chile has been an international and collaborative endeavour, and I developed a belief that science brings countries and cultures together in a special way. I had entered Middlebury thinking I would study international relations, and through the physics degree and astronomy research I found myself immersed in international initiatives.

Next I enrolled in the PhD programme at Yale University (USA), where the astronomy department has a joint agreement with the Universidad de Chile in Santiago. Chasing the latest international telescope projects, I chose a thesis with Héctor Arce that would use ALMA observations to study protostellar outflows. We made some preliminary observations with CARMA where I learned interferometry, and during the time of ALMA Early Science, I spent 18 months in Santiago with funding from a Fulbright fellowship. I worked with Diego Mardones at the Universidad de Chile, and I participated in ALMA Commissioning and Science Verification with Alison Peck and Richard Hills (and the entire ALMA Commissioning Science Verification team, of course).

Thanks to the Fulbright Fellowship from 2012, I developed a connection with the US Embassy in Chile, and I was able to participate in various “diplomatic” and educational outreach events. Diplomacy was also happening all the time within the ALMA project. The ALMA control room is a unique place where English, Spanish, and Japanese (among other languages) are spoken, while an international team operates an amazingly powerful, complex, and expensive telescope. To me, the *sala de control* (control room) is incredible because it is where so many of my interests come together. Did I mention that in high school I had studied Japanese?

I finished my PhD in 2015, when I came to ESO as a fellow with duties at ALMA. As a US citizen with a European contract, living in Chile and working for an international telescope project, I have become a sort of scientific ambassador. My childhood interests in maths, science, language, and travel led me to this position, although the journey was not so clearly defined and along the way I accrued many frequent flyer miles (thanks to generous support from several government agencies!).

Hsi-Wei Yen

As far as I can remember I started to be interested in science, particularly astronomy, when I was a kid. I became fascinated by a book about space missions, shuttles and astronauts in the public library near my home. Strictly speaking, that is totally different from what I am working on now. Nevertheless, I did not do anything more extraordinary for my interest in astronomy besides occasionally reading books or magazines about science and astronomy. At that time, playing and watching TV were the most important things to me. Life was just normal until I entered senior high school.

There was an astronomy club in my high school and I was immediately attracted to it as I had been interested in astronomy for a long time. That was my first opportunity to get involved in amateur astronomy. The club was organised by a small group of students who loved astronomy. We had a 10-cm refracting telescope, a 20-cm reflecting telescope, equatorial mounts and cameras. These instruments were all bought and donated by former members. I remember I also saved money and donated it to the club. With the donations from all the members in that year we were finally able to buy a new equatorial mount and replace the old one. We really participated in the club with passion. Together with astronomy clubs in other high schools, twice a year

Hsi-Wei Yen

we invited lecturers and organised talks, like a small workshop, for three or four days. In addition, every two or three weeks we took our instruments to mountains, found places without light pollution (which is relatively difficult in my home town of Taipei) and observed the night sky. I even knew how to recognise almost all the constellations on the sky, though I have totally lost that skill now.

After the fantastic years at the astronomy club in the high school, I entered the physics department in the National Taiwan University. It was a simple decision for me to select physics as my major. First, I was interested in science, especially fundamental science. Second, I actually had no plan for my future career and I thought that as a physicist there could be many options for future career. After my first two years in college, I realised that physics and mathematics are very difficult. I was not sure whether I could stay in the field for my future career after graduation or not.

Fortunately, I met my first mentor in my astronomy career in that year, Paul T. P. Ho. He was the director of the Academia Sinica Institute of Astronomy and Astrophysics (ASIAA). He organised a journal club particularly for undergraduate students, which I joined. There were about five students. We met every weekend. I still remember the first paper we read and discussed: the classical review paper of star formation written by Shu, Adams, and Lizano in 1987. After that, we chose papers ourselves and introduced them in turn. I was deeply attracted to astronomi-

cal research. As astronomers, we have the biggest laboratory in the world: the entire Universe. In most cases, the only experiments that astronomers can do is to observe. From the limited information obtained from observations, astronomers try to find underlying physics. That process is fascinating to me.

Then, by answering an advertisement from Paul Ho, I joined the summer student programme at ASIAA in my third year of college and started my first scientific research project. I worked with a postdoc on the Spitzer IRAC data of an H II region to study whether the H II region triggers the surrounding star formation activities. After the summer student programme I continued to work at ASIAA on a different topic with Nagayoshi Ohashi and Shigehisa Takakuwa, who later became my thesis supervisors. When I was in the fourth year of college I had taken most of the required courses so I spent time at ASIAA doing research. My project was about gas kinematics in a young, low-mass protostellar source observed with the SubMillimeter Array (SMA).

After I graduated from the physics department, I entered the Graduate Institute of Astrophysics in the National Taiwan University. My PhD thesis project was about observational studies of low-mass star-forming regions with the SMA and single-dish radio telescopes. In my third year of the PhD programme, the Atacama Large Millimeter/submillimeter Array (ALMA) came online. It was a really exciting moment to see images of star-forming regions with unprecedented sensitivity. In particular, I had SMA and ALMA images of the same source on the same scale so I could see how powerful ALMA is, and that was just cycle 0 with the limited number of antennae and baseline lengths! I was very impressed and excited about the future of my research field. After I received my PhD I worked at ASIAA for three years in my first postdoc position. Then I moved to ESO Headquarters in Garching as a fellow in 2016.

Here in Germany, the environment and culture are very different from those in Taiwan, my home country. I found it difficult to settle down at the beginning but now I enjoy life here very much. I feel very excited to be working at ESO. My favourite part is its diversity. At ESO, there are so many experts from different fields and with different expertise. This creates a lot of chances to gain new knowledge about astronomy. With new collaborations and access to the Very Large Telescope, I started a new project in the infrared. This aims to probe the inner regions (a few au) around protostars, and will pro-vide complementary information to my previous studies at radio wavelengths. With the opportunities here I am also extending my research from star formation to protoplanetary disks and planet formation. Several exciting new projects have started and I am looking to forward to obtaining new data and making new discoveries.

Personnel Movements

Arrivals (1 July–30 September 2017)

Europe

Alas Da Cunha Dias Da Silva, Nelma (PT)	Administrative Assistant
Anderson, Richard (DE)	Fellow
Aoki, Misa (JP)	Student
Aros Pinochet, Francisco Ignacio (CL)	Student
Barcons, Xavier (ES)	Director General
Bhattacharya, Souradeep (IN)	Student
Hamanowicz, Aleksandra (PL)	Student
Hopgood, Joshua (UK)	Detector Engineer
Jerabkova, Tereza (CZ)	Student
Kellerer, Aglaé (FR)	Optical Engineer
Lapeyre, Pascal (FR)	ELT DMS Site Manager
Manara, Carlo (IT)	Fellow
Mancino, Sara (IT)	Student
Scholtz, Jan (CZ)	Student
van de Ven, Glenn (NL)	Astronomer
Verinaud, Christophe (FR)	AO Physicist/Analyst

Chile

Angel, Maria Ester (CL)	Secretary/Technical Assistant
Garcés, Eduardo (CL)	Instrumentation Engineer
Minniti, Javier (AR)	Student
Paladini, Claudia (IT)	Operation Staff Astronomer
Razza, Alessandro (IT)	Student
Sedaghati, Elyar (IR)	Fellow
Thomas, Romain (FR)	Fellow

Departures (1 July–30 September 2017)

Europe

Bristow, Pamela (UK)	Scientific Reports Typist
de Zeeuw, Tim (NL)	Director General
Ellis Richard, (UK)	Visiting Senior Scientist
Geeraert, Patrick (BE)	Director of Administration
Hallakoun, Naama (IL)	Student
Immer, Katharina (DE)	Fellow
Kakkad, Darshan (IN)	Student
McClure, Melissa (US)	Fellow
Popping, Gergely (NL)	Fellow
Szécsényi, Orsolya (HU)	Contract Officer
Visser, Ruud (NL)	Fellow
Walsh, Jeremy (UK)	Astronomical Editor
Xu, Siyi (CN)	Fellow

Chile

Aubel, Karla (CL)	Telescope Instruments Operator
Girard, Julien (FR)	Operations Astronomer
Pantoja, Blake (US)	Student

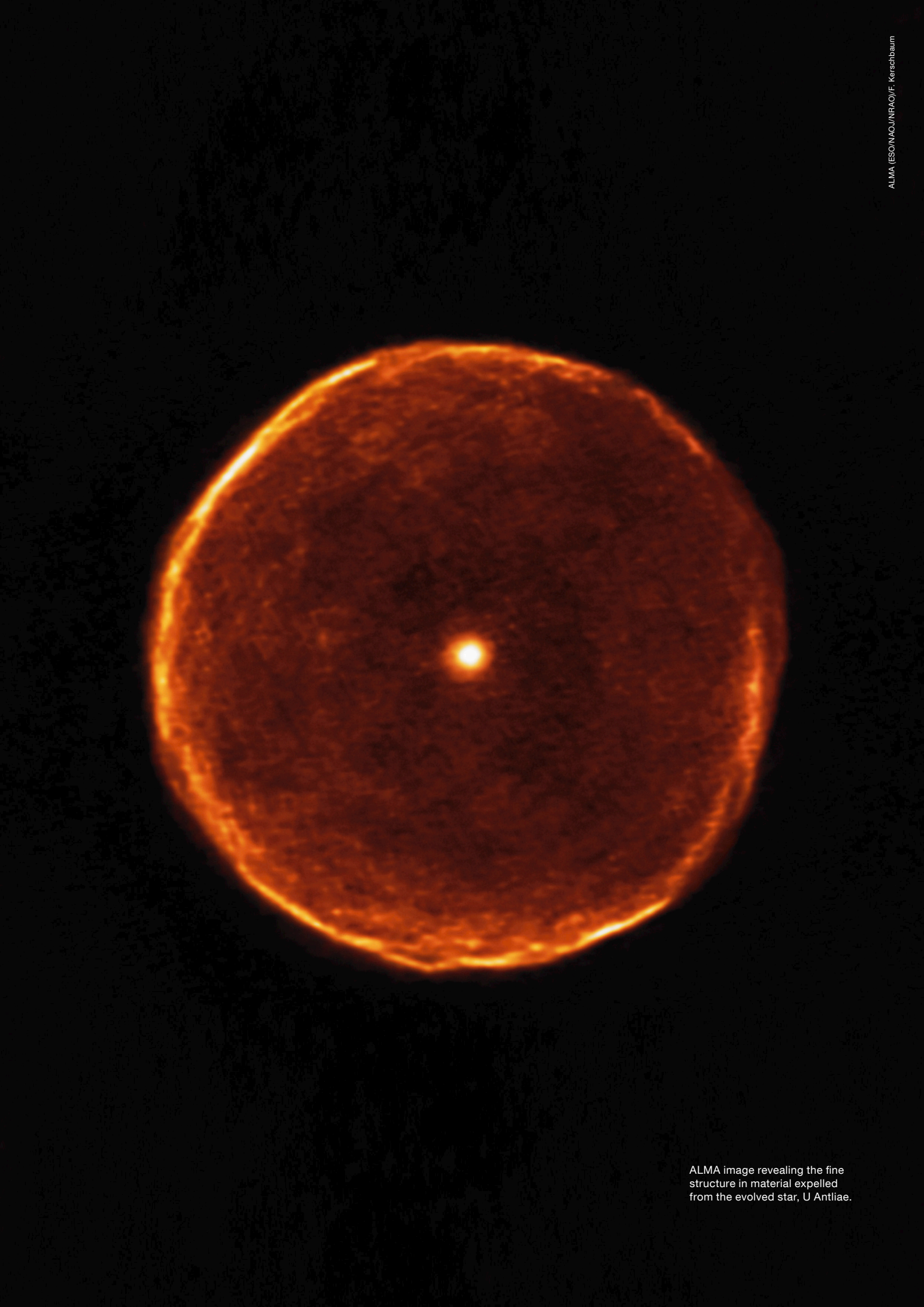

ALMA (ESO/NAOJ/NRAO)/F. Kerschbaum

ALMA image revealing the fine structure in material expelled from the evolved star, U Antliae.

ESO, the European Southern Observatory, is the foremost intergovernmental astronomy organisation in Europe. It is supported by 16 countries: Austria, Belgium, Brazil, the Czech Republic, Denmark, France, Finland, Germany, Italy, the Netherlands, Poland, Portugal, Spain, Sweden, Switzerland and the United Kingdom. ESO's programme is focused on the design, construction and operation of powerful ground-based observing facilities. ESO operates three observatories in Chile: at La Silla, at Paranal, site of the Very Large Telescope, and at Llano de Chajnantor. ESO is the European partner in the Atacama Large Millimeter/submillimeter Array (ALMA). Currently ESO is engaged in the construction of the Extremely Large Telescope.

The Messenger is published, in hardcopy and electronic form, four times a year: in March, June, September and December. ESO produces and distributes a wide variety of media connected to its activities. For further information, including postal subscription to The Messenger, contact the ESO education and Public Outreach Department at:

ESO Headquarters
Karl-Schwarzschild-Straße 2
85748 Garching bei München, Germany
Phone +49 89 320 06-0
information@eso.org

The Messenger:
Editors: Gaitee A. J. Hussain, Jeremy R. Walsh;
Graphics: Mafalda Martins; Ed Janssen;
Layout, Typesetting: Mafalda Martins, Jutta Boxheimer;
Design, Production: Jutta Boxheimer;
www.eso.org/messenger/

Printed by G. Peschke Druckerei GmbH
Taxetstraße 4,
85599 Parsdorf, Germany

ISSN 0722-6691

Contents

Front cover: The top image shows La Silla in 1968 (Period 1) when time was offered on only one telescope. The images below are of the La Silla Paranal Observatory in 2017 including the full range of telescopes offered for observing time in Period 100. The middle image is La Silla, the Very Large Telescope is in the lower image, with insets showing the Visible Infrared Survey Telescope for Astronomy and the Atacama Pathfinder EXperiment. Patat et al. (p. 5) describe the evolution of programmes over this time. Credits: ESO/B. Tafreshi, ESO/J. Dommaget, Iztok Bončina/ESO